SOME ASPECTS OF HARMONICS EXTRACTION AND MITIGATION IN POWER DISTRIBUTION SYSTEM

DISSERTATION

SUBMITTED IN PARTIAL FULFILLMENT OF THE REQUIREMENTS
FOR THE AWARD OF THE DEGREE
OF

MASTER OF TECHNOLOGY
IN
POWER SYSTEM

Submitted by:

ANAND AHIRWAR
Roll No. 2K14/PSY/03

Under the supervision of

Dr. ALKA SINGH

DEPARTMENT OF ELECTRICAL ENGINEERING
DELHI TECHNOLOGICAL UNIVERSITY
(Formerly Delhi College of Engineering)
Bawana Road, Delhi-110042

2016

DEPARTMENT OF ELECTRICAL ENGINEERING

DELHI TECHNOLOGICAL UNIVERSITY

(Formerly Delhi College of Engineering)

Bawana Road, Delhi-110042

CERTIFICATE

I, Anand Ahirwar, Roll No. 2K14/PSY/03 student of M. Tech. (Power System), hereby declare that the dissertation/project titled "SOME ASPECTS OF HARMONICS EXTRACTION AND MITIGATION IN POWER DISTRIBUTION SYSYTEM" under the supervision of Dr. ALKA SINGH of Electrical Engineering Department, Delhi Technological University in partial fulfillment of the requirement for the award of the degree of Master of Technology has not been submitted elsewhere for the award of any Degree.

Place: Delhi

Date: 28.07.2016

ANAND AHIRWAR

GUIDE:

Dr. ALKA SINGH

Associate Professor

EED, DTU

ACKNOWLEDGEMENT

I take this opportunity to express my sincere gratitude to all those who have been instrumental in the successful completion of this dissertation.

Dr. Alka Singh, Associate Professor, Department of Electrical Engineering, Delhi Technological University, my project guide, has guided me for the successful completion of this dissertation. It is worth mentioning that she always provided the necessary guidance and support. I sincerely thank her for her wholehearted guidance.

I would like to express my sincere thanks to **Mr. Prakash Chittora**, PhD.-Electrical Engineering Department, Delhi Technological University for his help and guidance.

I am grateful for the help and cooperation of **Prof. Madhusudan Singh**, Head of the Department of Electrical Engineering, Delhi Technological University, for providing the necessary laboratory facilities and cooperation. And I wish to thank all faculty members whoever helped to finish my project in all aspects.

I would also like to thank my beloved parents, who always give me strong inspirations, moral support, and helpful suggestions. Without them, my study career would never have begun. It is only because of them, my life has always been full of abundant blessing. To all the named and many unnamed, my sincere thanks. Surely it is Almighty's grace to get things done fruitfully.

Anand Ahirwar

2k14/PSY/03

ABSTRACT

This thesis presents work on some power quality issues and mitigation techniques. It consists of six chapters. Chapter one presents a review of power quality issues and self-excited induction generator systems. Chapter two consists of techniques for harmonic extraction in presence of non-linear load. Techniques used for harmonic extraction include d-q transformation, notch filter and p-q theory. Chapter three presents a number of conventional control algorithms for estimation of reference of supply currents and compensation of harmonics in presence of non-linear load in a three-phase-three-wire distribution system. This chapter discusses modeling and control of DSTATCOM which is operated in closed loop feedback for mitigation of power quality problems. The algorithms discussed in this chapter include Synchronous Reference Frame Theory, Instantaneous Reactive Power Theory, Modified Instantaneous Symmetrical Component Theory and Notch Filter. These algorithms have been modeled and the performance of system is discussed and compared. Chapter four presents harmonic extraction and mitigation techniques based on conventional and modified versions of p-q theory in presence of non-linear load under distorted grid. Results have been presented for power factor correction and voltage regulation in presence of non-linear load. Chapter five discusses the modelling and control of Self-Excited Induction Generator for voltage regulation.

TABLE OF CONTENTS

LIST OF FIGURES

LIST OF TABLES

LIST OF ABBREVIATIONS

ac	Alternating current
DC	Direct Current
GTO	Gate Turn-Off Thyristor
IGBT	Insulated Gate Bipolar Transistor
PQ	Power Quality
FACTS	Flexible Alternating Current Transmission System
SSSC	Static Synchronous Series Compensator
IPFC	Interline Power Flow Controller
TCSC	Thyristor Controlled Series Compensator
TCSC-FC	Thyristor Controlled Series Compensator-Fixed Capacitor
DSTATCOM	Distribution Static Compensator
UPFC	Unified Power Flow Controller
DVR	Dynamic Voltage Restorer
UPQC	Unified Power Quality Controller
PCC	Point of Common Coupling
SEIG	Self-Excited Induction Generator
DFT	Discrete Fourier Transform
MAFC	Multiple Adaptive Feed Forward Cancellation
SRFT	Synchronous Reference Frame Theory
IRPT	Instantaneous Reactive Power Theory
SSC	Shunt Switching Compensator
VSC	Voltage Source Converter
ANF	Adaptive Notch Filter
PLL	Phase Locked Loop
ISCT	Instantaneous Symmetric Component Theory
UPF	Unity Power Factor

ELC	Electronic Load Controller
DVFC	Decoupled Voltage and Frequency Controller
WECS	Wind Energy Conversion System
PFC	Power Factor correction
ZVR	Zero Voltage Regulation
CHE	Complete Harmonics Elimination
LPF	Low Pass Filter
FFT	Fast Fourier Transform
EMD	Empirical Decomposition Transformation
EPLL	Enhanced Phase Locked Loop
THD	Total Harmonic Distortion

CHAPTER-1

INTRODUCTION

GENERAL

With the development of alternating current (ac) transmission and distribution, power system at the end of 19^{th} century were based on sinusoidal voltage with constant frequency. This made the design of transformers, transmission lines, machines and transmission of power for long distances much easier. With the rise of sinusoidal voltage sources the next problem was to bring the load currents in phase with source voltage to make the power system more efficient and effective. So the concept of reactive power was introduced to represent the component of electric power due to the load current that is not in phase with the source voltage. The concept of apparent power and power factor was also introduced. Apparent power was explained to be total power delivered or consumed in the power system if the sinusoidal source voltages and load currents were perfectly in phase with each other. On the other hand, power factor was explained to give a relation between actual power delivered or consumed in the power system and apparent power at a same point.

For a long time, the problem of power factor correction was solved by using capacitor banks or in some cases reactors.

In the last fifty years or so, non-linear load that consumes non sinusoidal currents had increased significantly and problems like voltage deviation during load change and power transfer limitation have been observed due to reactive power unbalancing. Most of the AC loads consume reactive power due to presence of reactance. Heavy consumption of reactive power results in poor voltage quality. Today these problems have caused a substantially higher impact on reliable and secure power supply.

The development of semiconductors devices like Gate Turn-Off Thyristor (GTO) and Insulated Gate Bipolar Transistor (IGBT) allowed new power electronic configurations to be introduced for the tasks of power transmission and load flow control. The use of power electronics devices, solid state switching devices and the equipment showing

non-linear voltage/current characteristics has been rising these days. Maintaining the electric power quality (PQ) in a distribution system is presently of great concern.

The term power quality generally refers to maintaining good quality of power at generation, transmission, distribution and usage of electric power supply. Transient disturbances are likely to occur in power system due to several reasons. These disturbances cause electric pollution of the power system which is of great concern in power quality study and analysis. Power quality problems may be caused by a number of ways and some natural causes include lightning, flashover, equipment failure and faults (around 60%) and other causes such as voltage distortions and notches (around 40%). At consumer end, a number of equipment draw non -linear current which injects harmonics in the power system. Power quality is referred in terms of voltage, currents, or frequency deviation of supply system that can result in failure or mal-operation of consumer's equipment.

The detrimental effects of these problems can shorten the life of power system; decrease the reliability of the system, and cause control and protective devices of the power system to malfunction. Hence detection of these disturbances and distortions and compensating them are play a very important role in power systems.

Non-linear loads cause distortion in voltage and current waveforms in the distribution system. Such power quality problems like sag, swell, interruption, flicker, transients and harmonics cause huge disturbance in the power distribution system. These power quality problems become much more serious with the use of power electronic devices. The causes and effects of power quality problems are mentioned in **Table 1.1** (which is taken from reference [2]).

A lot of research work is being done worldwide to overcome the problems due to poor power quality. Some of these measures involve the use of passive filters and some involve the use of Custom Power Devices (CPD). Flexible Alternating Currents Transmission system (FACTS) devices are a counterpart of CPD used in power transmission systems.

Table 1.1: POWER QUALITY DISTURBANCES: CAUSES AND EFFECTS [2]

Problems	Category	Categorization	Causes	Effects
Transients	• Impulsive • Oscillatory	• Peak, rise time and duration. • Peak magnitude and frequency components.	• Lightning strikes, capacitor switching. • Line, capacitor or load switching.	• Power system resonance. • System resonance.
Short duration voltage variation	• Sag • Swell • Interruption	• Magnitude, duration. • Magnitude, duration. • Duration	• Motor staring, single line to ground fault. • Capacitor/large load switching, faults. • Temporary faults	• Protection malfunction, production loss. • Protection malfunction, stress on home appliances. • Production loss, fire alarm malfunction.
Long duration voltage variation	• Sustained interruption • Under voltage • Over voltage	• Duration • Magnitude, duration • Magnitude, duration	• Faults • Switching-on load, capacitor de-energization. • Switching-off load, capacitor energization.	• Production loss • Increase in losses, heating • Damage to household appliances.
Waveform distortion	• DC offset • Harmonics • Notching • Noise	• Volts, amperes • THD • THD • THD	• Geomagnetic disturbances, rectification • Non-linear loads • Power Electronic converters • Arc-furnace, arc-lamp, power converters	• Transformer saturation. • Increased losses, poor power factor • Damage to capacitive components. • Capacitor over-loading.
Voltage Flicker		• Frequency of occurrence, modulating frequency	• Arc-furnaces, arc-lamps.	• Human health, irritation, headache, migraine.
Voltage Fluctuation		• Intermittent	• Load change	• Protection malfunction, change in light intensity.

Flexible AC Transmission Systems (FACTS) devices offer a fast and reliable control over the transmission parameters, i.e. voltage, line impedance, and maintaining phase angle between the sending and receiving end voltage. Most widely known FACTS devices are Static Synchronous Series Compensator (SSSC), Interline Power Flow Controller (IPFC), Thyristor Controller Series Compensator (TCSC), Thyristor Controlled Series Compensator-Fixed Capacitor (TCSC-FC), Distribution Static Compensator (DSTATCOM), Unified Power Flow Controller (UPFC) etc. An overview of major FACTS devices is shown in **Fig. 1.1** (which has been taken from reference [2]). Some of the FACTS devices used at lower voltage level in the distribution system are categorised into Custom power devices. Three custom power devices viz. Distribution Static Compensator (DSTATCOM), Dynamic voltage Restorer (DVR) and Unified Power Quality Controller (UPQC) are popular. DSTATCOM is very well known, effective and can provide cost effective solution for the compensation of reactive power and unbalance loading in distribution system. DSTATCOM is shown to provide the reactive power compensation, harmonics elimination, regulating point of common coupling (PCC) voltage, load balancing and neutral current compensation. A significant part of the Thesis will deal with power quality problems and their mitigation using DSTATCOM.

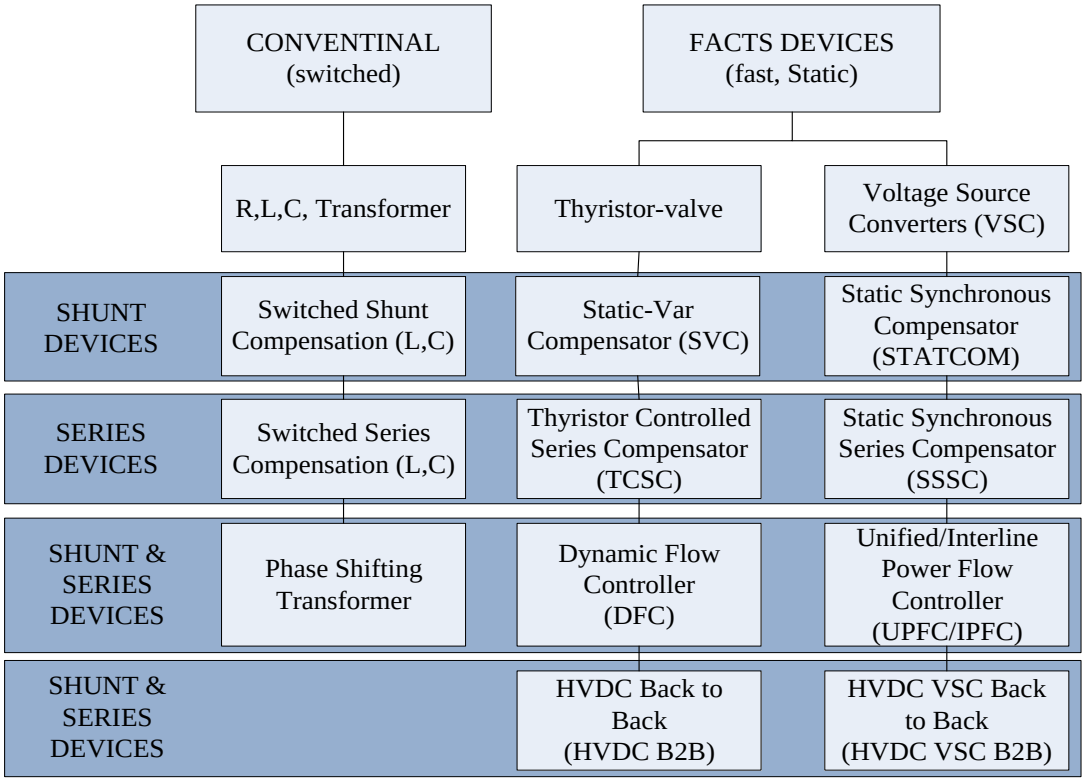

Fig. 1.1: Overview of major FACTS Devices [2].

Today the main sources for generation of electricity are fossil fuels like coal, oil and natural gas and these sources are non-renewable in nature. These fossil fuels have limited reserves in nature and will be exhausted in the near future. Apart from these limitations, the fossil fuels produce pollutant gases when they burn which is of great concern for the ecosystem. So, more attention is being given to renewable energy such as wind, micro-hydro, tidal, solar, bio-fuel etc. Out of these, wind energy seems to be most promising source because it is clean and abundant resource without producing any emissions.

Induction generators are commonly used for wind powered energy generation. An induction generator is low cost, has rugged construction and gives a good dynamic response over the conventional synchronous generator.

A three phase induction machine can act as self-excited induction generator when a capacitor bank is used to supply the reactive power required by the generator to start operating. In grid connected induction generator driven by wind turbine the magnetic field is produced by excitation current drawn from the grid. Fig. 1.2 shows the operation of self-excited induction generator driven by wind turbine.

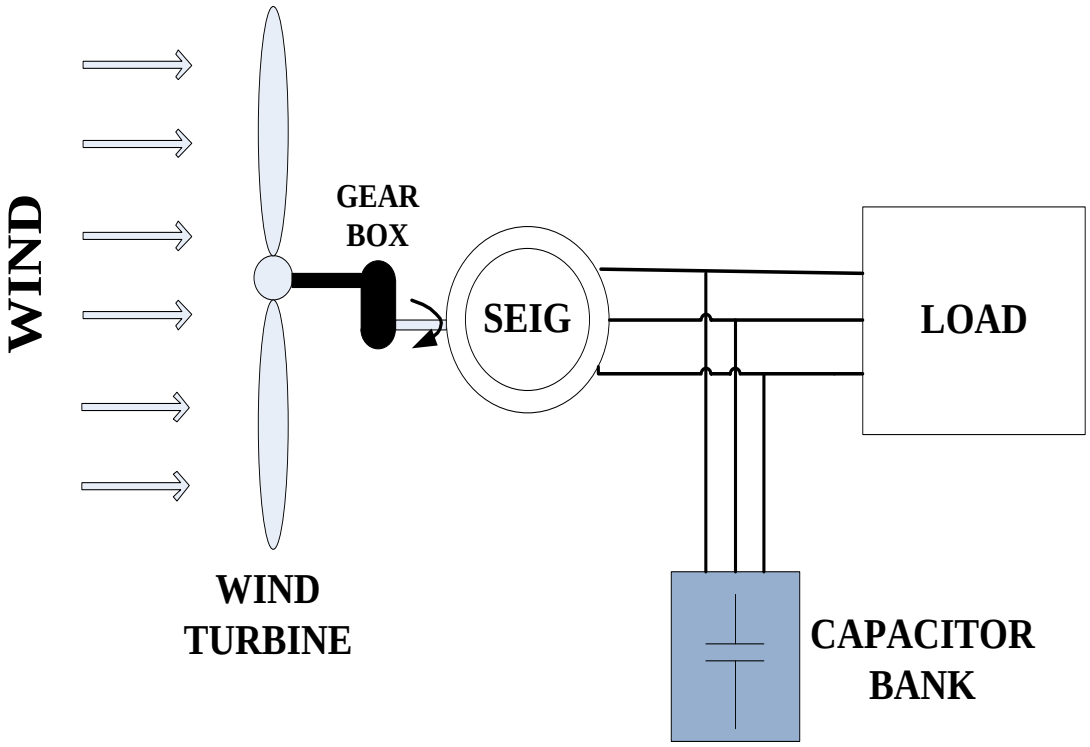

Fig. 1.2: Schematic Diagram of Wind Driven SEIG

1.2 LITERATURE REVIEW

Harmonics in supply voltage or current are indicators of poor power quality. They cause a lot of disturbances in the distribution system such as electromagnetic interference, overheating if cables and low power factor. Despite of existing active power filter technologies being present, research is still on-going on in search of effective harmonic detection methods.

Various methods for detection of fundamental and harmonics component in grid connected power system like Discrete Fourier Transform (DFT), Recursive DFT, Synchronous Fundamental d-q Frame, 5^{th} Harmonic d-q Frame, p-q Theory and 5^{th} Generalised Integrator are explained by B. Chen, G. Pin, Wai Man Ng, T. Parisini and S.Y. Ron Hui in [8]. A novel modulation function integral observer (MF Observer) that offers instantaneous convergence without complexity has also been developed.

A comparison between the popular d-q method that dominates over three phase active filter and DSTATCOM applications and Multiple Adaptive Feed Forward Cancellation (MAFC) method has been presented in [9] by L. Qian, D. Cartes and Hui Li. Real-time hardware tests of both MAFC method and d-q method have been performed for study in steady-state and dynamic transient. Two different non-linear loads, a diode rectifier front end motor drive system and a thyristor rectifier dc motor drive system have been used to verify the real-time hardware in loop test.

A Distribution Static Compensator (DSTATCOM) can be used to compensate reactive power and unbalancing in loading in the distribution system [10],[13-15]. Performance of DSTATCOM depends on control scheme used to extract reference current components. Instantaneous Reactive Power (IRP) theory and Synchronous reference Frame (SRF) theory for compensating reactive power and unbalancing in loading are compared with a new Adaline based control algorithm in [6] by B. Singh and J. Solanki. This adaline based control algorithm proves to be simple and requires less computational efforts.

Instantaneous Reactive Power (IRP) theory defines a set of instantaneous power in the time domain. It can be applied to three phase system with or without neutral conductor. Thus it is not only valid in steady-state and also during transients. Some other conventional power theories treat a three phase system as three separate single-phase

systems but the p-q theory deals with all three phases at a same time as a unity system. This theory is given by H. Akagi, E.H. Watanabe and M. Aredes in [3].

L.S. Czarnecki proposed an approach to generate reference current for shunt switching Compensator (SSCs) control using Instantaneous Reactive Power (IRP) p-q theory in [12] in 2009. On the other hand J. Bangarraju, V. Rajagopal and A. Jayalaxmi proposed Instantaneous Reactive Power (IRP) theory control algorithm for three-leg Voltage Source Converter (VSC) based on Dynamic Voltage Regulator (DVR) in [11].

An algorithm based on the concept of adaptive notch filter (ANF) is proposed to estimate power system frequency and its rate of change of power system signal. M. Malekpour, M. Farshadnia and M. Mojiri proposed an algorithm in [19] that extracts harmonics and fundamental component of voltage and current signals to estimate the parameters of the signal such as frequency, amplitude and phase in presence of disturbances, noise and distortion. B. Singh, K. Kant and S.R. Arya proposed in [20] the implementation of a Distribution Static Compensator (DSTATCOM) using an algorithm based on Notch Filter to mitigate power quality issues. Use of Shunt Active Power Filter (SAPF) to compensate reactive power and mitigate harmonics currents of non-linear load is presented by G.W. Chang in [16]. A comparison of performance of algorithm based on Adaptive Notch Filter(ANF) and a newly introduced algorithm based on an enhanced Phase Locked Loop (PLL) is presented in [18] by M. Karimi-Ghartemani, A.R. Bakhshai, and M. Mojiri.

A four-leg Voltage Source Converter (VSC) based Distribution Static Compensator (DSTATCOM) for load/neutral current compensation in three-phase four-wire distribution system is proposed in [10] by S. Kumar and B. Singh. The reference currents are extracted by using Instantaneous Symmetrical Component Theory (ISCT) that is modified for voltage regulation and is used with indirect current control technique for controlling the Distribution Static Compensator (DSTATCOM) currents.

Active filtering generally discussed in the literature focus on compensation techniques where the source voltages are sinusoidal where compensation of harmonic currents with reactive power gives unity power factor (UPF) which results in harmonics free supply currents. But when the source voltages are non-sinusoidal some difficulties arise in compensating. Conventional control algorithms may fail under distorted grid condition.

Salmerón and R. S. Herrera in [21] and S. Mohammad-Reza Rafiei, H. A. Toliyat, R. Ghazi, and T. Gopalarathnam in [22] proposed techniques for load compensation under distorted source voltages.

Depletion of fossil fuels and the growing concern about pollution in the environment has led to increase in research about generation of power using renewable resources. Self-Excited Induction Generators (SEIG) are gaining an advantage in this field due to their small size, low cost and robust structure.

In [39-40] modeling of Self-Excited Induction Generator in d-q Reference frame has been shown. The advantage of d-q axes model or the dynamic model is that it can analyse the steady-state and transient conditions fiving a good solution of any dynamics. A three-phase induction machine can act as a Self-Excited Induction Generator when a three-phase capacitor bank is connected across the stator terminals of the machine. [37] Shows the modeling and analysis of this three phase capacitor bank.

To improve the performance of the self-excited induction generator (SEIG) many researchers have proposed many algorithms for harmonics compensation, maintaining unity power factor, voltage regulation, frequency control and performance of SEIG under load variations.

Performance of SEIG under load variations and transients and compensation of harmonic currents using a DSTATCOM has been studied by various researchers in [32-36] and [53]. As SEIG has poor voltage regulation and it requires an adjustable source for reactive power to maintain constant terminal voltage, a number of papers have been published in this area of research for design and analysis if DSTATCOM based voltage regulator for SEIG in [27-28] and [48-52].

When SEIG is used for generating power a problem of power balancing with varying consumer load may arises. This problem can be solved by the use of an Electronic Load Controller (ELC) that consists of a rectifier-chopper system feeding resistive dump load whose power is varied by the duty cycle of the chopper. Since the generated power has to be maintained constant to balance the constant input power from the turbine, ELC has been used to dissipate the excess power in consumer load. Modeling and control strategies of this Electronic Load Controller (ELC) are shown in [30, 35, 41-42].

In variable power applications like biogas, gasoline and diesel engines driven Induction Generator where the speed is constant, compensator like DSTATCOM serves the purpose of voltage regulation and the frequency is maintained constant because of the constant speed of the prime mover. But in cases where frequency varies due to variation in consumer loads and a constant prime mover a necessity of a controller to maintain frequency constant is required. [34, 43-47] presents an approach towards designing controller that maintains both voltage and frequency in such conditions. For regulating the voltage the controller controls the reactive power and to control the frequency the controller controls the active power. Such a controller is known as Decoupled Voltage and Frequency Controller (DVFC). It is a combination of a Distribution Static Compensator (DSTATCOM) and an Electronic Load Controller (ELC). Here the Distribution Static Compensator (DSTATCOM) acts as a voltage regulator, harmonic/neutral current compensator and load balancer whereas; the Electronic Load Controller (ELC) is used to maintain constant power at the terminals of the generator which in turn maintains the frequency of the system.

Analysis and control of grid connected Wind Energy Conversion System (WECS) with DSTATCOM has been studied in [23-25].

1.3 MOTIVATION OF THE THESIS

The motivations of the thesis are as follows:

- Non-linear loads draw non-linear currents from the power system. Distorted load currents having harmonics propagate into the interconnected system and are identified to be the key factors affecting poor power quality. So harmonic detection is a critical element for active power filters. Instantaneous p-q theory, synchronous reference frame theory, notch filter and adaptive notch filter have proven to be very effective in estimating the harmonics content of single phase and three phase systems.
- Harmonic mitigation using DSTATCOM is attempted. The reference signal generated by the control algorithm of a grid-connected power converter should be synchronized with the fundamental component of the grid voltage. This has motivated to generate the reference current signal in shunt active power filter

based upon the knowledge of fundamental component of the grid voltage and load currents. Thus, a precise estimation of this fundamental component is intended for power factor correction, voltage regulation, harmonic reduction and load balancing. Some conventional control algorithms have been studied and compared here.

- This is followed by investigating the grid connected DSTATCOM performance in the presence of source distortions due to harmonics . the motivation here is to find out how the conventional algorithms behave and modifications required to achieve IEEE standards.

- The next problem undertaken is to investigate the effect of connecting a SEIG based system to the utility grid and electric load and how the power quality is affected with various load combinations.

- Shunt active power filter can compensate current harmonics by injecting equal-but-opposite harmonic compensating currents into the grid. It motivates to develop the dynamic model of stand-alone SEIG and analyse the whole system with different conditions and then develop a control algorithm to compensate the current harmonics.

1.4 OBJECTIVE OF THE THESIS

The objectives of this thesis are as follows-

- To propose various methods for estimation of fundamental amplitude and frequency in order to achieve accurate and fast results considering all possible disturbances in the distribution system such as voltage distortion and harmonics.

- To develop various reference current generation algorithms that can self-regulate the dc-link voltage.

- To propose robust control techniques and test their performance under variations of load, harmonic currents and load balancing etc.

- To develop and study IRPT algorithm and its modification for DSTATCOM control under distorted grid.

- Analysing and modeling of self-excited induction generator in MATLAB/SIMULINK.

- To analyse the dynamic response and voltage build-up process of self-excited induction generator under different loading conditions.

- To design and simulate a control strategy based on synchronous reference frame theory to compensate harmonics and reactive power requirement and maintaining the PCC voltage while a linear/non-linear load is connected to the grid connected SEIG.

1.5 OUTLINE OF THESIS

The chapters included in this thesis are organised as follows-

- CHAPTER 1 presents the basic introduction and gives an overview of the problems related to power quality and different ways of mitigating these problems, literature review of different control algorithm is presented in this thesis in order to measure, monitor and compensate the disturbances present in the distribution system

- CHAPTER 2 presents three strategies in order to monitor and extract harmonics present in the system in presence of non-linear load at consumers end. These include d-q transformation, notch filter and p-q theory.

- CHAPTER-3 comprises of four control algorithms for estimation of reference of load current and compensation of reactive power requirement of non-linear loads and maintaining unity power factor. These control algorithms are as follows-

    1. Synchronous Reference Frame Theory (SRFT)
    2. Instantaneous p-q Theory

3. Modified Instantaneous Symmetrical Component Theory
4. Adaptive Notch Filter

- CHAPTER 4 presents comparison of three different methods when the pure sinusoidal three phase voltage sources are replaced with distorted grid. These methods are discussed to obtain the reference currents using instantaneous p-q theory. The three methods are as follows-

  1. p-q theory (PFC mode)
  2. p-q Theory (ZVR mode)
  3. Complete Harmonic Elimination (CHE) Method

- CHAPTER 5 presents the analysis and dynamic response and voltage build-up process of self-excited induction generator under different loading conditions and designing and simulating a control strategy based on synchronous reference frame theory to compensate harmonics and reactive power requirement and maintaining the PCC voltage while a linear/non-linear load is connected to the grid connected SEIG.

- CHAPTER 6 gives the future scope of work.

CHAPTER-2

SOME ALGORITHMS FOR HARMONICS EXTRACTION [8-9]

INTRODUCTION

The problems emerging due to poor power quality are a cause of great concern these days. A lot of research is being done worldwide to mitigate these problems. Polluted supply in distribution system leads to a number of problems to consumers and in the industrial areas. These disturbances in power system can be either due to natural causes or artificially induced in the distribution system. Natural causes of these disturbances can be lightning strikes, flashover, failures in equipment used or faults. On the other hand, the disturbances that are artificially induced in the system can be due to use of non-linear loads at the consumers end. Non-linear loads draw non-linear currents from the system and in doing, they induce harmonics currents into the system which pollutes the grid voltage and currents. A sinusoidal component of a periodic wave or quantity having a frequency that is an integral multiple of the fundamental frequency is known as harmonic. For example, a component having a frequency five times the fundamental frequency is called a fifth harmonic [2].
There are a number of ways for compensating these harmonics currents in order to obtain pollution free supply. But for compensation of harmonics, detection of harmonic components present in the system is very important.

There are two ways of detecting the total harmonic content.

1. By obtaining the sum of the fundamental component and the dc component and subtracting this sum from the input current waveform.
2. By adding several low-order harmonic components together to form an approximation of harmonic current.

This chapter contains three methods for detection of harmonics, these methods are:

1. d-q Transformation
2. Notch Filter
3. p-q theory

Fig. 2.1 shows a general diagram representing the fundamental components and the harmonic components in a signal.

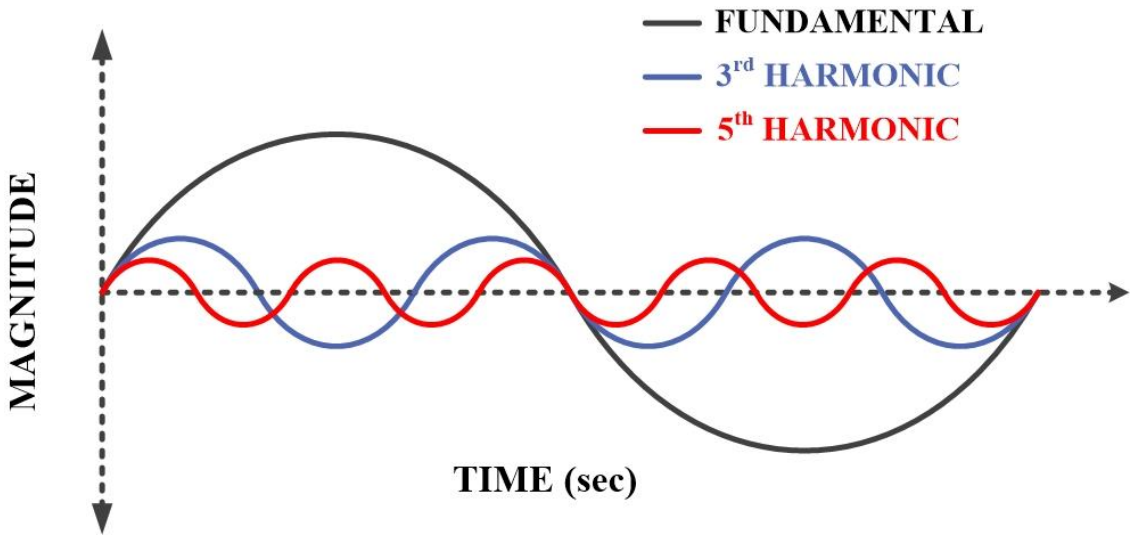

Fig. 2.1: General Diagram of Fundamental and Harmonic Components

2.2 METHODS FOR EXTRACTING HARMONICS

Three methods are discussed in this Section that deal with harmonic extraction.

2.2.1 d-q Transformation [8]

In this method we sense the load currents (i_{La}, i_{Lb}, i_{Lc}) and the phase voltages (v_{sa}, v_{sb}, v_{sc}) in the distribution system. The load currents are converted into d-q frame using Park's transformation so that the fundamental component appears a DC component, with the use of a low pass filter this DC component can be filtered and converted back from d-q frame to a-b-c frame using Park's transformation.

This procedure of extracting the fundamental component can be used for extracting the harmonic components by tuning the Phase Locked Loop (PLL) to the individual harmonic frequency. The sum of the fundamental component and these harmonic components will give an approximate load current signal. Fig. 2.2 shows the schematic diagram for the extraction of the fundamental and harmonic components.

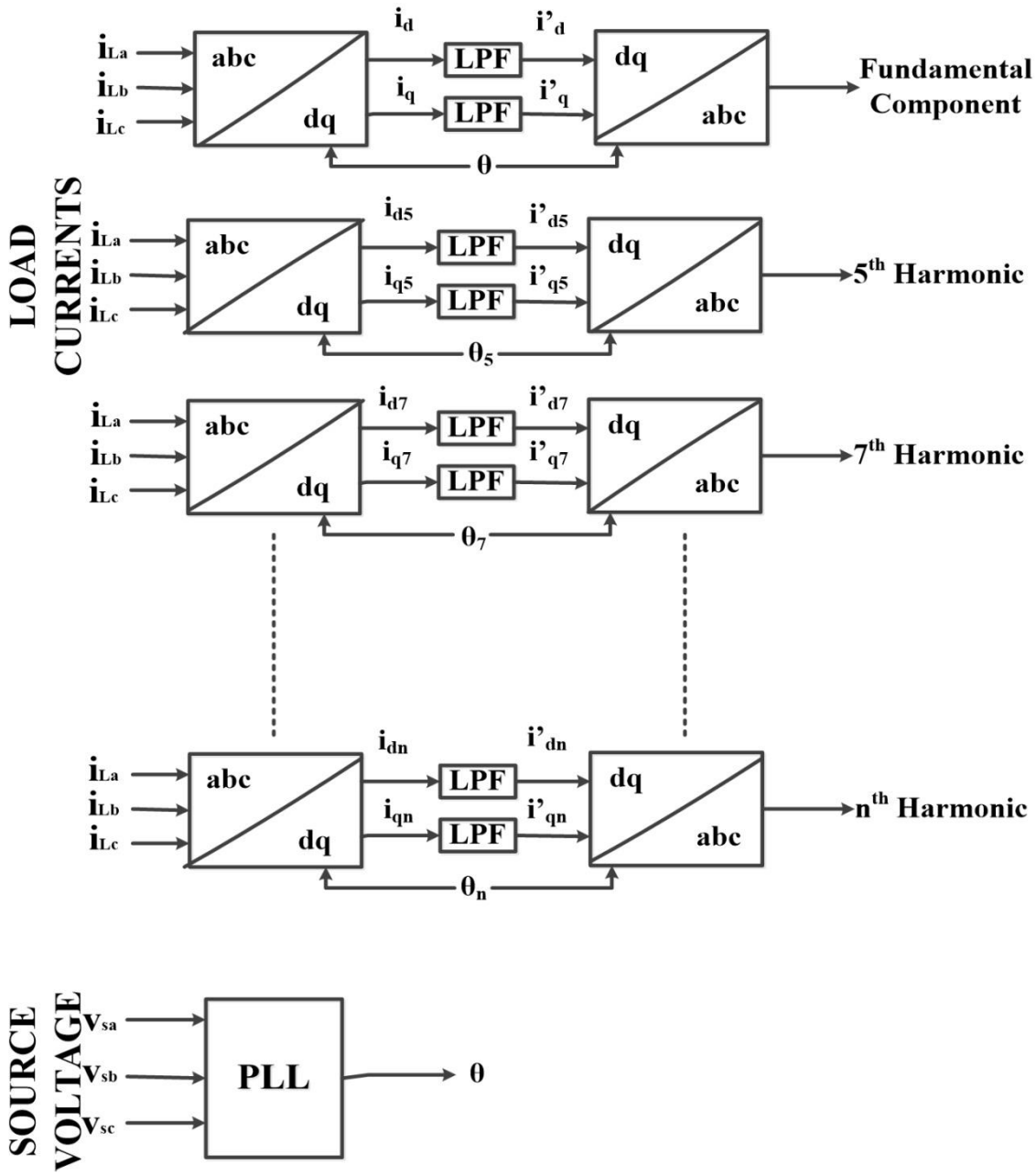

Fig. 2.2: Extraction of Fundamental and Harmonic Component using d-q Transformation [8]

In this scheme we first convert the load currents (i_{La}, i_{Lb}, i_{Lc}) are converted into d-q frame by using Park's transformation.

$$\begin{bmatrix} i_{Ld} \\ i_{Lq} \end{bmatrix} = \frac{2}{3}\begin{bmatrix} cos\,\theta & -sin\,\theta \\ cos\left(\theta - \frac{2\pi}{3}\right) & -sin\left(\theta - \frac{2\pi}{3}\right) \\ cos\left(\theta + \frac{2\pi}{3}\right) & sin\left(\theta + \frac{2\pi}{3}\right) \end{bmatrix}\begin{bmatrix} i_{La} \\ i_{Lb} \\ i_{Lc} \end{bmatrix} \quad (2.1)$$

These currents thus obtained from the Park's Transformation i.e. ($i_{Ld}\ and\ i_{Lq}$) are passed through a Low Pass Filter (LPF) to obtain the DC components of 'i_{Ld}' and 'i_{Lq}'. The d-q components of the load currents contain both fundamental and harmonic components as shown:

$$i_{Ld} = i_{dDC} + i_{dAC} \quad (2.2)$$

$$i_{Lq} = i_{qDC} + i_{qAC} \quad (2.3)$$

A Phase Locked Loop (PLL) is used to synchronize these signals with the fundamental/harmonic component's frequency.

Then the filtered DC components are i_{dDC} and i_{qDC} are converted back to a-b-c frame by using inverse Park's transformation to obtain the fundamental/harmonic component.

$$\begin{bmatrix} i_{refa} \\ i_{refb} \\ i_{refc} \end{bmatrix} = \begin{bmatrix} cos\,\theta & sin\,\theta \\ cos\left(\theta - \frac{2\pi}{3}\right) & sin\left(\theta - \frac{2\pi}{3}\right) \\ cos\left(\theta + \frac{2\pi}{3}\right) & sin\left(\theta + \frac{2\pi}{3}\right) \end{bmatrix}\begin{bmatrix} i_{dDC} \\ i_{qDC} \end{bmatrix} \quad (2.4)$$

Adding all the harmonic components and the fundamental component gives us the approximate load current present in the grid.

Fig. 2.3 shows the simulation diagram of this method developed using Matlab.

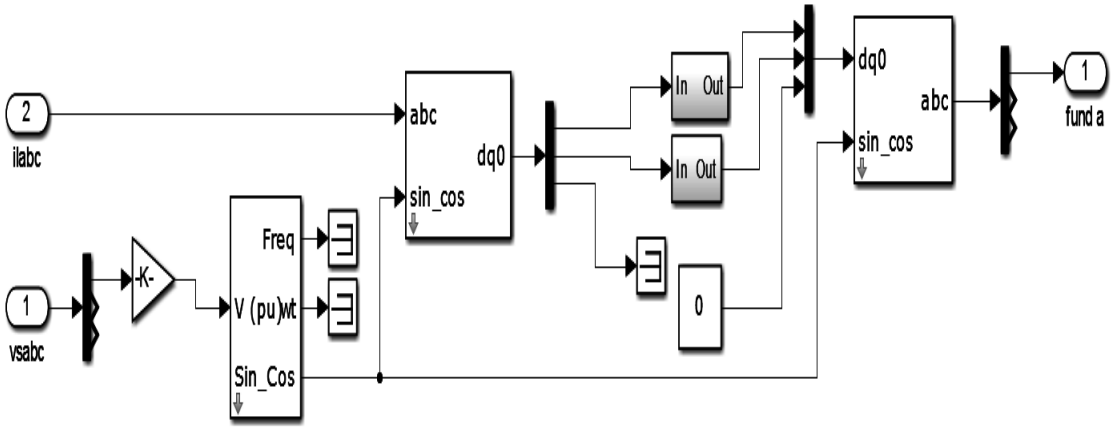

Fig. 2.3: Simulation Diagram of d-q Transformation for Extracting Fundamental/Harmonic Component

2.2.1.2 Results with d-q transformation

Fig. 2.4 shows a comparison between the original load current and its extracted fundamental component, $5^{th}/7^{th}/11^{th}/13^{th}/17^{th}/19^{th}$ harmonic components and the comparison between the original and calculated load currents using d-q Transformation.

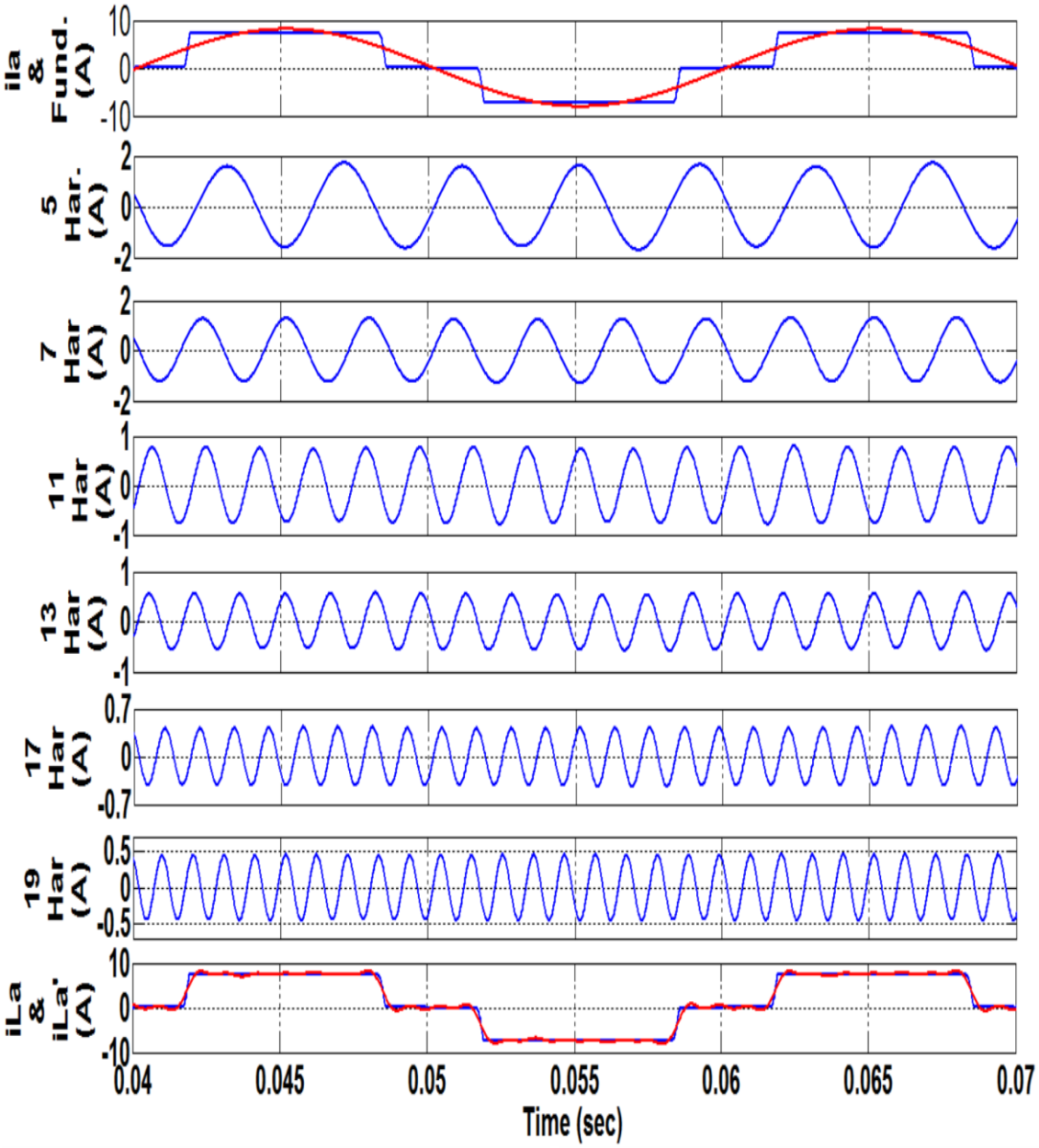

Fig. 2.4: Fundamental/Harmonic Components of Load current and Comparison between Original/Calculated Load Currents using d-q Transformation

Load is modelled as a three-phase diode rectifier circuit with R-L circuit connected at the DC link. Fig. 2.5 and Fig. 2.6 show the FFT analysis of original load current in phase-a and calculated load current in phase-a respectively, the total harmonic disorder in original load current is found to be 29.25% and in the calculated load current is 29.15%.

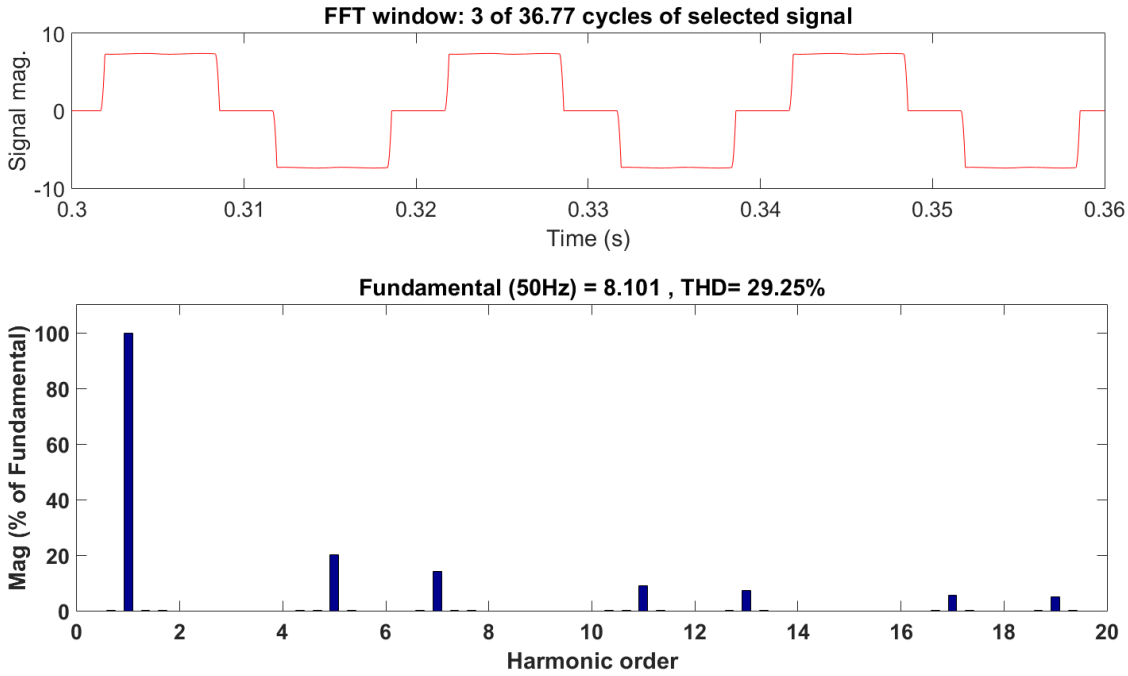

Fig. 2.4: FFT Analysis of Original Load Current using d-q Transformation

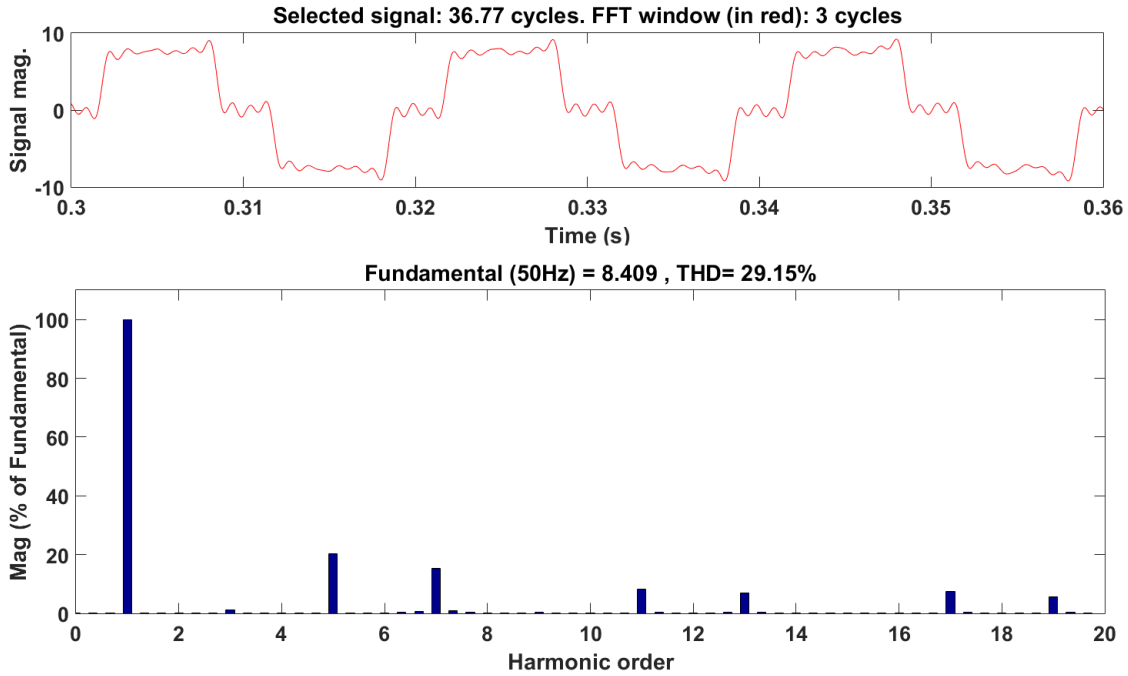

Fig. 2.5: FFT Analysis of Calculated Load Current using d-q Transformation

2.2.2 Harmonic Extraction using Notch Filter [20]

There are many power quality problems such as poor power factor of loads, network pollution due to harmonics injection by the nonlinear. A notch filter extracts the fundamental frequency component of the load currents by allowing only a specific frequency to pass through it (which in this case is the fundamental frequency. These components of load currents are used to estimate reference supply currents. The load currents (i_{La}, i_{Lb}, i_{Lc}) are sensed and passed through the notch filter in order to obtain the fundamental/harmonic components of the load currents individually. We vary θ synchronizing it to the fundamental/harmonic component's frequency in order to extract the fundamental/harmonic component of load current. The equations defining the characteristics of a notch filter are [18]:

$$e(t) = u(t) - \dot{x} \tag{2.5}$$

$$\ddot{x} + \theta^2 x = 2\xi\theta e(t) \tag{2.6}$$

Here,

u(t) is the input signal.

e(t) is the error signal or the harmonic signal.

$\dot{x}$ is the estimate signal for input signal u(t).

θ is the frequency in rad/sec.

ξ is a real positive number that determine the performance of notch filter in terms of accuracy.

The simulation diagram of notch filter is shown in Fig. 2.7. In this scheme the notch filter is set to capture the fundamental and the harmonic components of the load current individually. Fig. 2.8 shows a block diagram of this scheme.

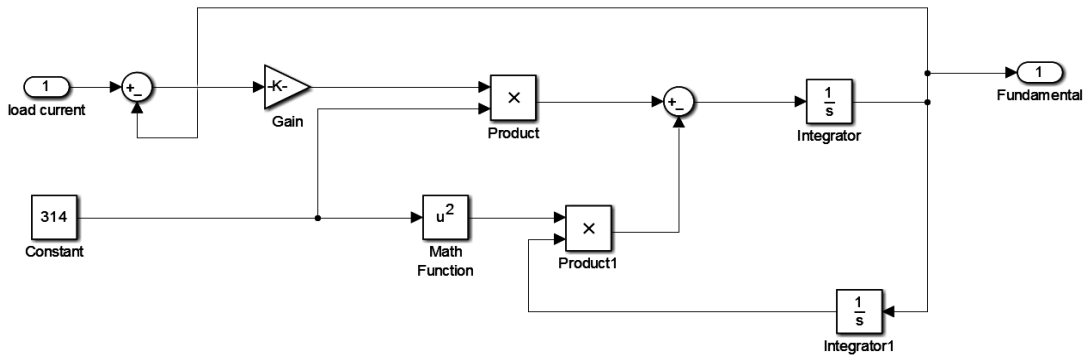

Fig. 2.7: Simulation Diagram of a Notch Filter

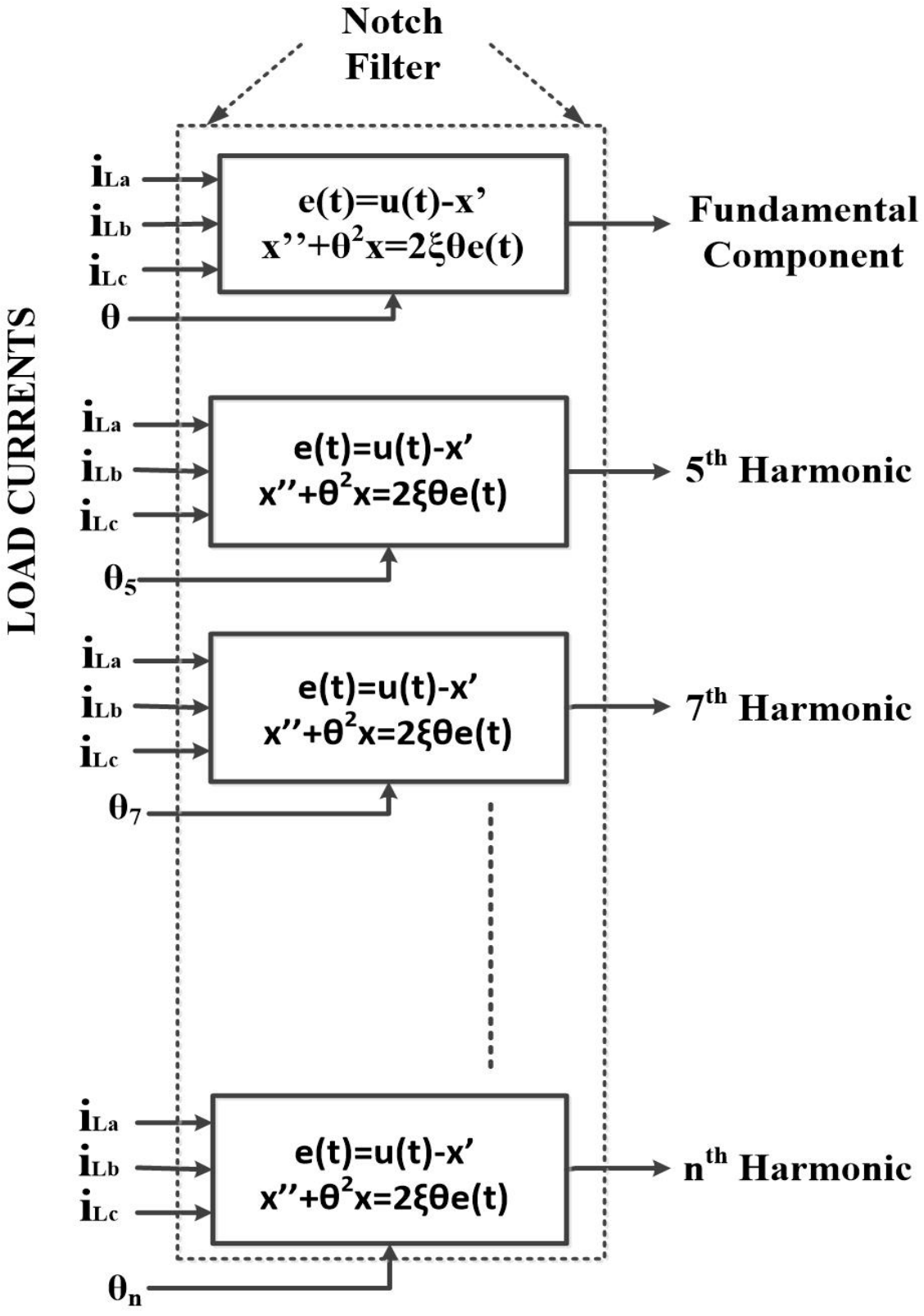

Fig. 2.8: Block Diagram of Extracting Fundamental/Harmonic Component using Notch Filter

Adding all the harmonic components and the fundamental component will give us the approximate load current present in the system.

2.2.2.2. Results with Notch Filter

Fig. 2.9 shows a comparison between the original load current and its extracted fundamental component, $5^{th}/7^{th}/11^{th}/13^{th}/17^{th}/19^{th}$ harmonic components and the comparison between the original and calculated load currents using notch filter

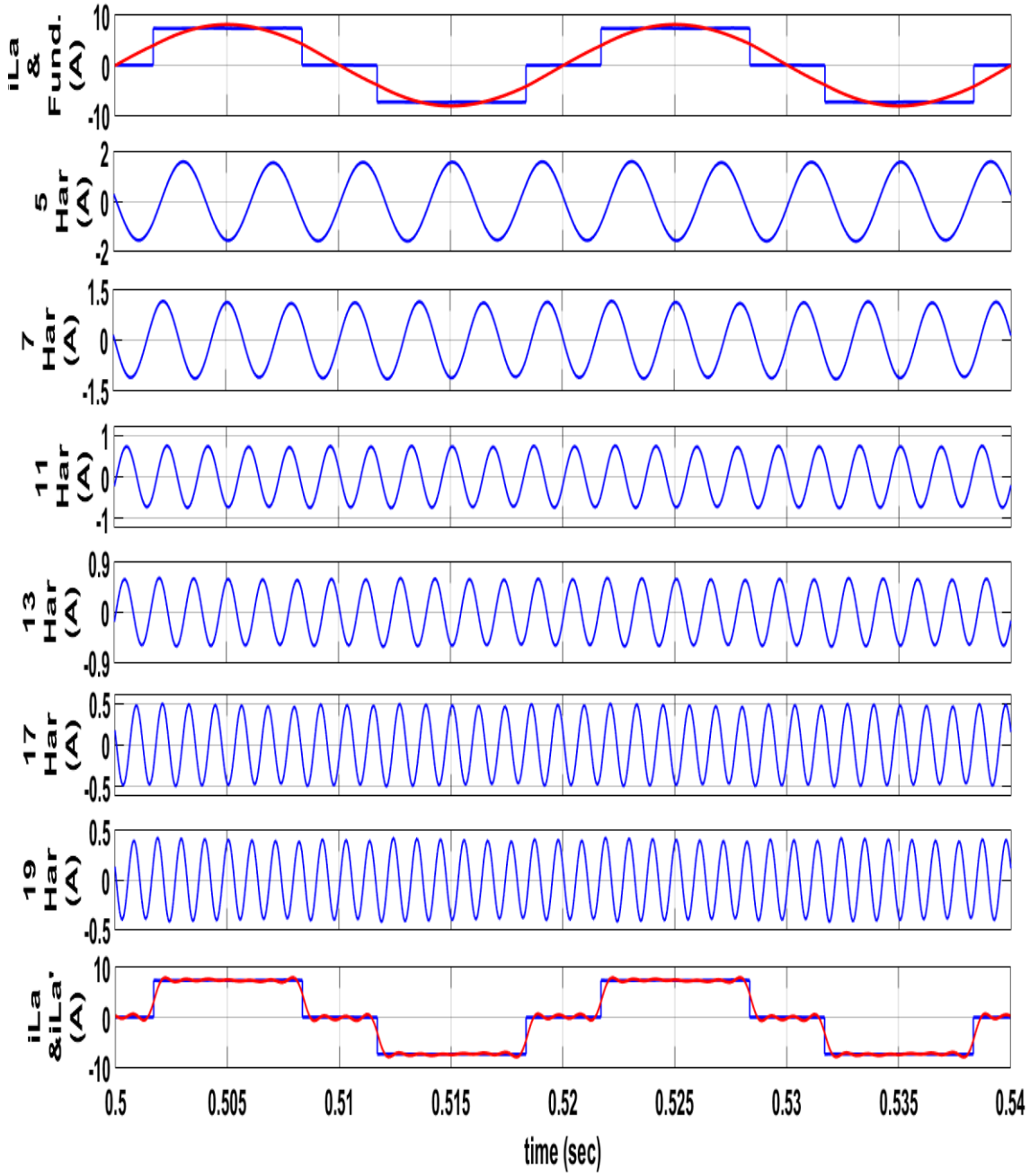

Fig. 2.9: Fundamental/Harmonic Components of Load current and Comparison between Original/Calculated Load Currents using Notch Filter

Fig. 2.10 and Fig. 2.11 show the FFT analysis of original load current in phase-a and calculated load current in phase-a respectively, the total harmonic disorder in original load current is found to be 29.25% and in the calculated load current is 26.02%.

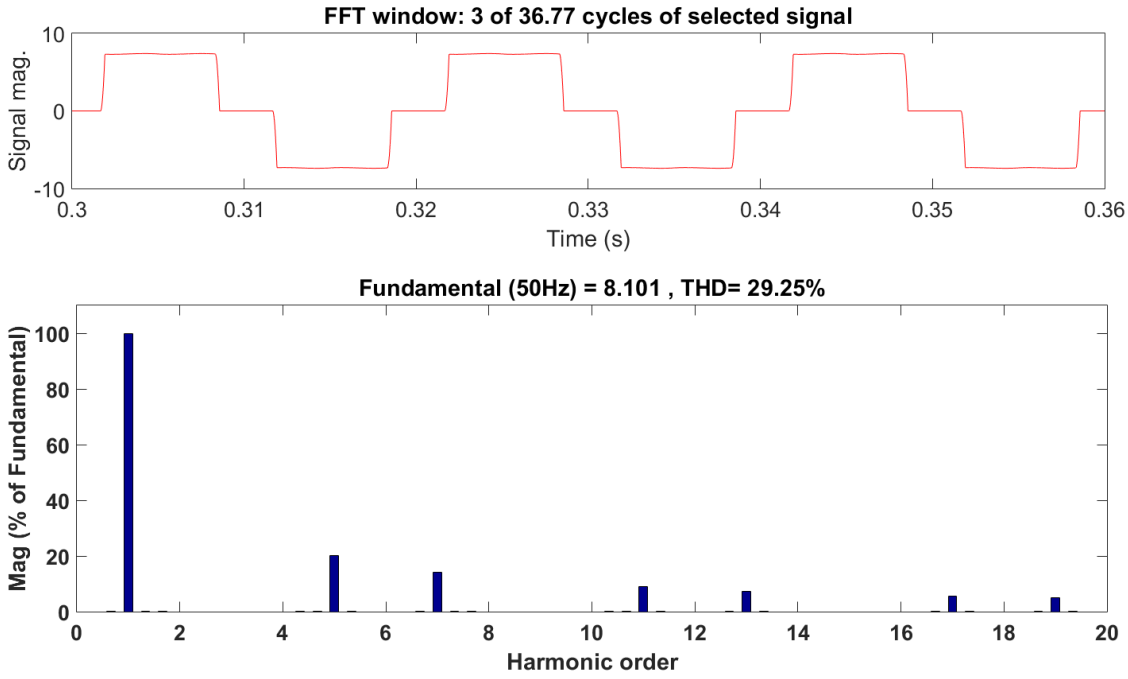

Fig. 2.10: FFT Analysis of Original Load Current using Notch Filter

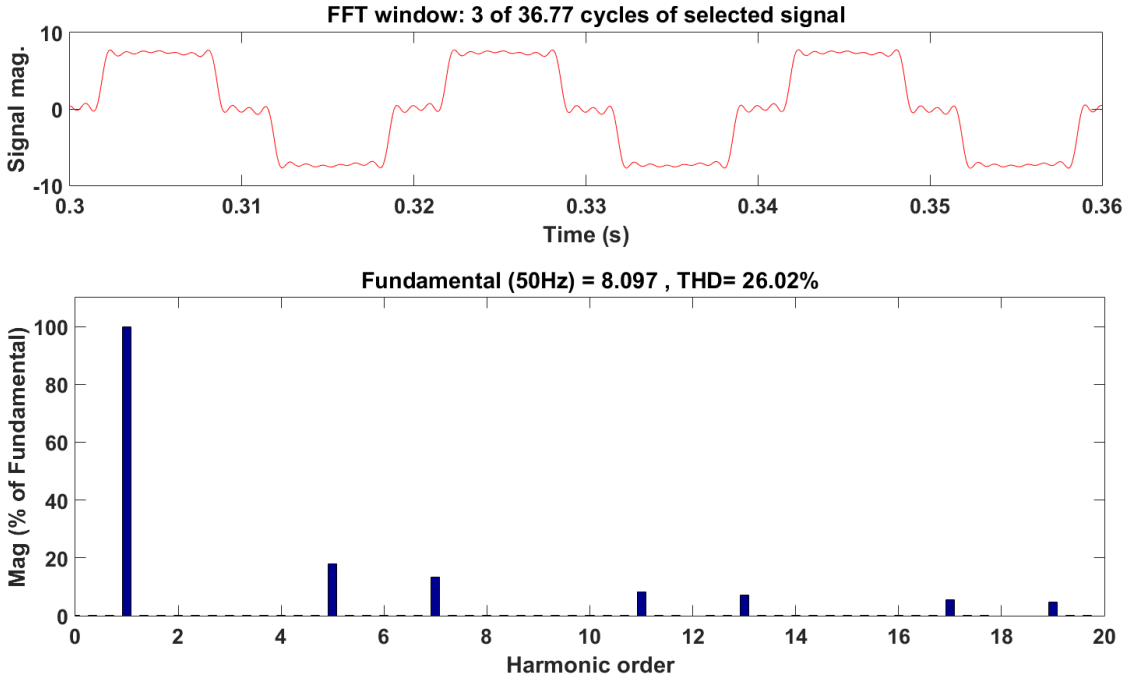

Fig. 2.11: FFT Analysis of Calculated Load Current using Notch Filter.

2.2.3 Harmonic Extraction using p-q Theory [9]

Another common approach for extraction of fundamental component and complete harmonics in the load currents is p-q theory. This scheme is not capable of extracting individual harmonic components and can work only. In a three phase system, in order to extract all the harmonics in load current, it needs to sense the load currents (i_{La}, i_{Lb}, i_{Lc}) and the phase voltages (v_{sa}, v_{sb}, v_{sc}) to measure the instantaneous active and reactive power of the system.

In this scheme, we extract the fundamental component of load current using p-q theory and subtract it from the load current in order to extract three phase harmonics from the load current.

Fig. 2.12 shows a block diagram for extracting three phase harmonic currents from load currents using p-q theory.

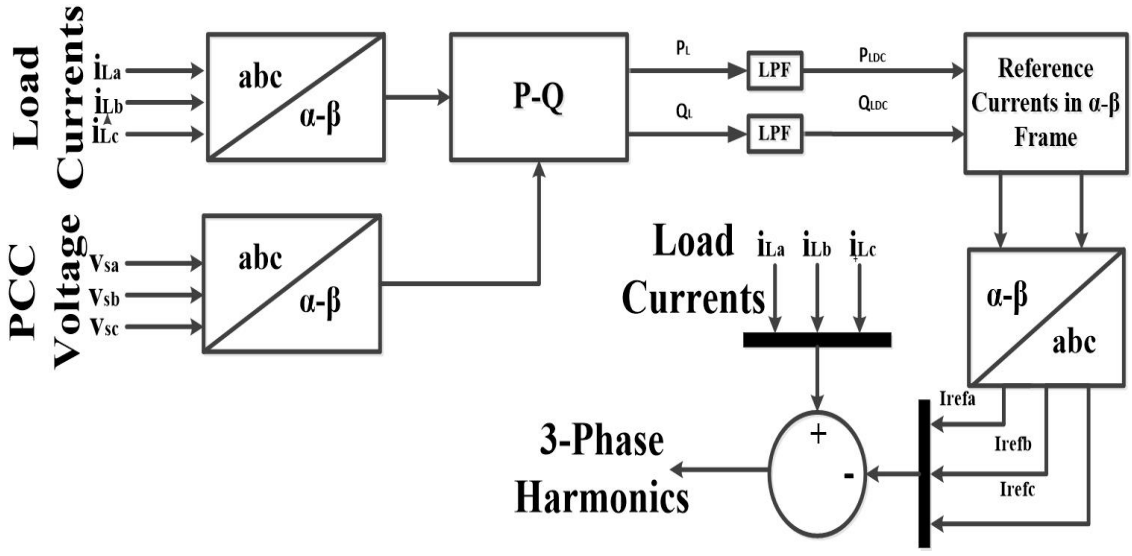

Fig. 2.12: Block Diagram of Extracting Harmonics using p-q Theory [2]

The p-q theory uses $\alpha\beta 0$ transformation, also known as the Clarke transformation to convert three phase voltages and currents in $\alpha\beta 0$ stationary reference frame. Eq. 2.7 and 2.8 discusses extraction of αβ components of voltage and currents respectively.

$$\begin{bmatrix} v_\alpha \\ v_\beta \end{bmatrix} = \sqrt{\frac{2}{3}} \begin{bmatrix} 1 & -\frac{1}{2} & -\frac{1}{2} \\ 0 & \frac{\sqrt{3}}{2} & -\frac{\sqrt{3}}{2} \end{bmatrix} \begin{bmatrix} v_{sa} \\ v_{sb} \\ v_{sc} \end{bmatrix} \tag{2.7}$$

$$\begin{bmatrix} i_\alpha \\ i_\beta \end{bmatrix} = \sqrt{\frac{2}{3}} \begin{bmatrix} 1 & -\frac{1}{2} & -\frac{1}{2} \\ 0 & \frac{\sqrt{3}}{2} & -\frac{\sqrt{3}}{2} \end{bmatrix} \begin{bmatrix} i_{La} \\ i_{Lb} \\ i_{Lc} \end{bmatrix} \tag{2.8}$$

Simulation diagram of $\alpha\beta 0$ transformation or the Clarke transformation is shown in Fig. 2.13.

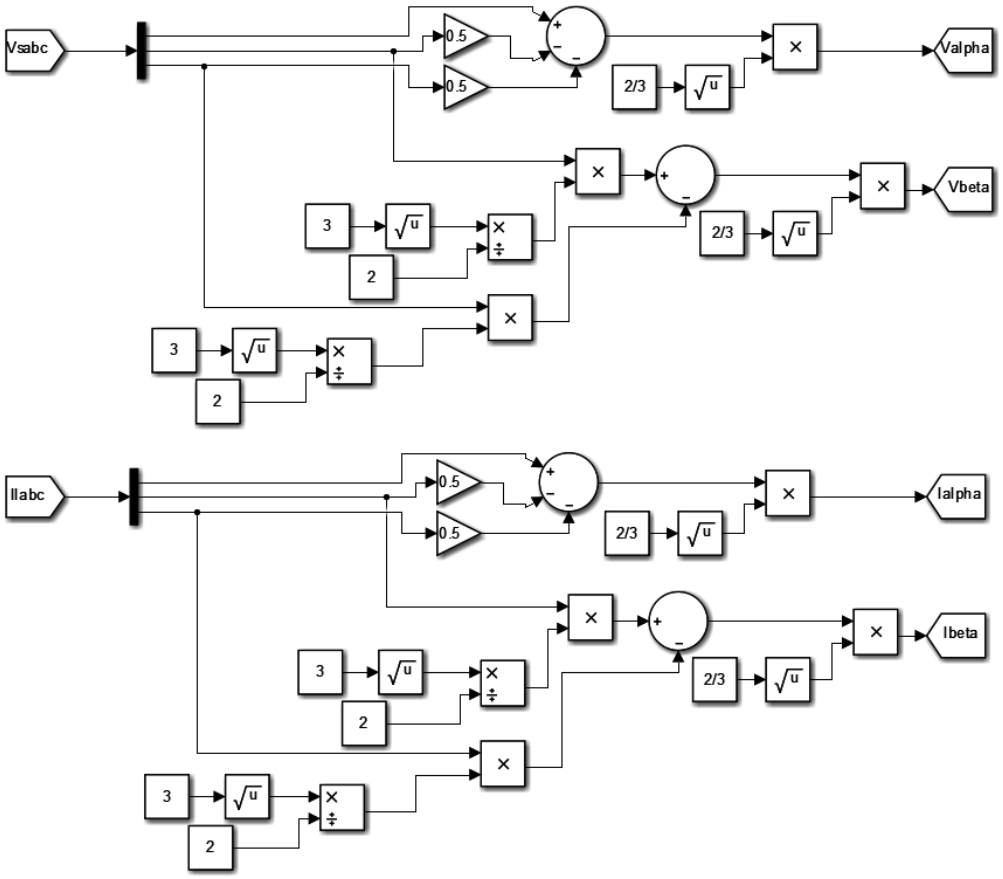

Fig. 2.13: Simulation Diagram of Clarke Transformation

The instantaneous active and reactive powers are calculated as:

$$\begin{bmatrix} P_L \\ Q_L \end{bmatrix} = \begin{bmatrix} V_\alpha & V_\beta \\ V_\beta & -V_\alpha \end{bmatrix} \begin{bmatrix} i_\alpha \\ i_\beta \end{bmatrix} \tag{2.9}$$

As these powers contain both the AC and DC components the AC component needs to be filtered out using a low pass filter.

$$\begin{bmatrix} P_L \\ Q_L \end{bmatrix} = \begin{bmatrix} \bar{P}_L + \tilde{P}_L \\ \bar{Q}_L + \tilde{Q}_L \end{bmatrix} \tag{2.10}$$

Here, $\bar{P}_L$ and $\bar{Q}_L$ are the DC components and $\tilde{P}_L$ and $\tilde{Q}_L$ are the AC components of the instantaneous active and reactive powers

The DC components are filtered using a low pass filter to obtain the DC components of instantaneous active and reactive powers also known as the fundamental of active and reactive powers.

These fundamental components of active and reactive powers are used to obtain the reference currents in α-β frame known as 'i_α^*' and 'i_β^*'. Fig. 2.14 shows the simulation diagram of calculation of fundamental components in α-β frame.

$$\begin{bmatrix} i_\alpha^* \\ i_\beta^* \end{bmatrix} = \frac{1}{v_\alpha^2 + v_\beta^2} \begin{bmatrix} v_\alpha & v_\beta \\ v_\beta & -v_\alpha \end{bmatrix} \begin{bmatrix} \bar{P}_L \\ \bar{Q}_L \end{bmatrix} \tag{2.11}$$

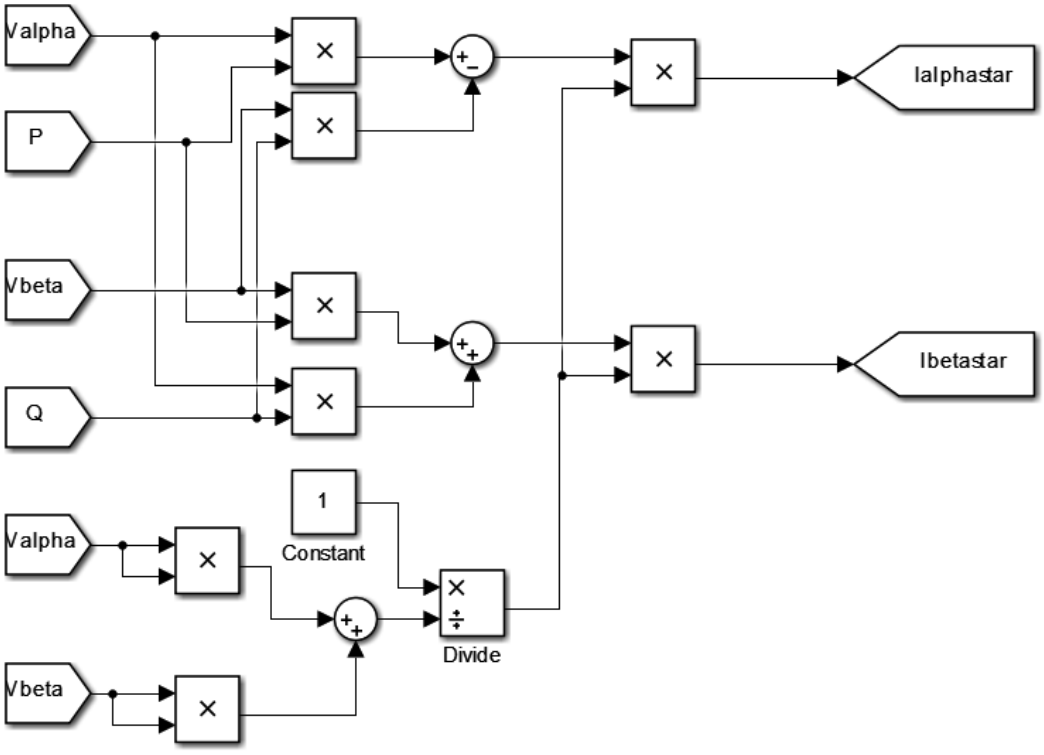

Fig. 2.14: Simulation Diagram of Calculation of Fundamental Component in α-β Frame.

The three-phase fundamental components of the load currents are estimated by inverse Clarke Transformation shown as:

$$\begin{bmatrix} i_{refa} \\ i_{refb} \\ i_{refc} \end{bmatrix} = \sqrt{\frac{2}{3}} \begin{bmatrix} 1 & 0 \\ -\frac{1}{2} & \frac{\sqrt{3}}{2} \\ -\frac{1}{2} & -\frac{\sqrt{3}}{2} \end{bmatrix} \begin{bmatrix} i_{\alpha}^{*} \\ i_{\beta}^{*} \end{bmatrix} \tag{3.24}$$

The Simulation diagram of estimation of three-phase fundamental components of the load currents by inverse Clarke transformation is shown in Fig. 2.15.

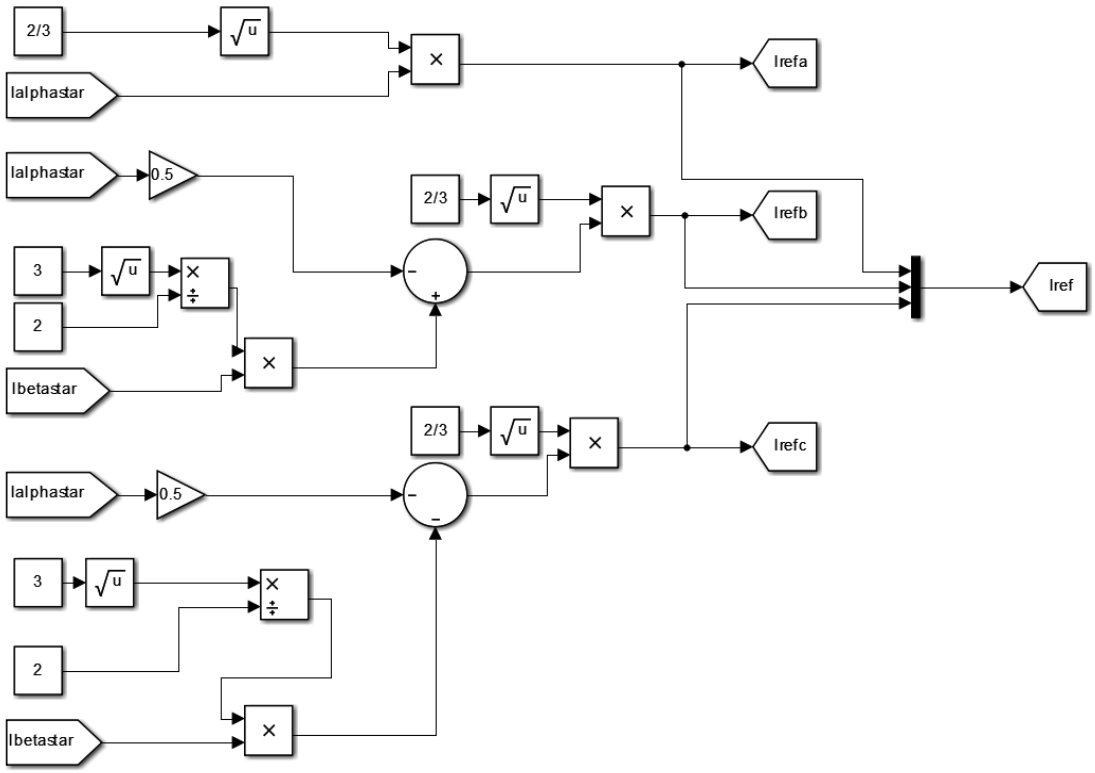

Fig. 2.15: Simulation Diagram of Estimation of Three- Phase Fundamental Components of the Load Currents by Inverse Clarke Transformation.

2.2.3.2 Results with p-q Theory.

Fig. 2.16 shows the three-phase load currents, its fundamental components and the extracted harmonic currents.

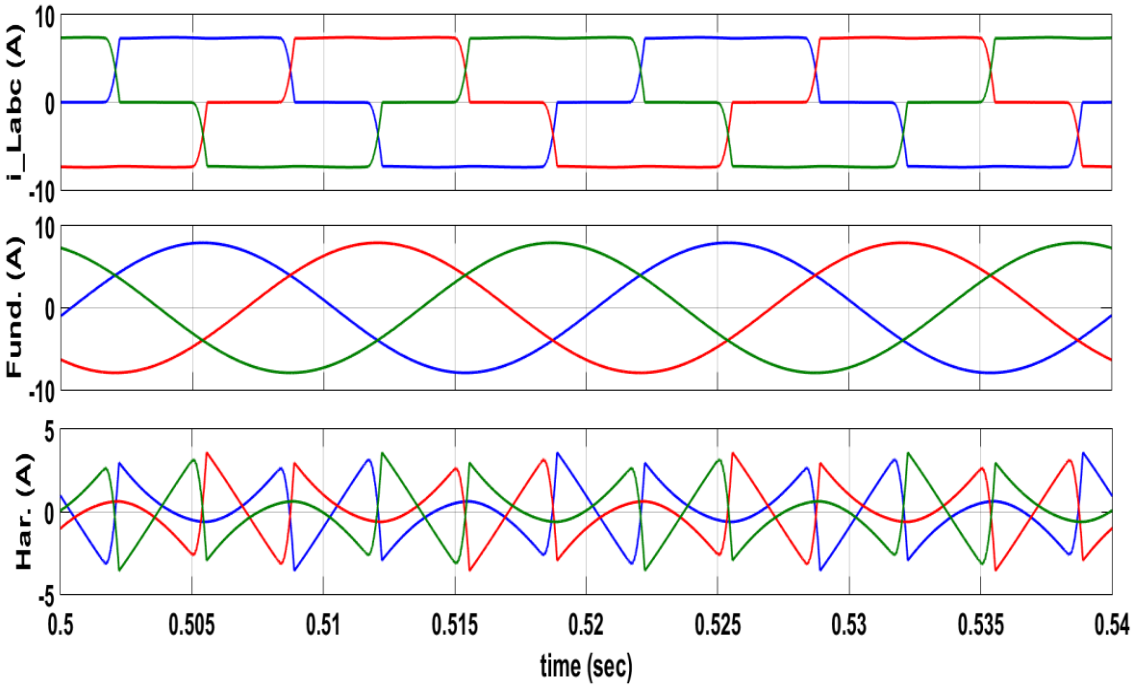

Fig.2.16: 3-Phase Load-Currents, Fundamental Components and Harmonics Current using p-q Theory.

Fig. 2.17 shows the FFT analysis of the load current, the total harmonic disorder found in load current phase-a is 29.25%

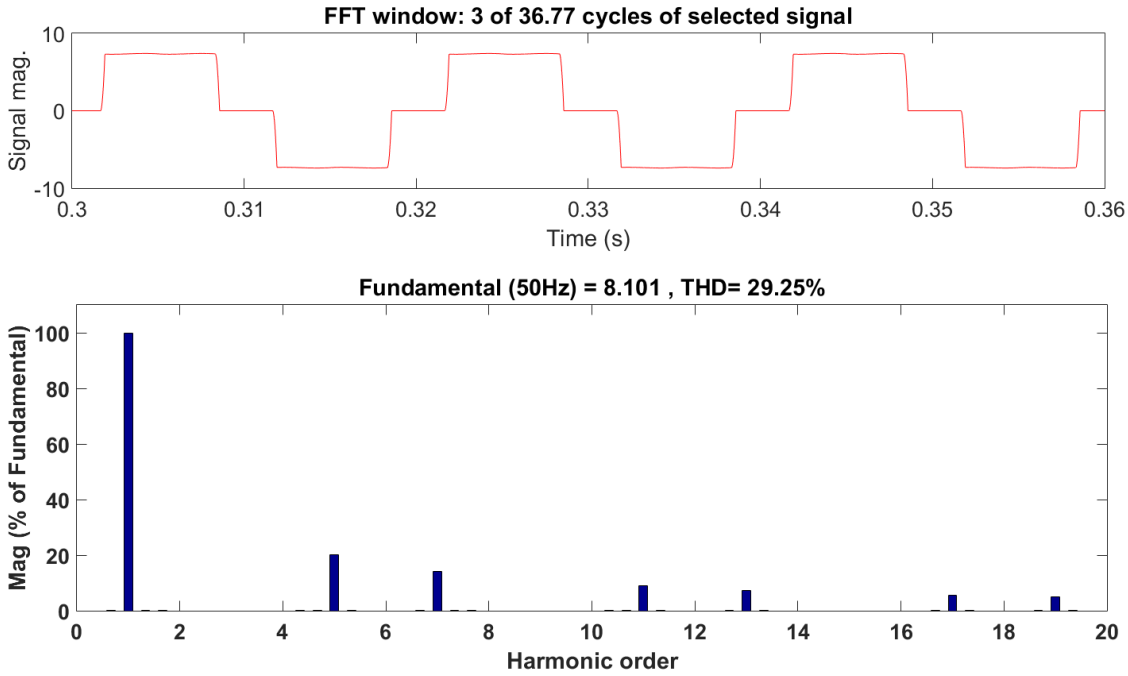

Fig. 2.17: FFT Analysis of Load Current using p-q Theory.

2.3 COMPAISION OF ALGORITHMS.

The comparison between all three algorithms for harmonics extraction studied in this chapter is shown in TABLE 2.1.

TABLE 2.1: COMPARISION OF PERFORMANCE OF d-q TRANSFORMATION, NOTCH FILTER AND p-q THEORY

	d-q Trans.	**Notch Filter**	**p-q Theory**
THD % in Original Load Current	29.25	29.25	29.25
THD % in Constructed Load Current	29.15	26.02	NA
Harmonic Extraction	Single-Phase/ Three-Phase	Single-Phase/ Three-Phase	Three-Phase only
Re-Construction of Load Current	yes	yes	no
Complexity of scheme	Easy	Easy	Easy

2.4 CONCLUSION

In this chapter three schemes viz d-q transformation, notch filter and p-q theory have been utilised to extract the harmonics from the load current. The load is modelled as a three phase diode rectifier feeding a r-L load having R=20Ω, L=100mH. The theory, equations and simulation models are well explained. A comparison is made in Table 2.1.

The table shows the performance of d-q transformation for extraction of harmonics and construction of load current from the fundamental and harmonics component is fairly accurate to the original load current of 29.25% THD.

The notch filter based method reconstructs the load current with a THD of 26.02%which is slightly different from the actual value of 29.25%. one of the reason could be that notch filter have been designed till 19^{th} order of harmonic. The p-q theory based approach can be designed to extract fundamental and separate remaining harmonic, although not individually.

CHAPTER-3

SOME ALGORITHMS FOR CONTROL OF DSTSTCOM

INTRODUCTION

Distribution Static Compensator (DSTATCOM) can be used to compensate the current based power quality disturbances like reactive power, neutral currents, fluctuations, harmonics and unbalanced currents. An IGBT based Current Controlled Voltage Source Converter (CC-VSC) with a DC bus capacitor is used as a DSTATCOM. In general, a DSTATCOM has a Voltage Source Converter (VSC) connected to a DC bus and AC side is connected across the consumer end of the distribution system in shunt. A control algorithm is used to generate reference currents that are compared to the supply currents in indirect current control of the VSC to generate gating pulses which are fed directly to the DSTATCOM. The gating pulses of the DSTATCOM can be generated by using PWM hysteresis current control [2]. Fig 3.1 shows a three-leg VSC-based three-phase-three-wire DSTATCOM.

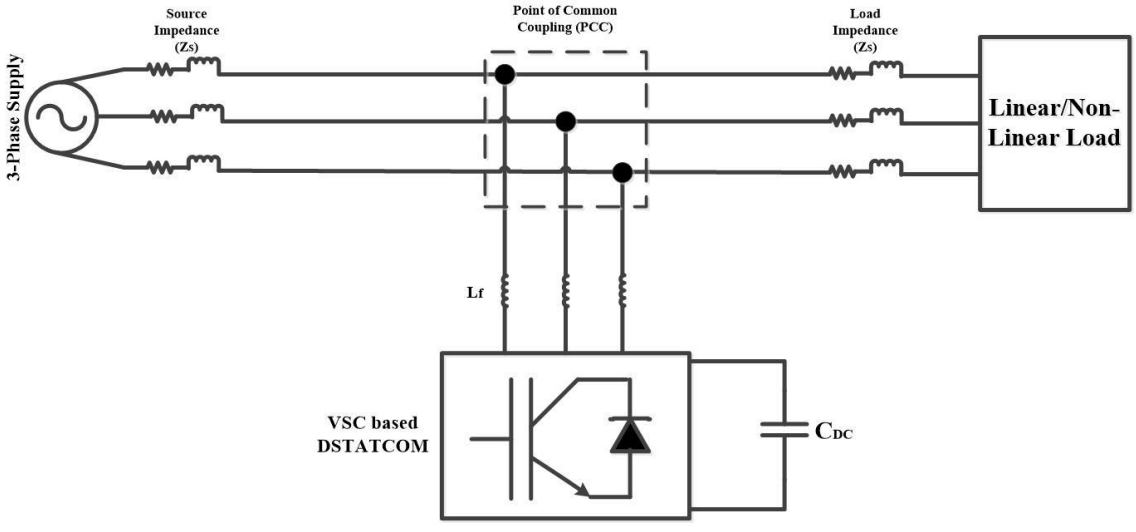

Fig. 3.1: Three-Leg VSC based Three-Phase-Three Wire DSTATCOM

The DSTATCOM also requires many passive elements like a DC bus capacitor, AC interacting inductors, isolation and injection transformers and small power filters.

The generation of reference currents for controlling the DSTATCOM can be estimated by many control algorithms [2]. These control algorithms can be classified as follows:

TABLE 3.1: CLASSIFICATION OF CONTROL ALGORITHMS [2].

TIME DOMAIN	**FREQUENCY DOMAIN**
• Unit Templates/PI Controller based theory	• Fourier Series Theory
• Power Balance Theory	• Discrete Fourier Transform Theory
• I cosϕ control algorithm	• Fast Fourier Transform Theory
• Instantaneous Reactive Power Theory	• Recursive Discrete Fourier Transform Theory
• Synchronous Reference Frame Theory	• Kalman Filter based control algorithm
• Instantaneous Symmetrical Component Theory	• Wavelet Transform Theory
• Neural Network Theory	• Stockwell Transformation Theory
• Enhanced Phase Locked Loop (EPLL) based control Algorithm	• Empirical Decomposition (EMD) Transformation Theory
• Conductance based control algorithm	• Hilbert-Huang Transformation Theory
• Adaptive Detecting control algorithm	

Generation of reference current signals for generating gating pulses for the DSTATCOM is performed by the following control algorithms in this chapter:

1. Synchronous Reference Frame (SRF) Theory
2. Instantaneous Reactive Power (IRP) Theory or p-q Theory
3. Modified Instantaneous Symmetrical Component Theory
4. Notch Filter

3.2 CONTROL ALGORITHMS

The first algorithm discussed for harmonic mitigation and other pq improvement features is SRFT.

3.2.1 Synchronous Reference Frame (SRF) Theory

A block diagram of this control algorithm is shown in Fig. 3.2.

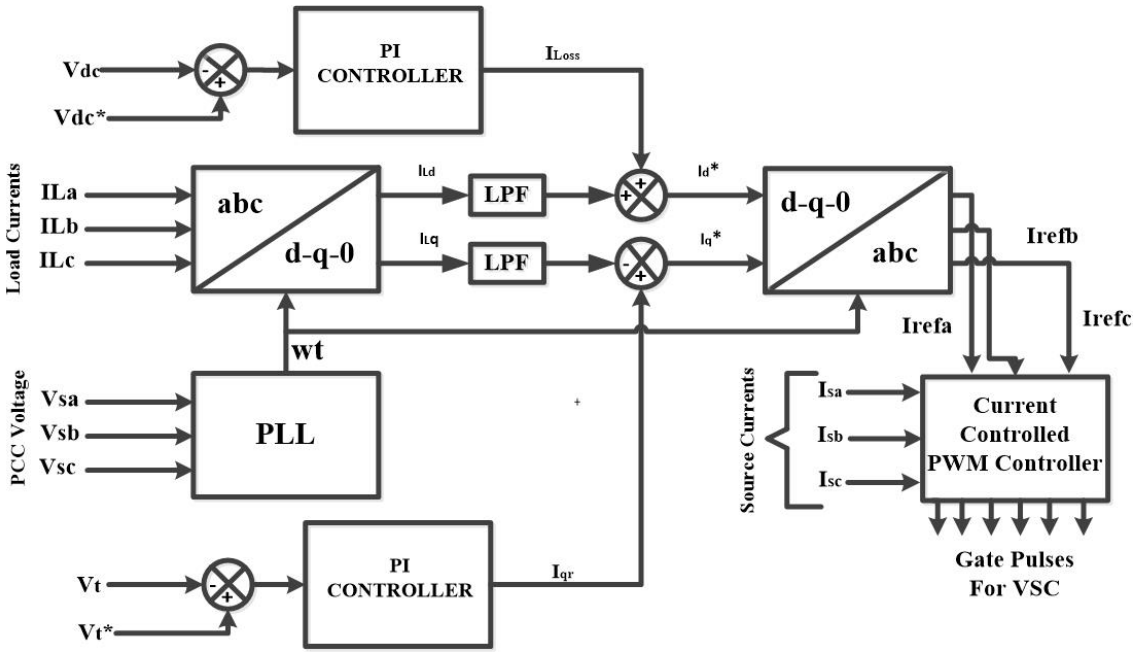

Fig. 3.2: Block Diagram of synchronous Reference Frame (SRF) Theory

3.2.1.1 Control Algorithm [6]

The load currents (i_{La}, i_{Lb}, i_{Lc}), point of common coupling (PCC) voltages (v_{sa}, v_{sb}, v_{sc}) and the DC bus voltage (V_{dc}) in the distribution system are sensed for generating the reference current signals.

The three-phase load currents (i_{La}, i_{Lb}, i_{Lc}) are converted into d-q frame using Park's Transform as follows:

$$\begin{bmatrix} i_{Ld} \\ i_{Lq} \end{bmatrix} = \frac{2}{3}\begin{bmatrix} cos\,\theta & -sin\,\theta \\ cos\left(\theta - \frac{2\pi}{3}\right) & -sin\left(\theta - \frac{2\pi}{3}\right) \\ cos\left(\theta + \frac{2\pi}{3}\right) & sin\left(\theta + \frac{2\pi}{3}\right) \end{bmatrix}\begin{bmatrix} i_{La} \\ i_{Lb} \\ i_{Lc} \end{bmatrix} \quad (3.1)$$

A Phase Locked Loop (PLL) is used to synchronize these signals with the PCC voltages.

The currents thus obtained from the Park's Transformation i.e. ($i_{Ld}\ and\ i_{Lq}$) are passed through a Low Pass Filter (LPF) to obtain the DC components of 'i_{Ld}' and 'i_{Lq}'. The d-q components of the load currents contain both fundamental and harmonic components as shown:

$$i_{Ld} = i_{dDC} + i_{dAC} \quad (3.2)$$

$$i_{Lq} = i_{qDC} + i_{qAC} \quad (3.3)$$

In Power Factor Correction (PFC) mode the control algorithm is developed in such a manner that the source must supply the active power component and switching losses to maintain the DC bus voltage.

The error between the reference DC bus voltage 'V_{dc}^{*}' and the sensed DC bus voltage 'V_{dc}' is given to a PI controller and the output thus obtained is the current 'i_{Loss}'.

$$V_{DC}(n) = V_{dc}^{*}(n) - V_{dc}(n) \quad (3.4)$$

$$i_{Loss}(n) = i_{Loss}(n-1) + K_{pd}\{V_{DC}(n) - V_{DC}(n-1)\} + K_{pi}V_{DC}(n) \quad (3.5)$$

Here,

n is the n^{th} sampling instant, K_{pd} and K_{id} are the proportional and integral gain of the PI controller respectively.

This current 'i_{Loss}' thus obtained is added to the DC component of direct-axis current i_{dDC} to obtain the reference direct-axis supply current.

$$i_{d}^{*} = i_{dDC} + i_{Loss} \quad (3.6)$$

In the Zero Voltage Regulation (ZVR) mode it is considered that the source must supply both the supply the active power component and switching losses to maintain the DC bus voltage and also the difference of quadrature-axis current 'i_{qDC}' of the load and the component obtained from the PI voltage controller 'i_{qr}' used for regulating the voltage at PCC.

A second PI controller is used to maintain the amplitude of PCC Voltage 'V_t'. The error between reference voltage 'V_t^*' and PCC voltage 'V_t' is considered as reactive power component of current 'i_{qr}'. The amplitude of PCC Voltage 'V_t' is calculated as:

$$V_t = \sqrt{\frac{2}{3}(V_{sa}^2 + V_{sb}^2 + V_{sc}^2)} \tag{3.7}$$

$$V_{te}(n) = V_t^*(n) - V_t(n) \tag{3.8}$$

$$i_{qr}(n) = i_{qr}(n-1) + K_{pd}\{V_{te}(n) - V_{te}(n-1)\} + K_{pi}V_{te}(n). \tag{3.9}$$

Here,

'n' is the nth sampling instant, K_{pd} and K_{id} are the proportional and integral gain of the PI controller respectively.

The reference quadrature axis supply current is given as:

$$i_q^* = i_{qr} - i_{qDC} \tag{3.10}$$

The reference currents are obtained by reverse Park's Transformation shown as:

$$\begin{bmatrix} i_{refa} \\ i_{refb} \\ i_{refc} \end{bmatrix} = \begin{bmatrix} cos\,\theta & sin\,\theta \\ cos\left(\theta - \frac{2\pi}{3}\right) & sin\left(\theta - \frac{2\pi}{3}\right) \\ cos\left(\theta + \frac{2\pi}{3}\right) & sin\left(\theta + \frac{2\pi}{3}\right) \end{bmatrix} \begin{bmatrix} i_d^* \\ i_q^* \end{bmatrix} \tag{3.11}$$

Fig. 3.3 shows the simulation diagram of Synchronous Reference Frame (SRF) Theory.

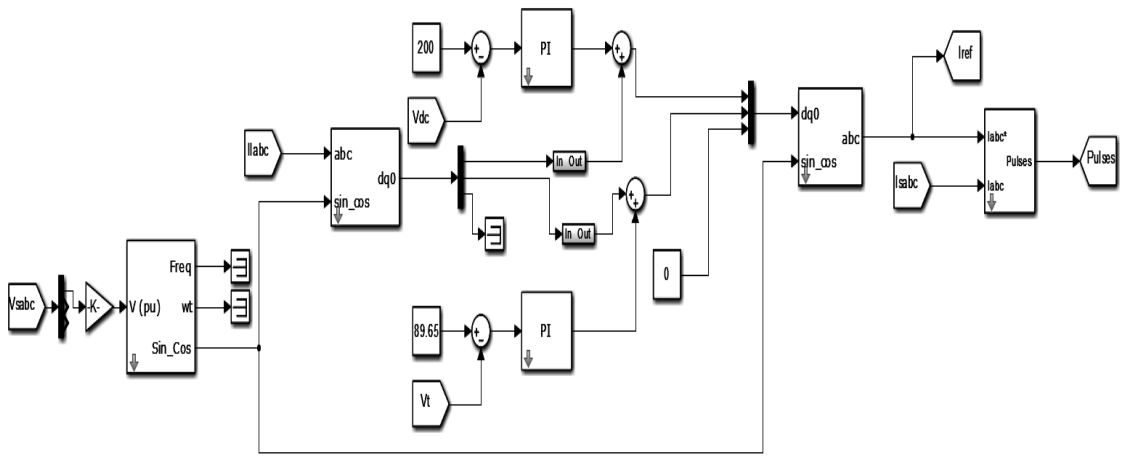

Fig. 3.3: Simulation Diagram of Synchronous Reference Frame (SRF) Theory in PFC mode

3.2.1.2 Results with SRF Theory

The performance of DSTATCOM controlled by SRFT in UPF and ZVR mode are shown.

3.2.1.2.1 Power Factor Correction (PFC) mode

The performance of VSC based DSTATCOM controlled by SRF theory in PFC mode is observed in Fig. 3.5 and the results of the intermediate in the control algorithm are also shown in Fig. 3.4. The intermediate signals plotted i_{dqo}, $i_{d(DC)}$, i_{Loss} and reference currents i_{ref}. In Fig.3.5, it is observed that the PCC voltage is sinusoidal, the phase 'a' of three phase non-linear load is disconnected at time t=0.3 sec. as we can see the dc link voltage V_{dc} rises momentarily and slowly starts to settle down at 200V. The supply currents are sinusoidal and reduced when phase-a of load gets disconnected.

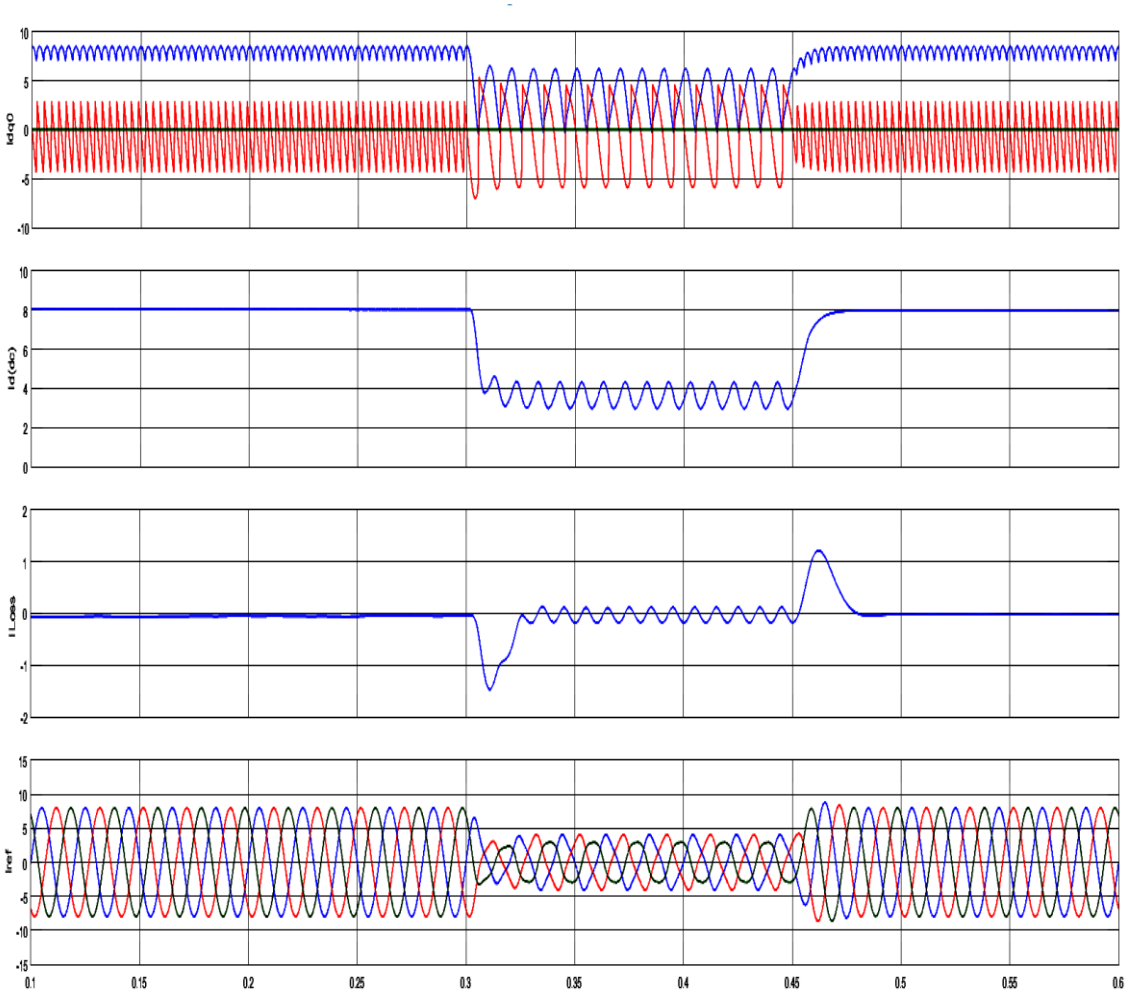

Fig. 3.4: Intermediate Results in PFC mode

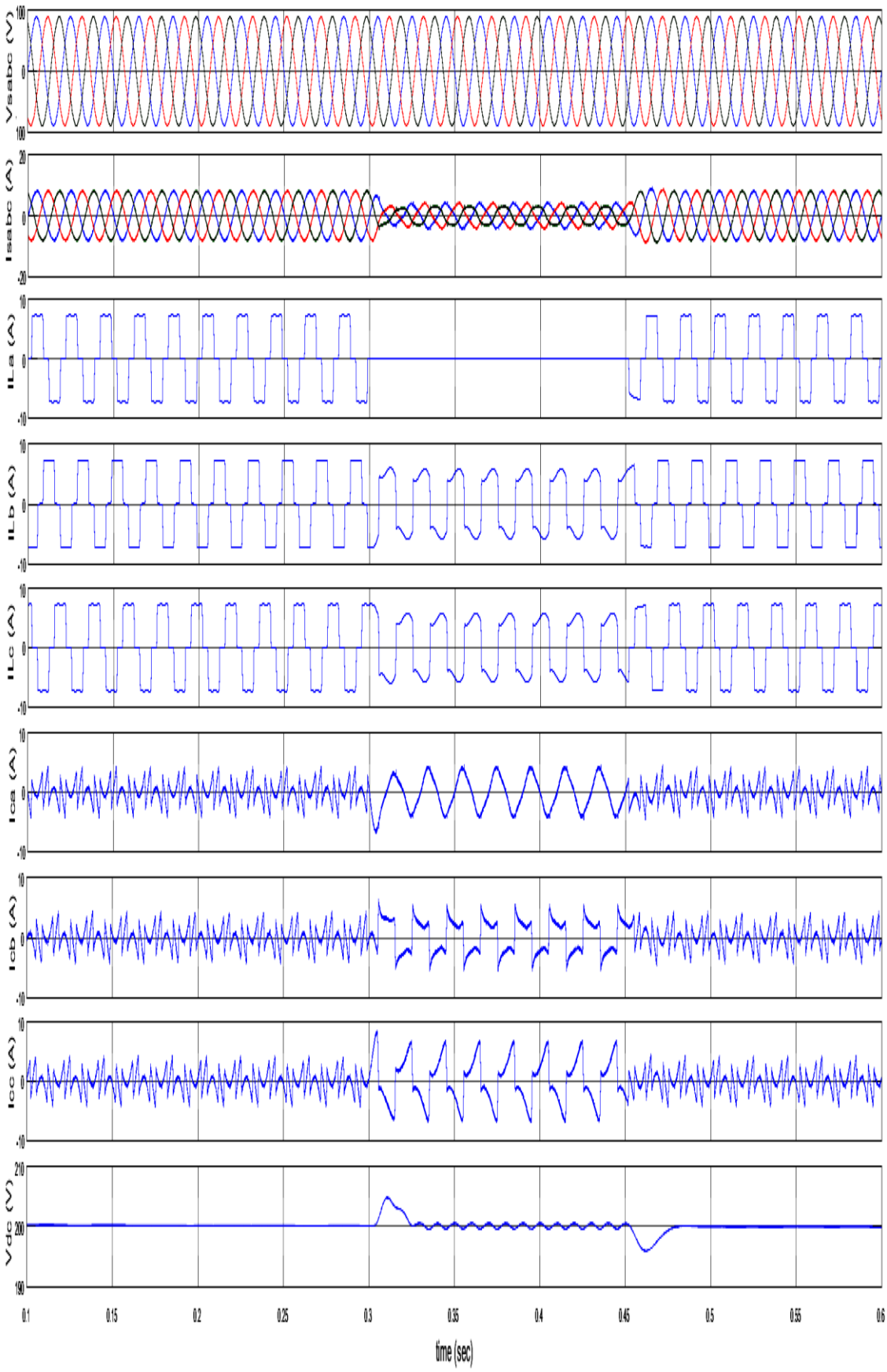

Fig. 3.5: Performance of DSTATCOM Controlled using SRF Theory in PFC mode

The FFT Analysis of PCC Voltage, Load Current, Source Current obtained by SRF theory in PFC mode in distribution system is shown below. The Total Harmonic Disorder (THD) in %age of the load current, PCC Voltage and Source currents are observed to be 27.26%, PCC voltage 0.01% and the source current 2.20%.

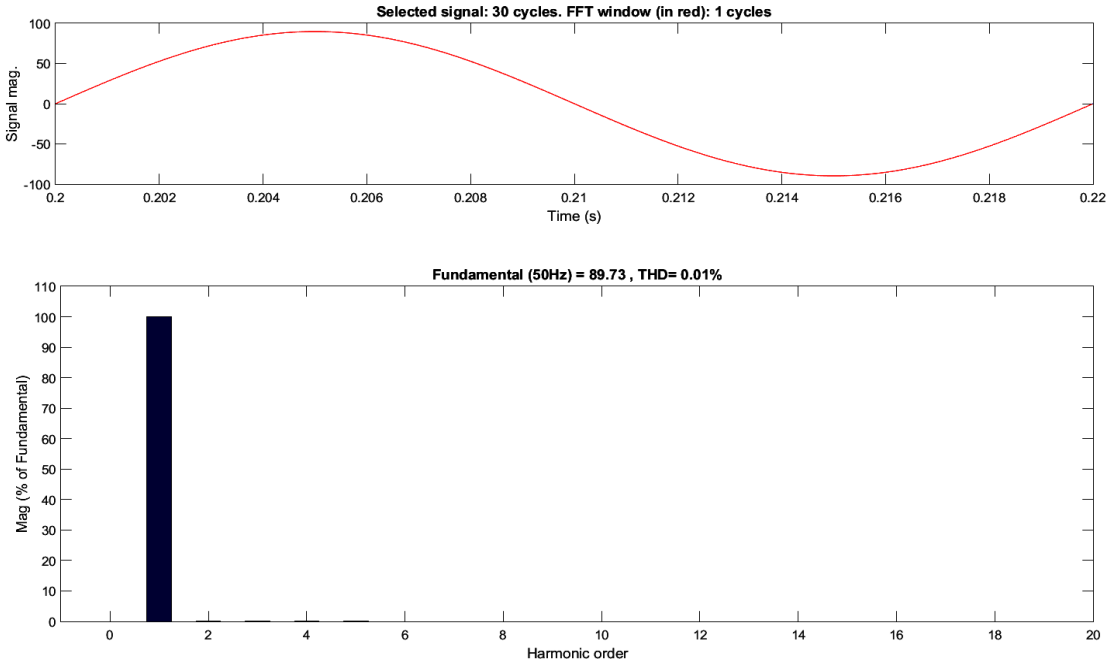

Fig. 3.6: FFT Analysis of PCC Voltage in PFC mode using SRFT

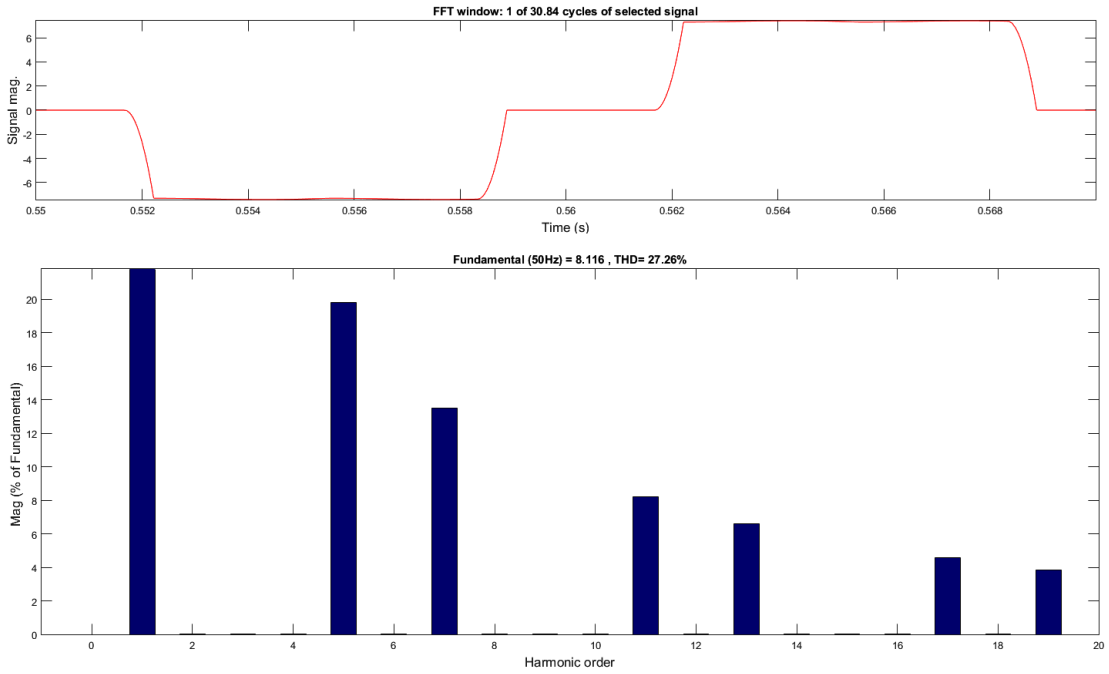

Fig. 3.7: FFT Analysis of Load Current in PFC mode using SRFT

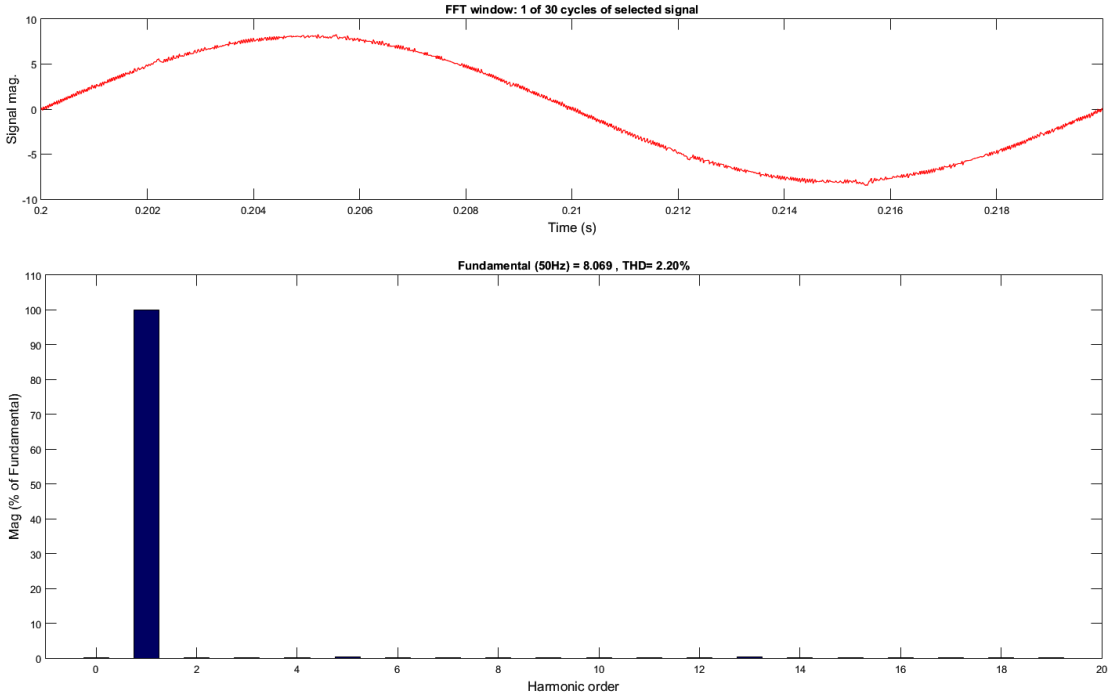

Fig.3.8: FFT Analysis of Source Current in PFC mode using SRFT

3.2.1.2.2 Zero Voltage Regulation (ZVR) mode

The performance of VSC based DSTATCOM controlled by SRF theory in ZVR mode is observed in Fig. 3.10 and the results of the intermediate in the control algorithm are also shown in Fig. 3.9. The intermediate signals plotted i_{dqo}, $i_{d(DC)}$, i_{Loss} , i_{qloss} and i_{qr} and reference currents i_{ref}. In Fig.3.10, it is observed that the PCC voltage is sinusoidal, the phase 'a' of three phase non-linear load is disconnected at time t=0.3 sec. as we can see the dc link voltage V_{dc} rises momentarily and slowly starts to settle down at 200V. the supply currents are sinusoidal and reduced when phase-a of load gets disconnected.

Also in this mode the magnitude of PCC Voltage i.e. V_t is also regulated, at time t=0.3 sec the magnitude of V_t rises momentarily but slowly settles down to 89.8V.

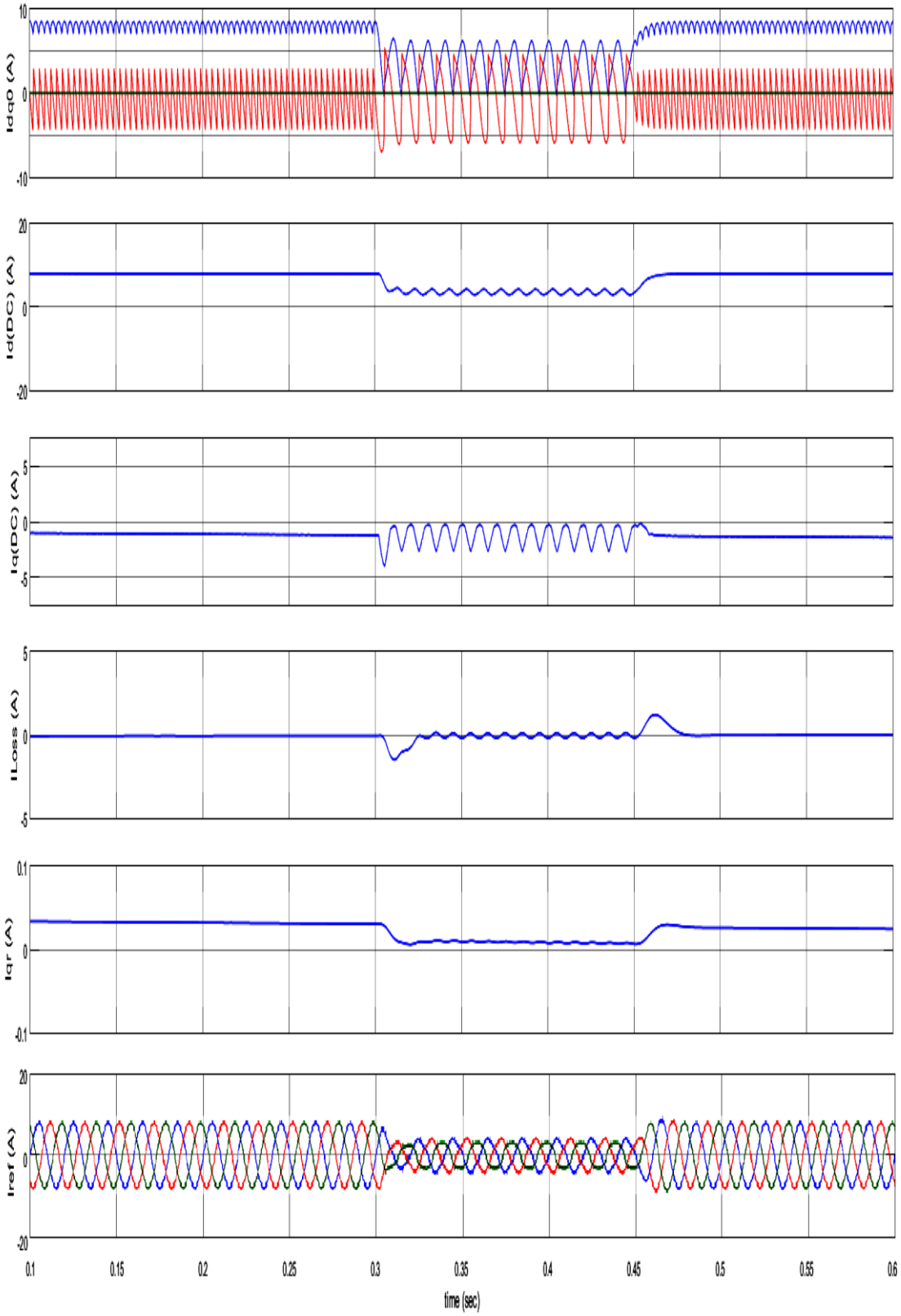

Fig: 3.9 Intermediate Results in ZVR mode using SRFT

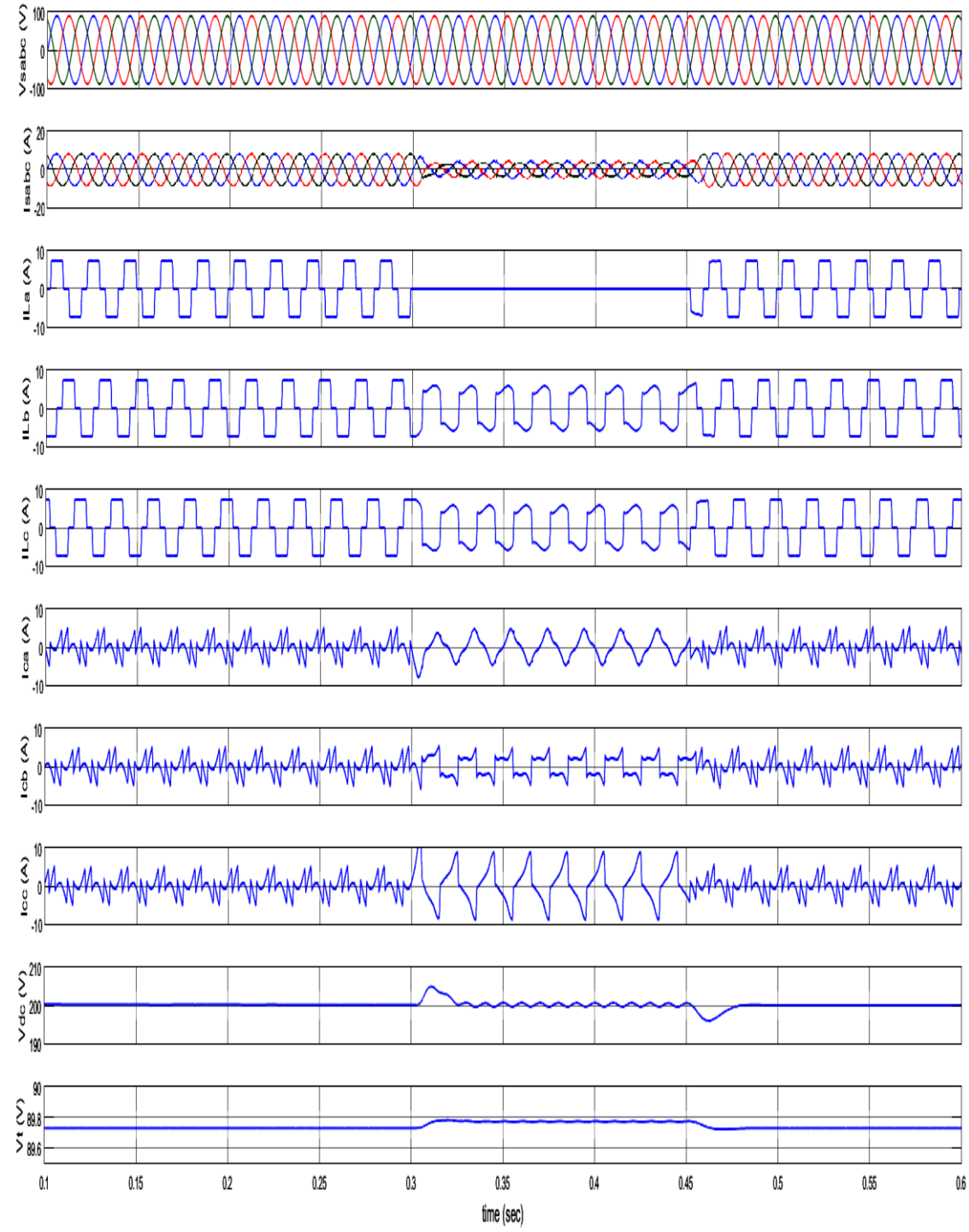

Fig. 3.10: Performance of DSTATCOM Controlled using SRF Theory in ZVR mode

The Total Harmonic Disorder (THD) in %age of the Source currents in ZVR mode is observed to be 2.04% as shown in Fig. 3.11.

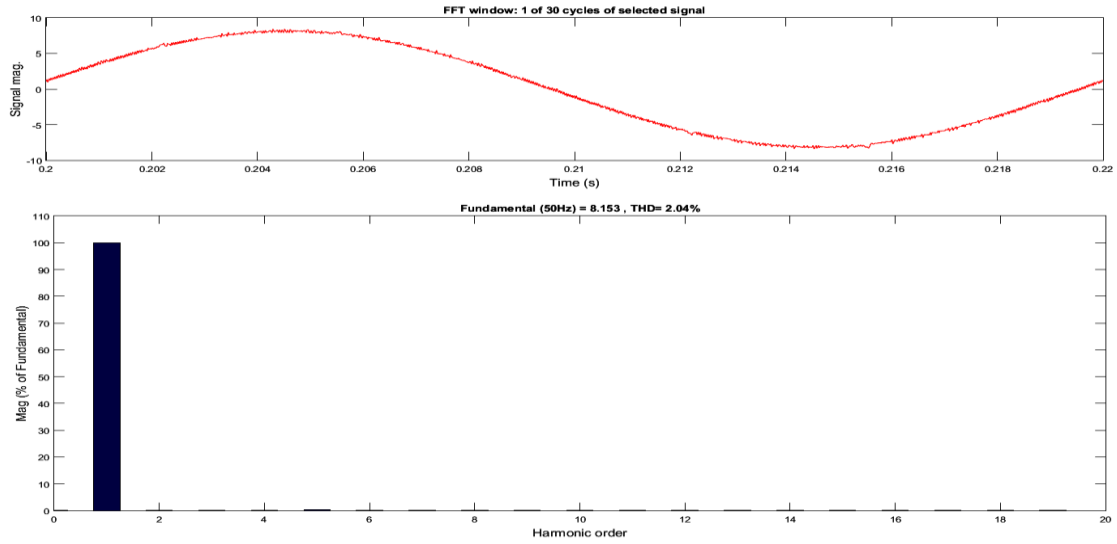

Fig.3.11: FFT Analysis of Source Current in ZVR mode using SRFT

3.2.2 Instantaneous Reactive Power (IRP) Theory

The Instantaneous Reactive Power (IRP) Theory or the p-q Theory is based on a set of instantaneous powers defined in the time-domain [3]. Three phase load currents (i_{La}, i_{Lb}, i_{Lc}), Point of Common Coupling (PCC) Voltages (v_{sa}, v_{sb}, v_{sc}) and the DC bus voltage (V_{dc}) in the distribution system are sensed for generating the reference current signals. A block diagram showing the structure of Instantaneous Reactive Power (IRP) Theory is shown in Fig. 3.12.

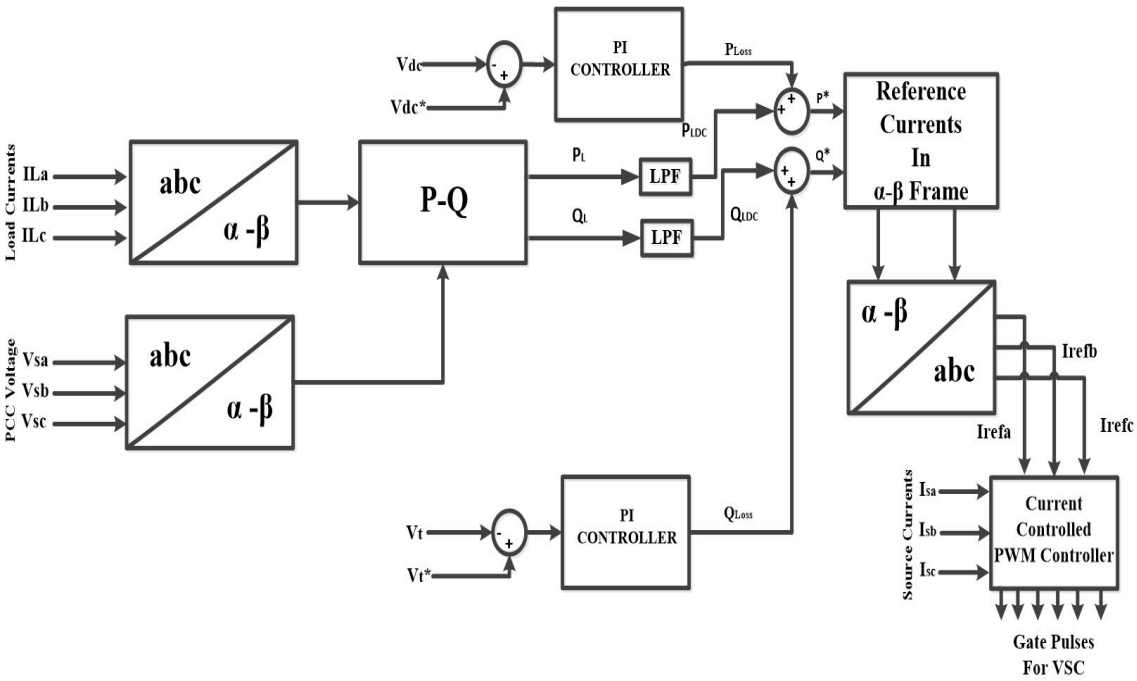

Fig. 3.12: Block Diagram of Instantaneous Reactive Power (IRP) Theory

3.2.2.1 Control Algorithm [13]

The p-q theory uses $\alpha\beta 0$ transformation, also known as the Clarke transformation to convert three phase voltages and currents in $\alpha\beta 0$ stationary reference frame

$$\begin{bmatrix} v_\alpha \\ v_\beta \end{bmatrix} = \sqrt{\frac{2}{3}} \begin{bmatrix} 1 & -\frac{1}{2} & -\frac{1}{2} \\ 0 & \frac{\sqrt{3}}{2} & -\frac{\sqrt{3}}{2} \end{bmatrix} \begin{bmatrix} v_{sa} \\ v_{sb} \\ v_{sc} \end{bmatrix} \tag{3.12}$$

$$\begin{bmatrix} i_\alpha \\ i_\beta \end{bmatrix} = \sqrt{\frac{2}{3}} \begin{bmatrix} 1 & -\frac{1}{2} & -\frac{1}{2} \\ 0 & \frac{\sqrt{3}}{2} & -\frac{\sqrt{3}}{2} \end{bmatrix} \begin{bmatrix} i_{La} \\ i_{Lb} \\ i_{Lc} \end{bmatrix} \tag{3.13}$$

Simulation diagram of $\alpha\beta 0$ transformation or the Clarke transformation is shown in Fig. 3.13.

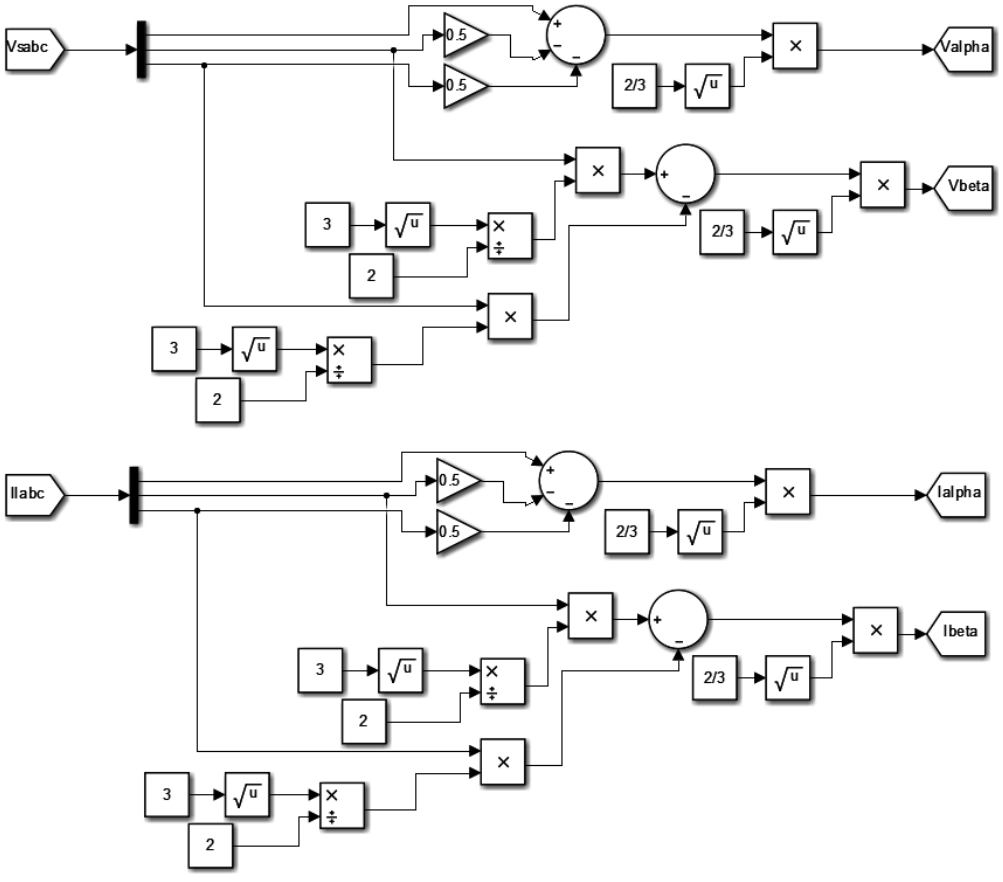

Fig. 3.13: Simulation Diagram showing Clarke Transformation

The instantaneous active and reactive powers are calculated as:

$$\begin{bmatrix} P_L \\ Q_L \end{bmatrix} = \begin{bmatrix} V_\alpha & V_\beta \\ V_\beta & -V_\alpha \end{bmatrix} \begin{bmatrix} i_\alpha \\ i_\beta \end{bmatrix} \tag{3.14}$$

As these powers contain both the AC and DC components the AC component needs to be filtered out using a low pass filter.

$$\begin{bmatrix} P_L \\ Q_L \end{bmatrix} = \begin{bmatrix} \bar{P}_L + \tilde{P}_L \\ \bar{Q}_L + \tilde{Q}_L \end{bmatrix} \tag{3.15}$$

Here, $\bar{P}_L$ and $\bar{Q}_L$ are the DC components and $\tilde{P}_L$ and $\tilde{Q}_L$ are the AC components of the instantaneous active and reactive powers. Two PI controllers are used to regulate the DC bus voltage 'V_{dc}' and PCC Voltage 'V_t' respectively.

The error in DC bus Voltage at nth sampling instant between the reference DC bus voltage 'V_{dc}^*' and the sensed DC bus voltage 'V_{dc}' is given as:

$$V_{DC}(n) = V_{dc}^*(n) - V_{dc}(n) \tag{3.16}$$

The output of the DC PI controller is known as the active power component loss 'P_{Loss}'

$$P_{Loss}(n) = P_{Loss}(n-1) + K_{pd}\{V_{DC}(n) - V_{DC}(n-1)\} + K_{pi}V_{DC}(n) \tag{3.17}$$

Here, K_{pd} and K_{id} are the proportional and integral gain of the PI controller respectively. P_{Loss} is added to the DC component of active power '$\bar{P}_L$' to acquire the fundamental component of active power given by 'P'.

$$P = \bar{P}_L + P_{Loss} \tag{3.18}$$

The error in PCC voltage at nth sampling instant between the amplitude of the reference PCC voltage 'V_t^*' and the amplitude of sensed PCC voltage 'V_t' is given as:

$$V_{te}(n) = V_t^*(n) - V_t(n) \tag{3.19}$$

$$V_t = \sqrt{\frac{2}{3}(V_{sa}^2 + V_{sb}^2 + V_{sc}^2)} \tag{3.20}$$

The output of the second PI controller is used to maintain constant PCC voltage at n[th] sampling instant and is given by 'Q_{Loss}'.

$$Q_{Loss}(n) = Q_{Loss}(n-1) + K_{pd}\{V_{te}(n) - V_{te}(n-1)\} + K_{pi}V_{te}(n) \tag{3.21}$$

Here, K_{pd} and K_{id} are the proportional and integral gain of the PI controller respectively. Q_{Loss} is added to the DC component of active power '$\bar{Q}_L$' to acquire the fundamental component of active power given by 'Q'.

$$Q = \bar{Q}_L + Q_{Loss} \tag{3.22}$$

Simulation diagram of calculation of fundamental component of instantaneous active and reactive powers is shown in Fig. 3.14.

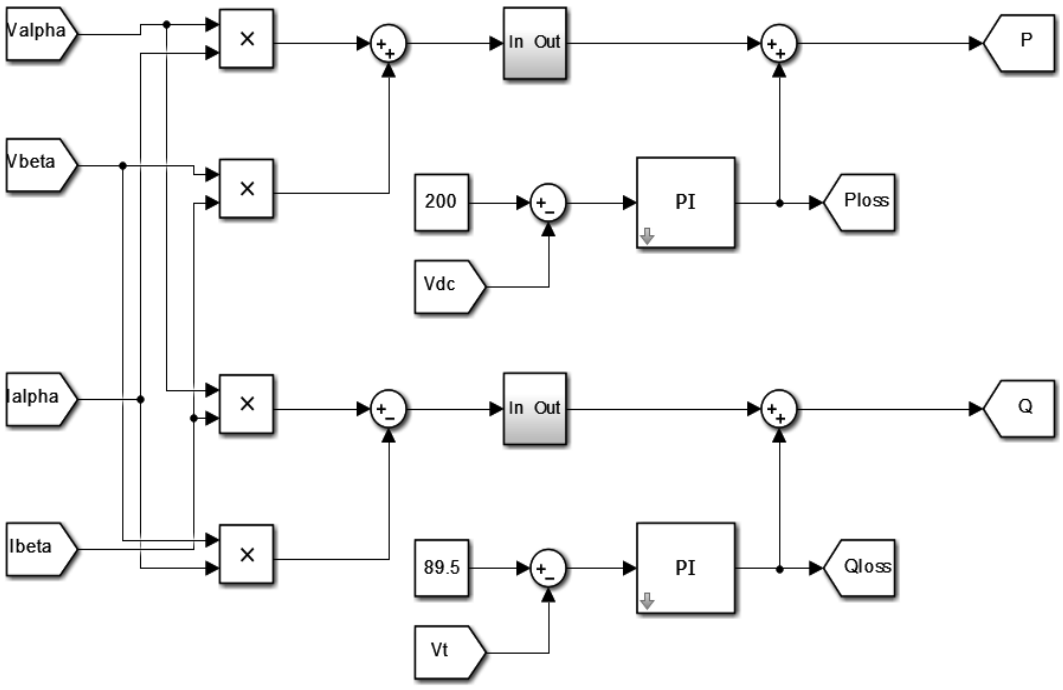

Fig.3.14: Simulation Diagram for Calculation of Fundamental Component of Instantaneous Active and Reactive Powers

These fundamental components of active and reactive powers are used to obtain the reference currents in α-β frame known as 'I_{α}^{*}' and 'I_{β}^{*}'.

$$\begin{bmatrix} i_{\alpha}^{*} \\ i_{\beta}^{*} \end{bmatrix} = \frac{1}{V_{\alpha}^{2}+V_{\beta}^{2}} \begin{bmatrix} v_{\alpha} & v_{\beta} \\ v_{\beta} & -v_{\alpha} \end{bmatrix} \begin{bmatrix} P \\ Q \end{bmatrix} \tag{3.23}$$

Fig. 3.15 shows the simulation diagram of calculation of reference currents in α-β frame.

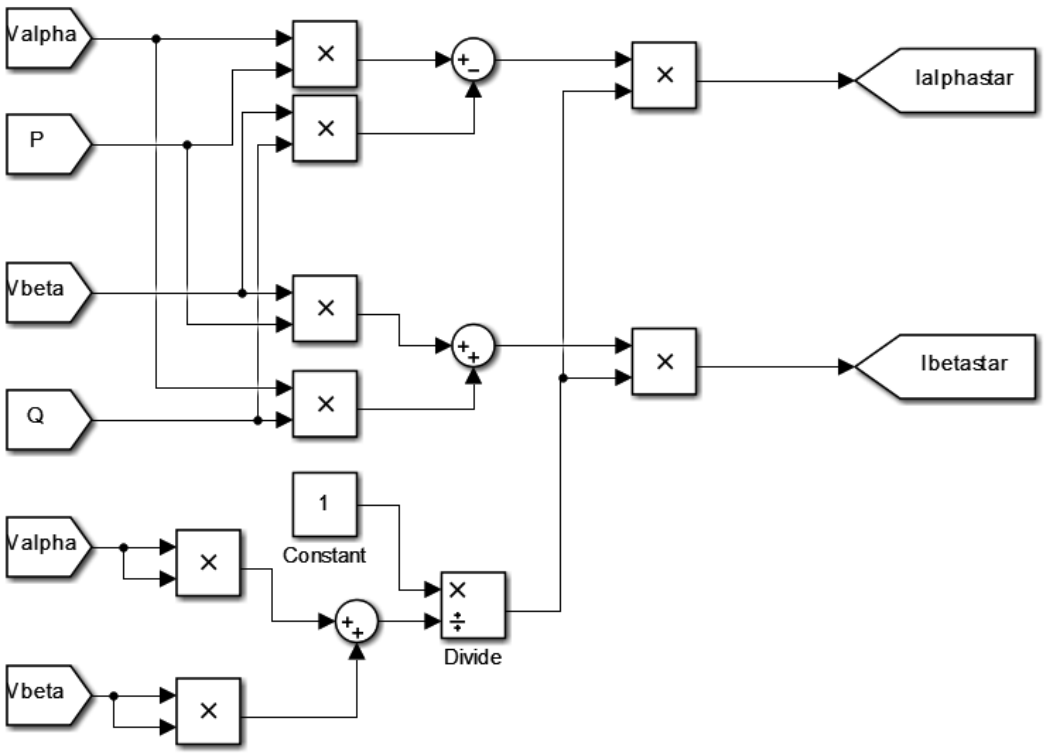

Fig. 3.15: Simulation Diagram of Calculation of Reference Currents in α-β Frame

The reference three-phase supply currents are estimated by inverse Clarke Transformation shown as:

$$\begin{bmatrix} i_{refa} \\ i_{refb} \\ i_{refc} \end{bmatrix} = \sqrt{\frac{2}{3}} \begin{bmatrix} 1 & 0 \\ -\frac{1}{2} & \frac{\sqrt{3}}{2} \\ -\frac{1}{2} & -\frac{\sqrt{3}}{2} \end{bmatrix} \begin{bmatrix} i_{\alpha}^{*} \\ i_{\beta}^{*} \end{bmatrix} \tag{3.24}$$

The Simulation diagram of estimation of reference three-phase supply currents by inverse Clarke transformation is shown in Fig. 3.16.

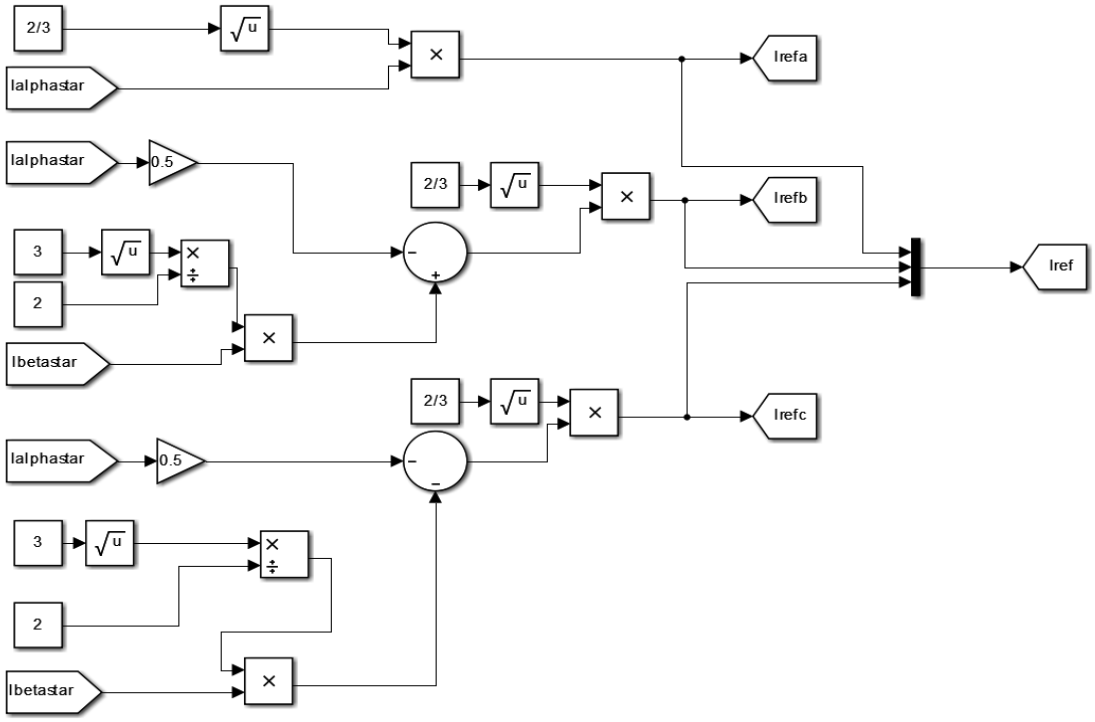

Fig. 3.16: Simulation Diagram of Estimation of Reference Three-Phase Supply Currents by Inverse Clarke Transformation

This Instantaneous Reactive Power (IRP) Theory can be easily modified for indirect current control. For Power Factor Correction (PFC) mode, Q=0.

$$Q = \bar{Q}_L + Q_{Loss} = 0 \tag{3.25}$$

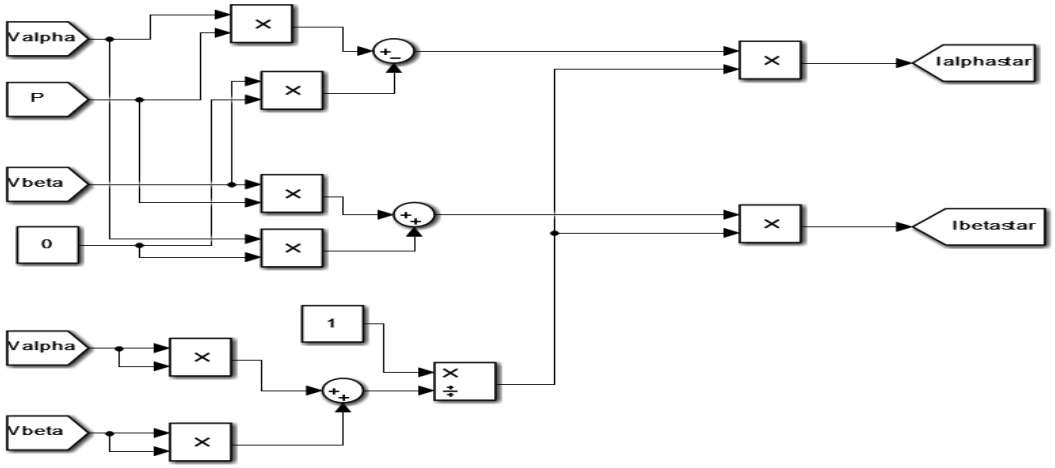

Fig. 3.17: Simulation Diagram of Calculation of Reference Currents in α-β Frame in PFC Mode

3.2.2.2 Results with IRPT

The performance of DSTATCOM controlled by IRPT in UPF and ZVR mode are shown.

3.2.2.2.1 Power Factor Correction (PFC) Mode

The performance of DSTATCOM controlled by IRP theory in PFC mode is observed in Fig. 3.19 and the results of the intermediate in the control algorithm are also shown in Fig. 3.18 which shows a plot of $v_\alpha, v_\beta, i_\alpha, i_\beta, P, i_\alpha^*, i_\beta^*, P_{Loss} and\ i_{ref}$.

In Fig.3.19 as we can see the PCC voltage is sinusoidal, the phase 'a' of three phase non-linear load is disconnected at time t=0.6 sec. as we can see the dc link voltage V_{dc} rises momentarily and slowly starts to settle down at 200V. The supply currents are sinusoidal and reduced when phase-a of load gets disconnected.

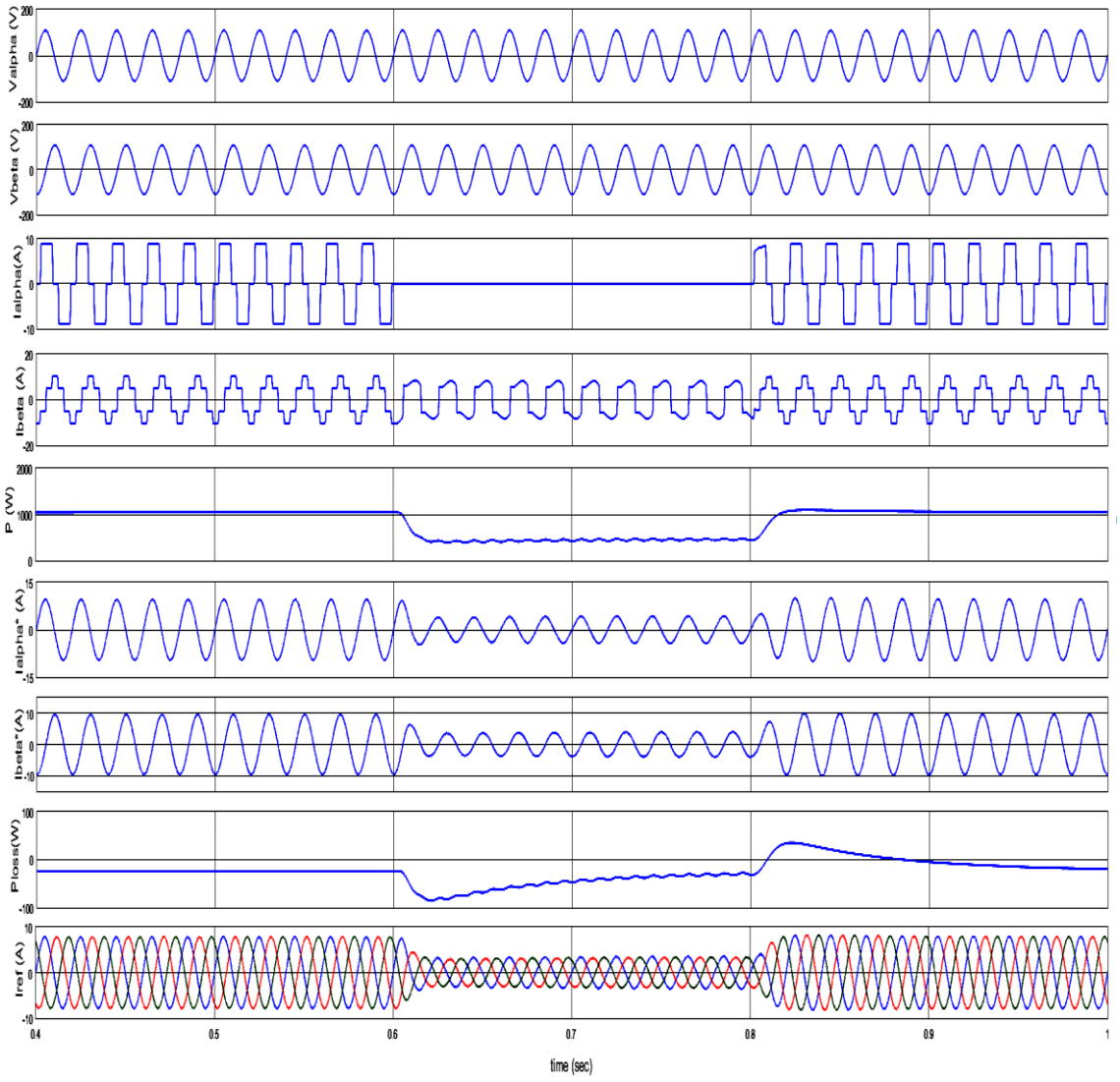

Fig. 3.18: Intermediate Results in PFC Mode using IRPT

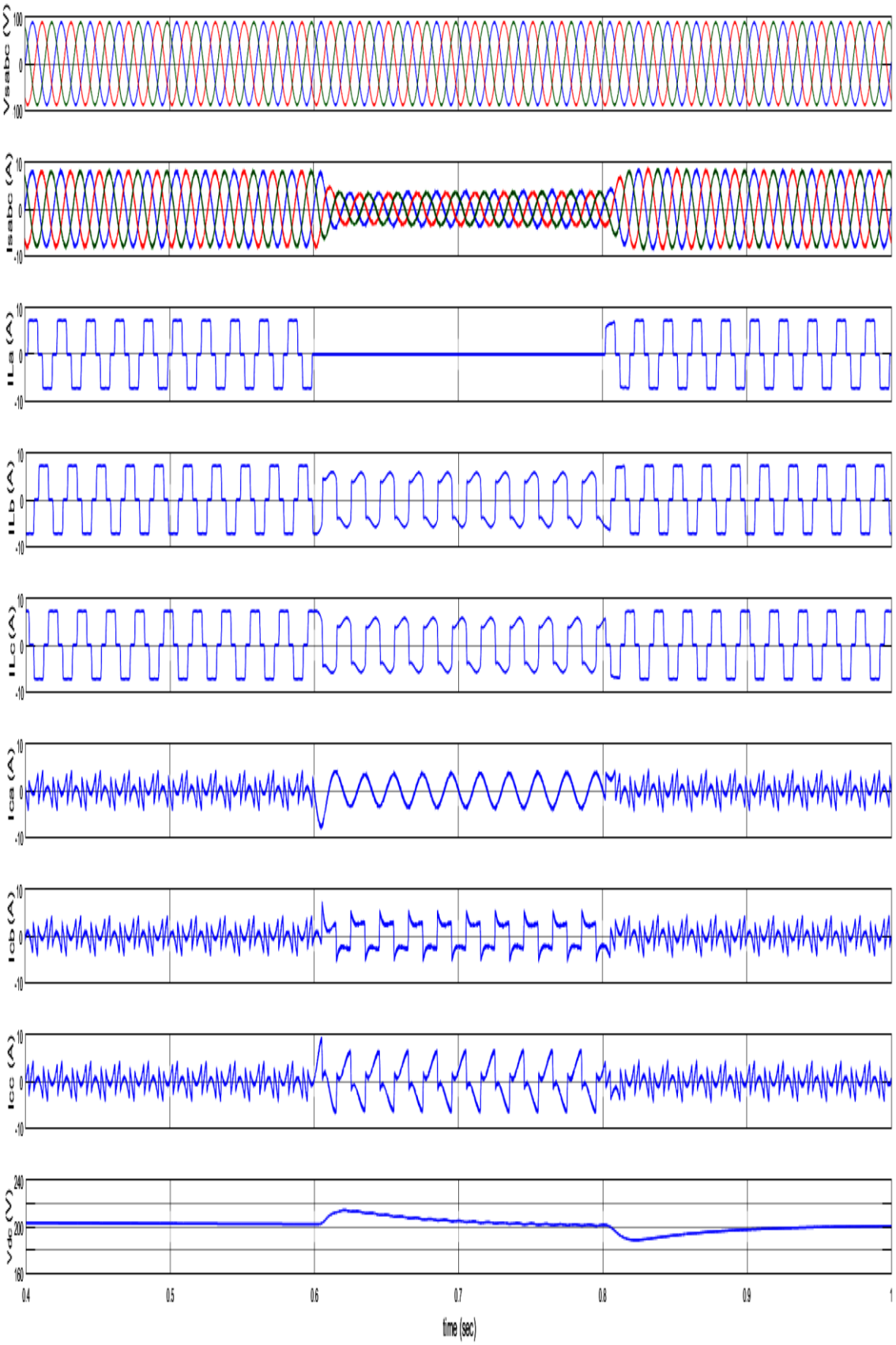

Fig. 3.19: Performance of DSTATCOM Controlled using IRP Theory in PFC mode using IRPT

The FFT Analysis of PCC Voltage, Load Current, Source Current obtained by IRP theory in PFC mode in distribution system is shown below. The Total Harmonic Disorder (THD) in %age of the load current, PCC Voltage and Source currents are observed to be 27.19%, PCC voltage 0.04% and the source current 3.87%.

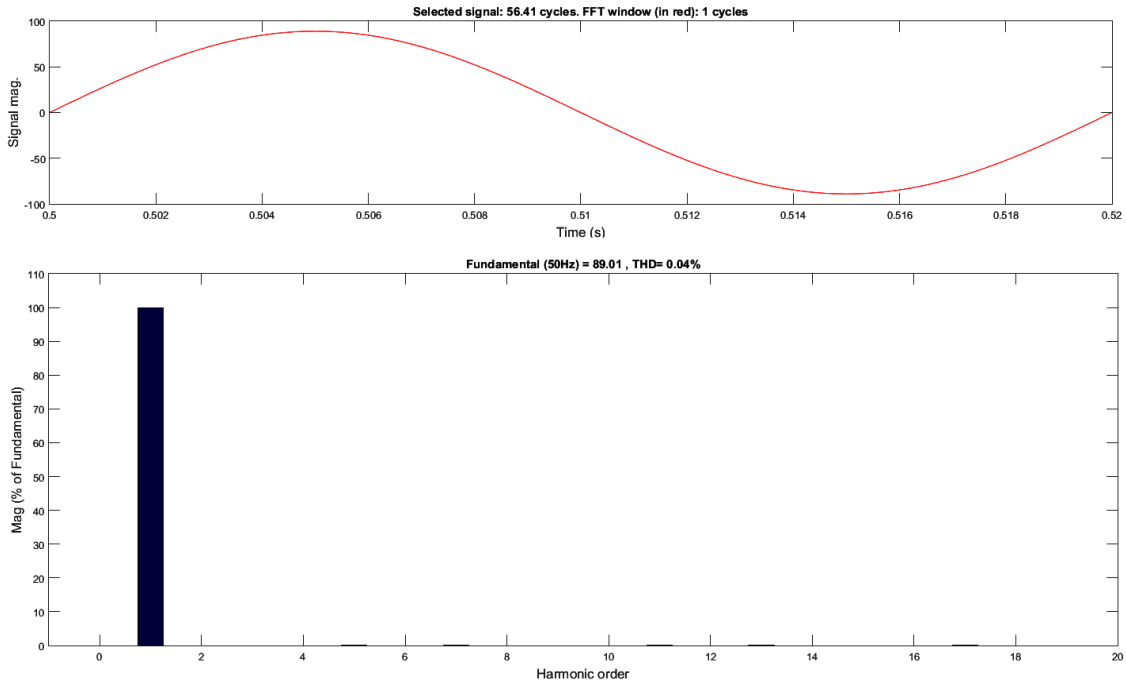

Fig. 3.20: FFT Analysis of PCC Voltage in PFC mode using IRPT

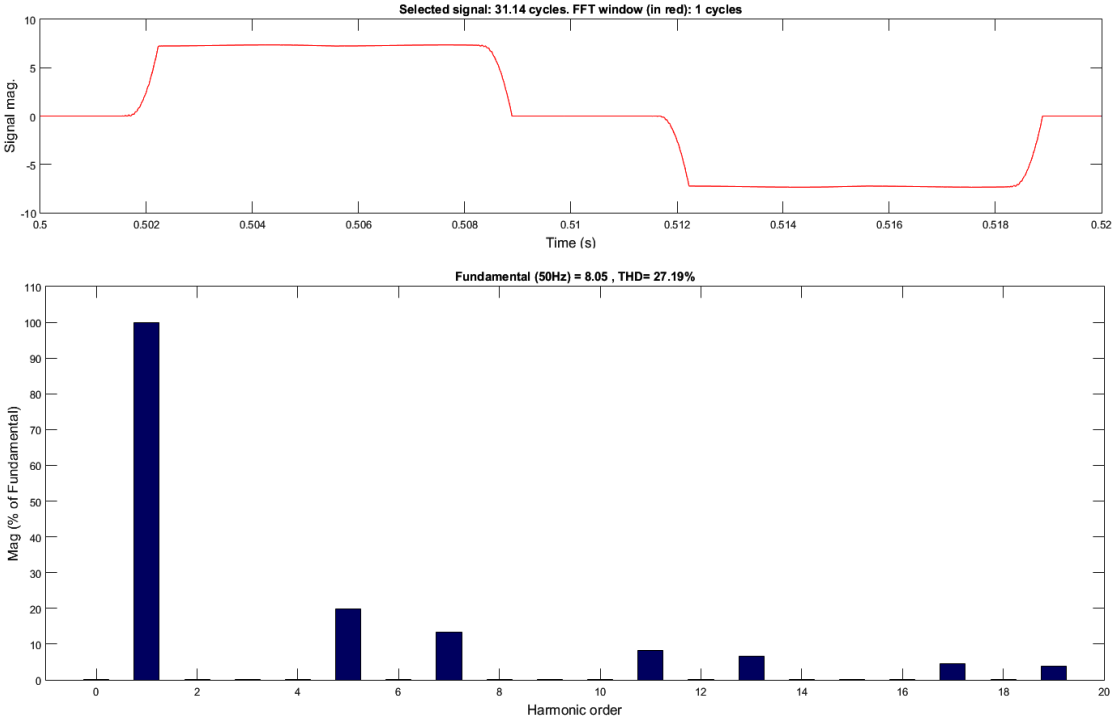

Fig. 3.21: FFT Analysis of Load Current in PFC mode using IRPT

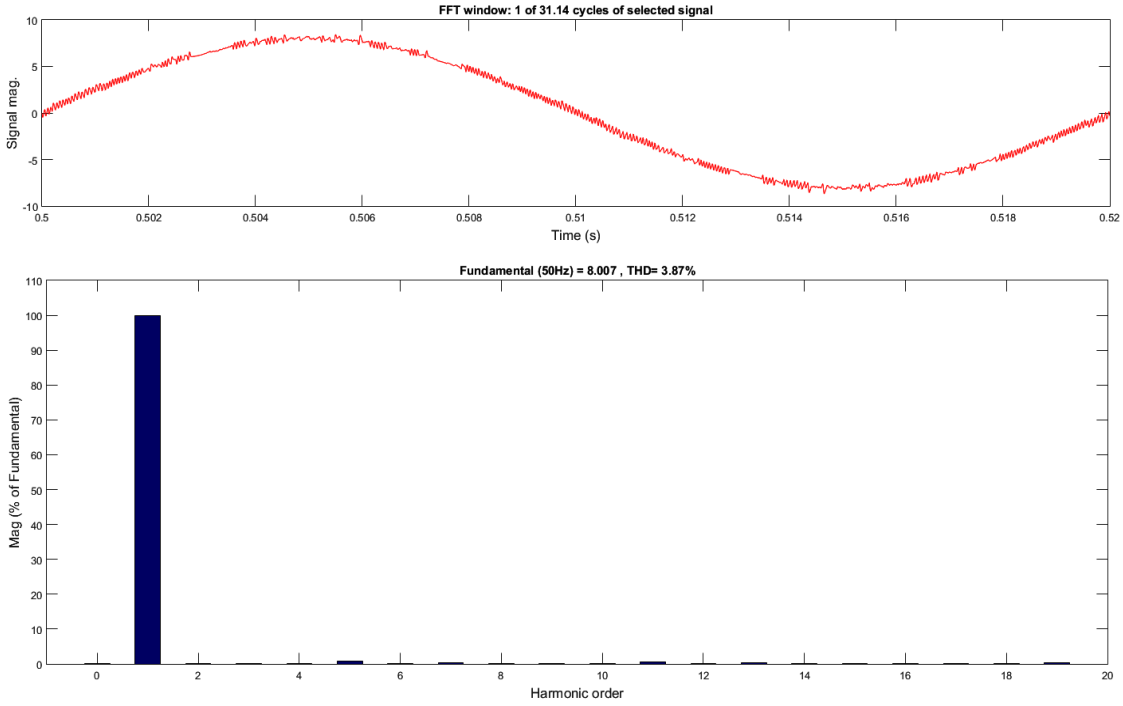

Fig. 3.22: FFT Analysis of Source Current in PFC mode using IRPT

3.2.2.2.2 Zero Voltage Regulation (ZVR) mode:

The performance of VSC based DSTATCOM controlled by IRP theory in ZVR mode is observed in Fig. 3.24 and the results of the intermediate in the control algorithm are also shown in Fig. 3.23 which shows a plot of $v_\alpha, v_\beta, i_\alpha, i_\beta, P, Q, i_\alpha^*, i_\beta^*, P_{Loss}, Q_{Loss} and\ i_{ref}$.

Fig.3.24 as we can see the PCC voltage is sinusoidal, the phase 'a' of three phase non-linear load is disconnected at time t=2.2 sec. as we can see the dc link voltage V_{dc} rises momentarily and slowly starts to settle down at 200V. The magnitude of PCC voltage is also regulated in ZVR mode, at time t=2.2 sec the magnitude of PCC voltage rises momentarily and slowly begins to settle down oscillating near 89.8V.

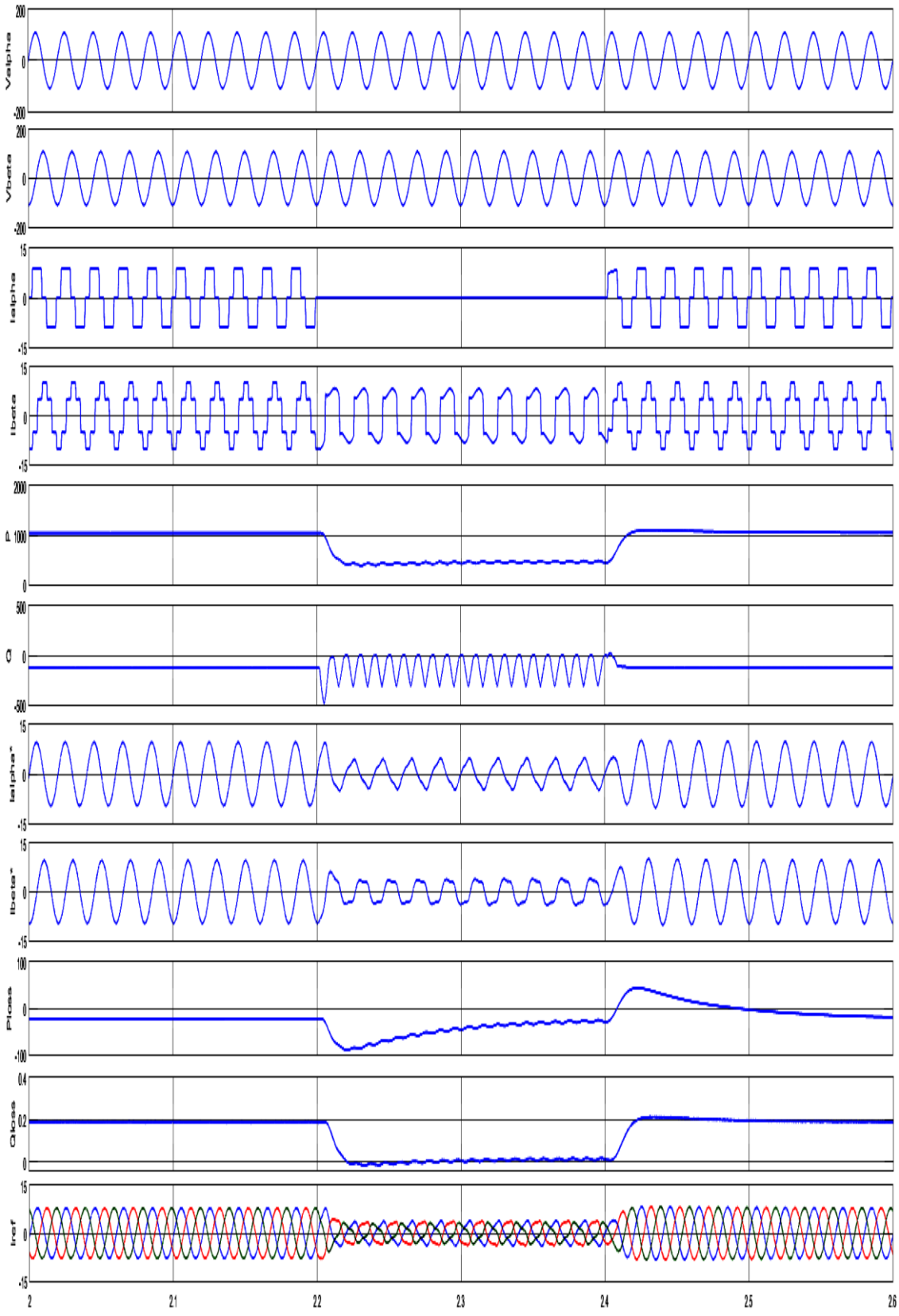

Fig. 3.23: Intermediate Results in ZVR Mode with IRPT

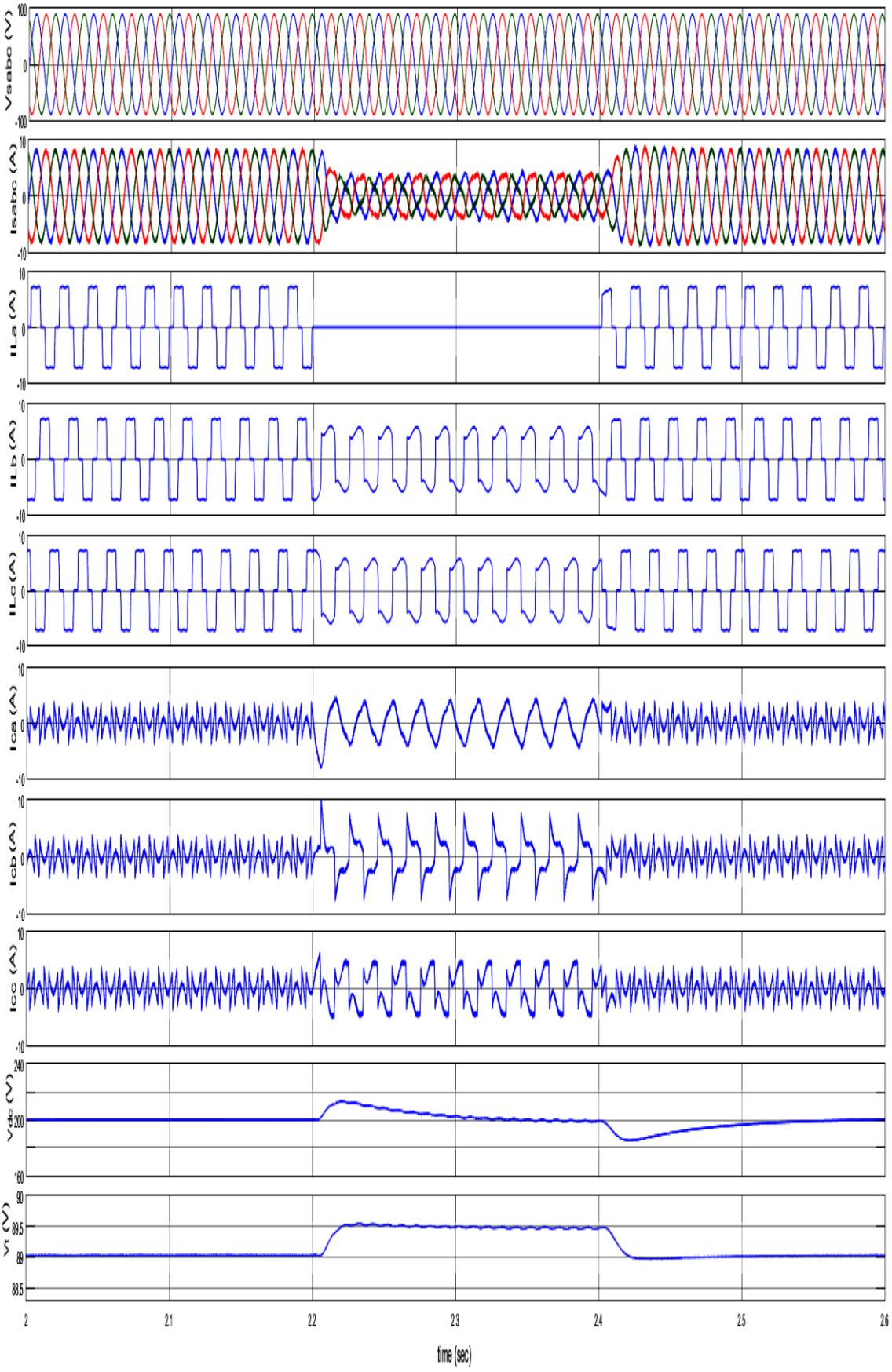

Fig. 3.24: Performance of DSTATCOM Controlled using IRP Theory in ZVR mode

The FFT Analysis of PCC Voltage, Load Current, Source Current, intermediate and the performance of DSTATCOM controlled by IRP theory in ZVR mode in distribution system is shown below. The Total Harmonic Disorder (THD) in %age of the load current, PCC Voltage and Source currents are observed to be 27.16%, PCC voltage 0.0% and the source current 3.70%.

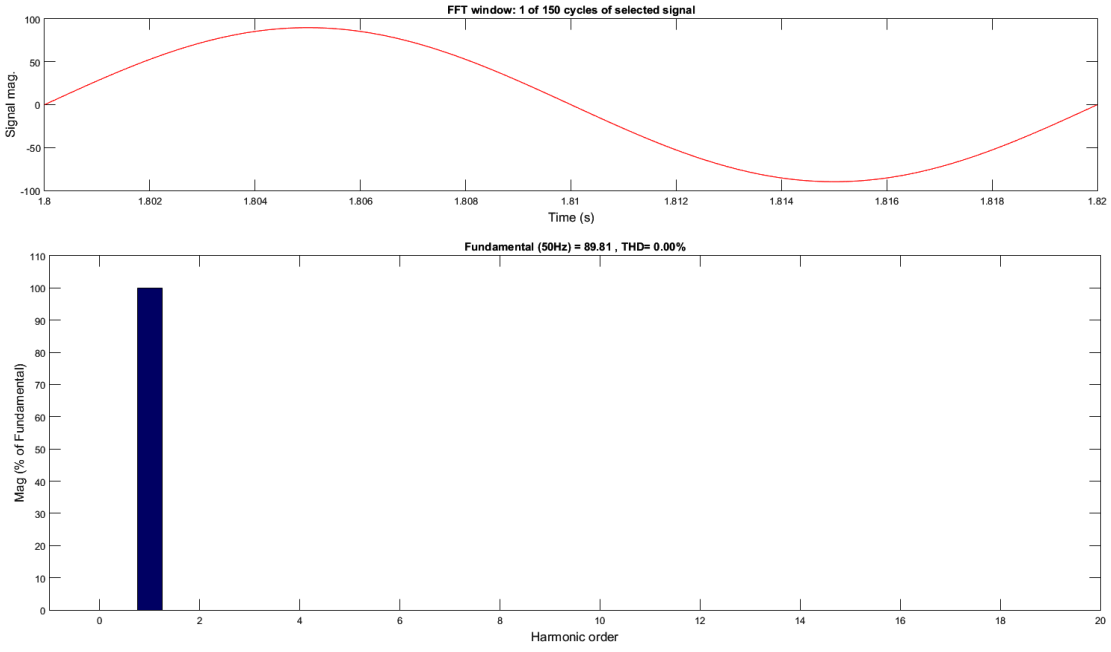

Fig. 3.25: FFT Analysis of PCC Voltage in ZVR mode using IRPT

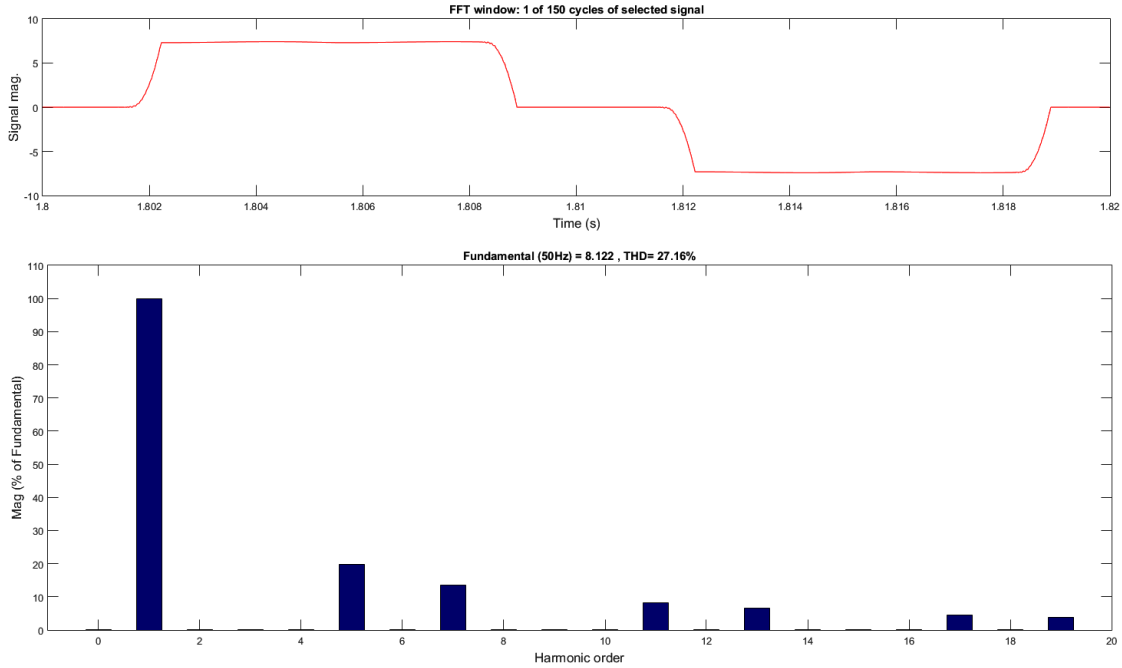

Fig. 3.26: FFT Analysis of Load Current in ZVR mode using IRPT

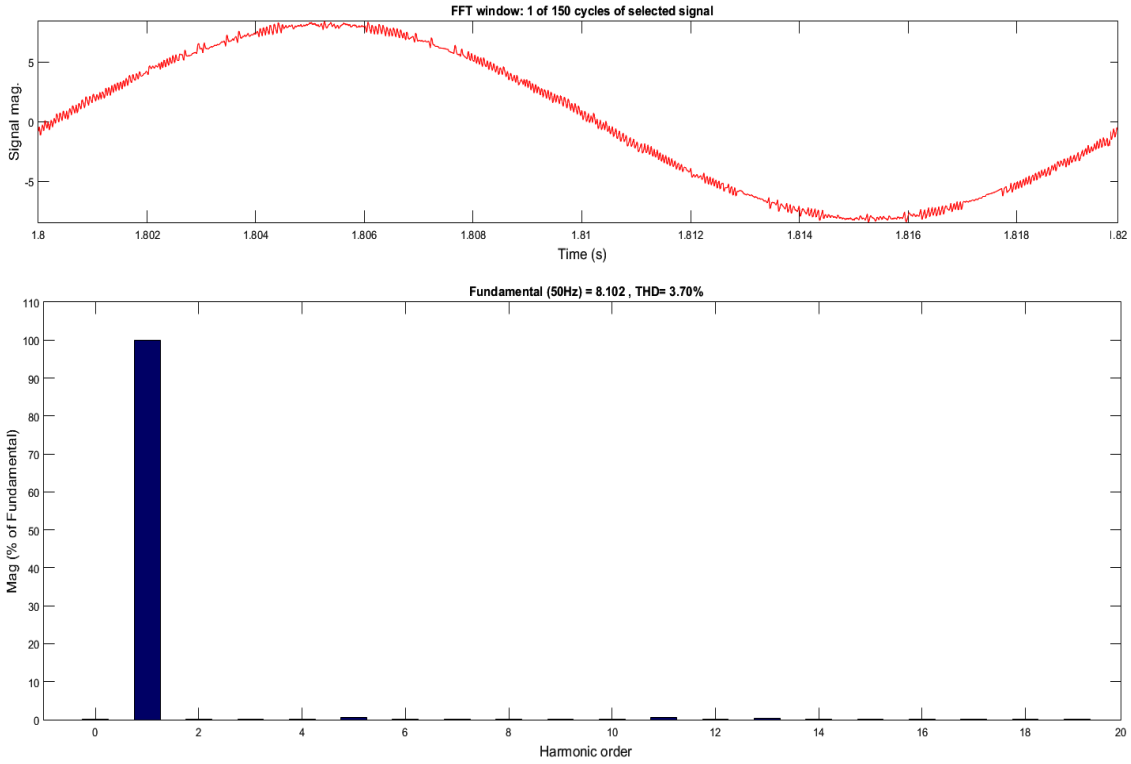

Fig. 3.27: FFT Analysis of Source Current in ZVR mode using IRPT

3.2.3 Modified Instantaneous Symmetrical Component (ISC) Theory

In this algorithm, the PCC voltages and the load currents are sensed to estimate the average power. The product of instantaneous values of PCC phase voltages and load currents gives the instantaneous load power. The instantaneous load power is filtered using a low pass filter to acquire the DC value of this instantaneous load power. The reference source-current are generated by using this DC component of instantaneous load power [2].

Fig. 3.28 shows a block diagram of Modified Instantaneous Symmetrical Component Theory.

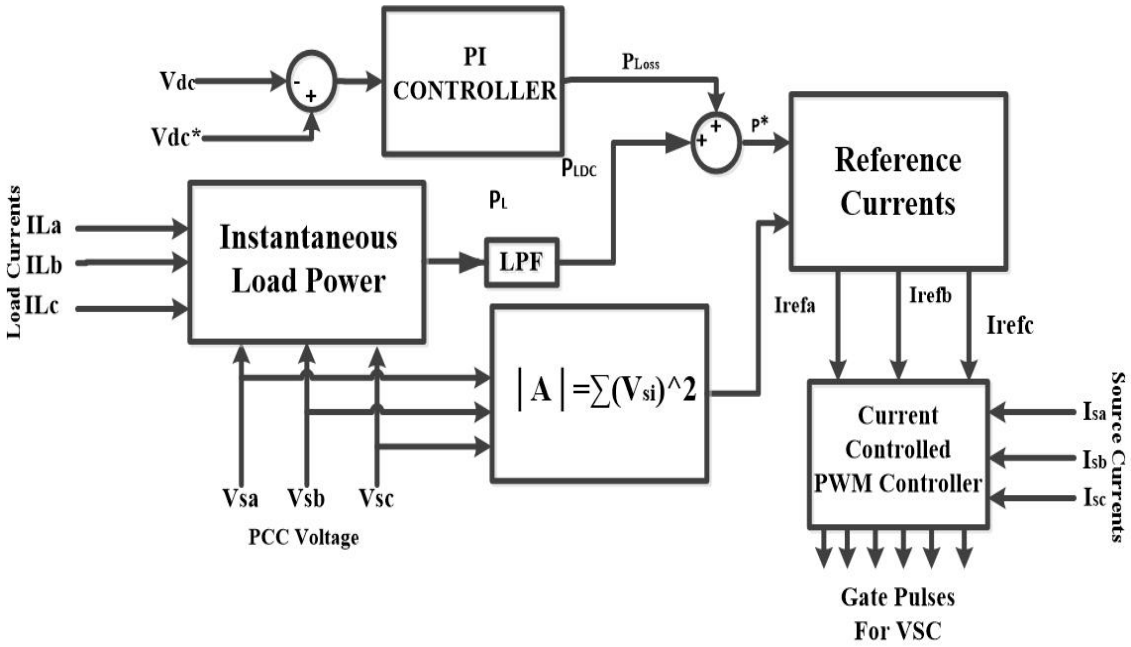

Fig. 3.28: Block Diagram of Modified Instantaneous Symmetrical Component Theory

3.2.3.1 Control Algorithm [10]

The instantaneous load currents (i_{La}, i_{Lb}, i_{Lc}), Point of Common Coupling (PCC) Voltages (v_{sa}, v_{sb}, v_{sc}) and the DC bus voltage (V_{dc}) in the distribution system are sensed for generating the reference current signals. The instantaneous load power is the product of instantaneous PCC phase voltages and the load currents.

$$P_L = v_{sa} i_{La} + v_{sb} i_{Lb} + v_{sc} i_{Lc} \tag{3.26}$$

As this instantaneous load power contains both AC and DC component, a low pass filter is used to filter the AC component. A PI controller is used to regulate the DC bus voltage 'V_{dc}'.

$$P = \bar{P}_L + \tilde{P}_L \tag{3.27}$$

The error in DC bus Voltage at nth sampling instant between the reference DC bus voltage 'V_{dc}^*' and the sensed DC bus voltage 'V_{dc}' is given as:

$$V_{DC}(n) = V_{dc}^*(n) - V_{dc}(n) \tag{3.28}$$

The output of the DC PI controller is known as the active power component loss 'P_{Loss}'

$$P_{Loss}(n) = P_{Loss}(n-1) + K_{pd}\{V_{DC}(n) - V_{DC}(n-1)\} + K_{pi}V_{DC}(n) \quad (3.29)$$

Here, K_{pd} and K_{id} are the proportional and integral gain of the PI controller respectively. P_{Loss} is added to the DC component of instantaneous load active power '$\bar{P}_L$' to acquire the fundamental component of active power given by 'P'.

$$P = \bar{P}_L + P_{Loss} \quad (3.30)$$

The simulation diagram of extracting the fundamental component of active power is shown below in Fig. 3.29.

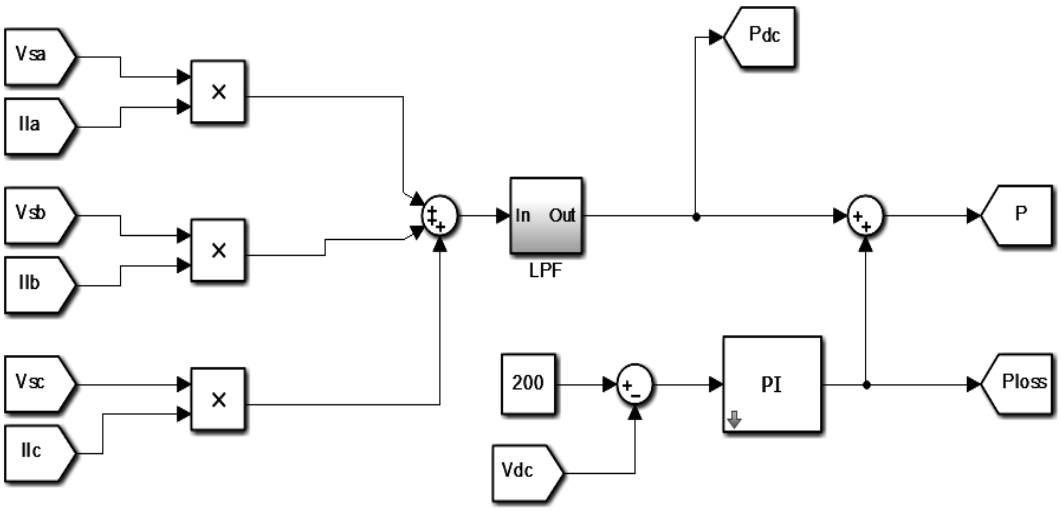

Fig. 3.29: Simulation diagram of Extracting the Fundamental Component of Active Power

$$|A| = \sum V_{si}^2 = 3(\text{rms phase voltage})^2 \quad (3.31)$$

The reference source currents are generated as follows:

$$\begin{bmatrix} i_{refa} \\ i_{refb} \\ i_{refc} \end{bmatrix} = \frac{P}{|A|} \begin{bmatrix} v_{sa} \\ v_{sb} \\ v_{sc} \end{bmatrix} \quad (3.32)$$

The simulation diagram to extract reference source currents is shown in Fig. 3.30.

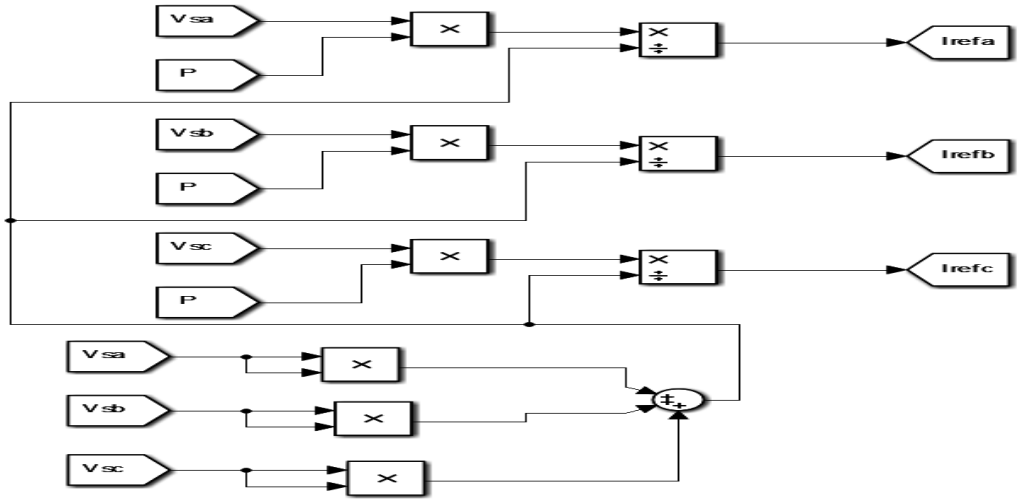

Fig. 3.30: Simulation Diagram to Extract Reference Source Currents

3.2.3.2 Results with Modified ISCT

The performance of VSC based DSTATCOM controlled by ISC theory in PFC mode is observed in Fig. 3.32 and the results of the intermediate in the control algorithm are also shown in Fig. 3.31 which shows a plot of $P_{DC}, P, P_{Loss} and\ i_{ref}$. Fig.3.24 as we can see the PCC voltage is sinusoidal, the phase 'a' of three phase non-linear load is disconnected at time t=0.6 sec. as we can see the dc link voltage V_{dc} rises momentarily and slowly starts to settle down at 200V. As we can also see that the source currents are sinusoidal and its magnitude reduces while phase-a of load is disconnected.

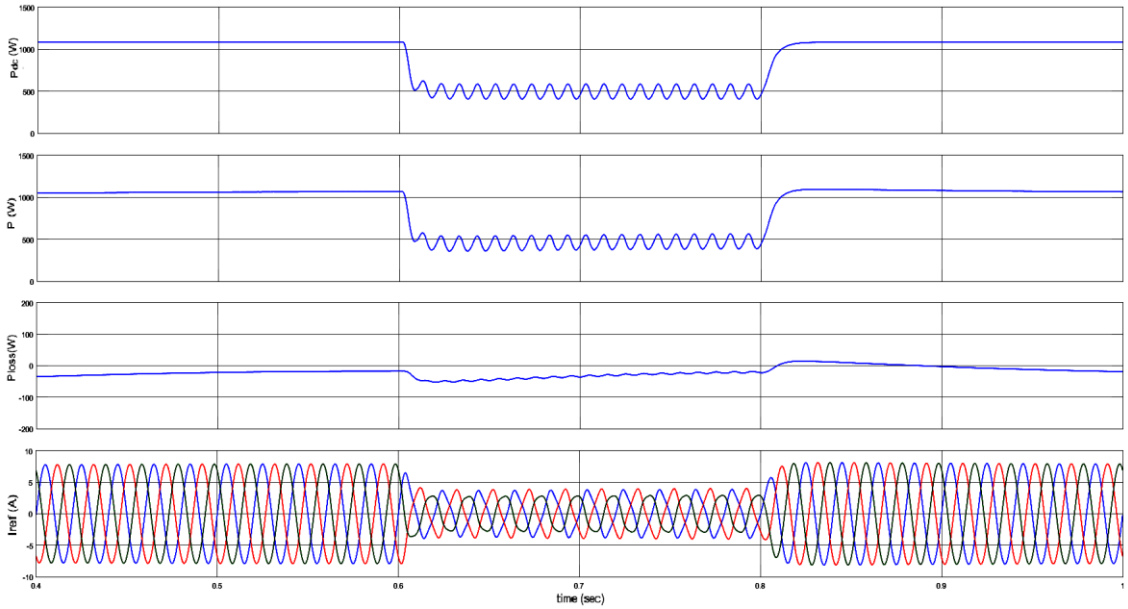

Fig. 3.31: Intermediate results in PFC mode using Modified ISCT

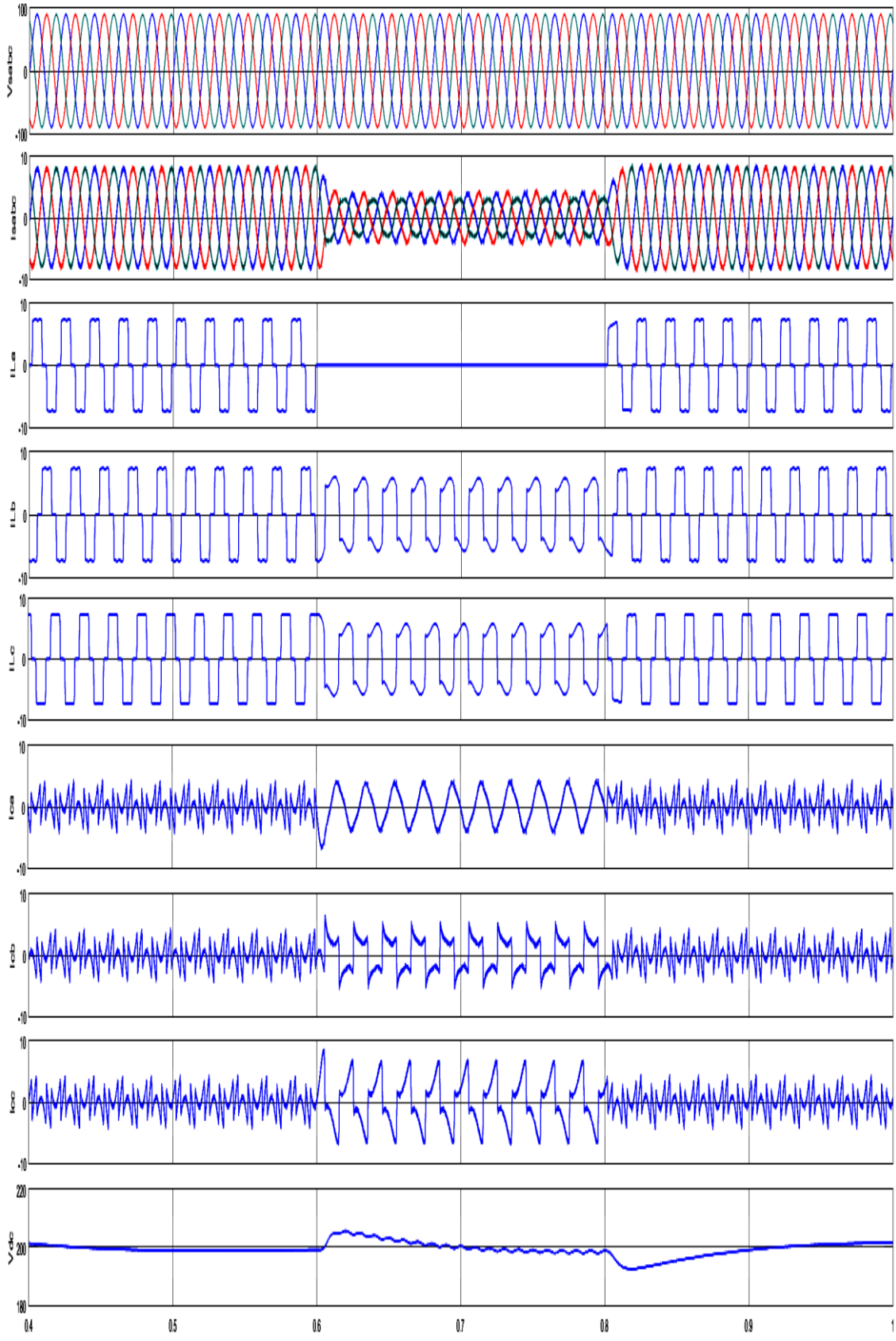

Fig. 3.32: Performance of DSTATCOM Controlled using Modified ISCT

The FFT Analysis of PCC voltage, load current and source current obtained by ISC theory in distribution system is shown below. The Total Harmonic Disorder (THD) in %age of the load current, PCC Voltage and Source currents are observed to be 27.26%, PCC voltage 0.30% and the source current 3.32%.

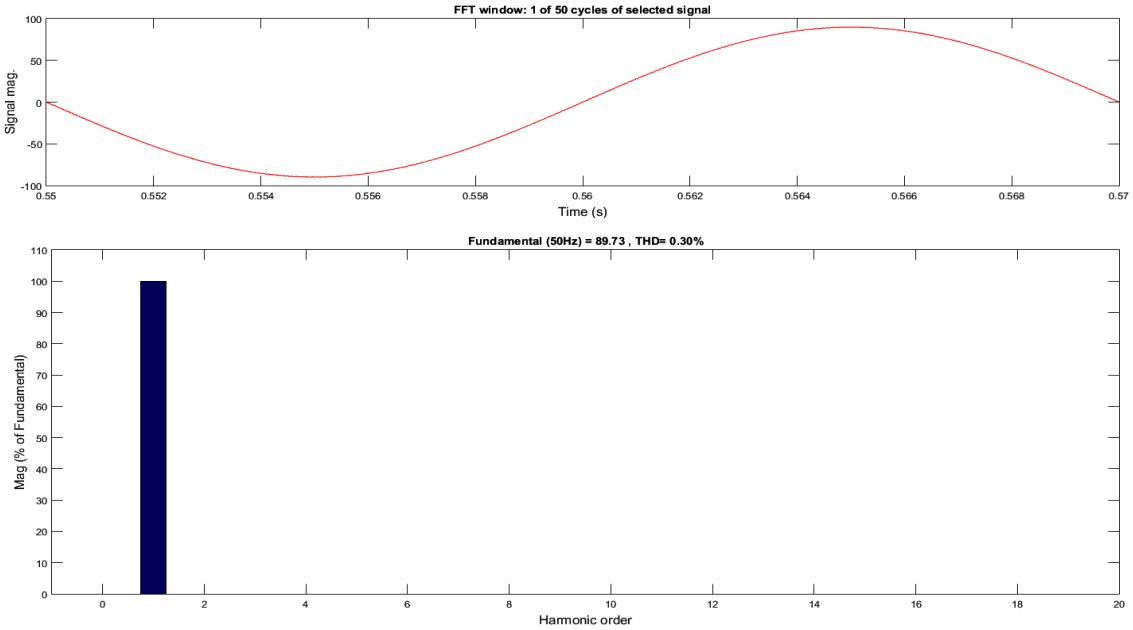

Fig. 3.33: FFT Analysis of PCC Voltage using Modified ISCT

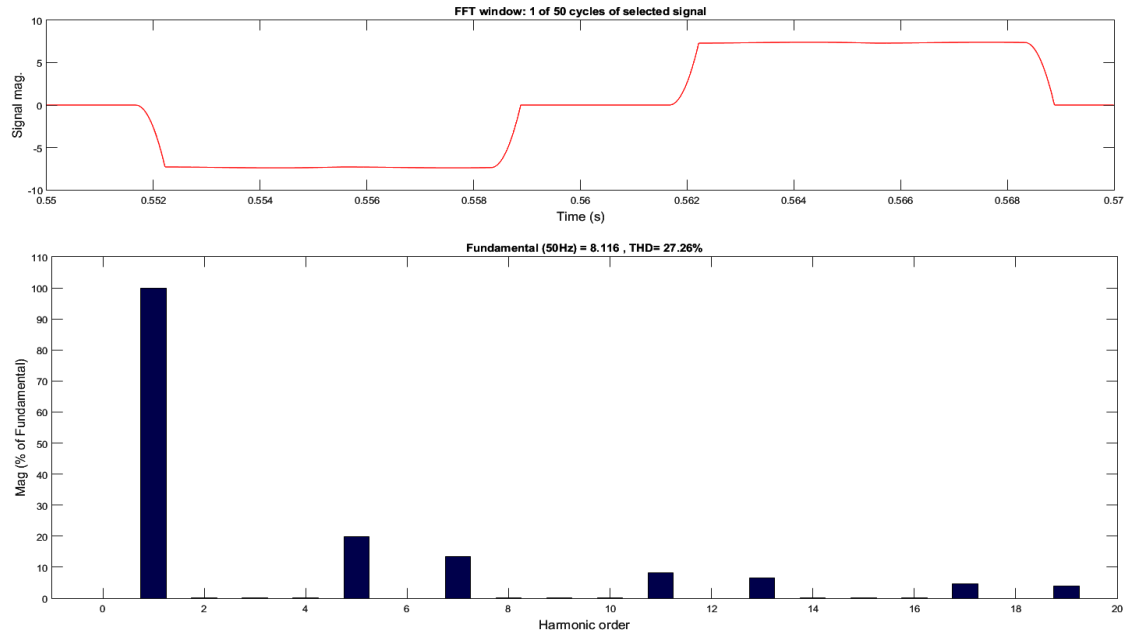

Fig. 3.34: FFT Analysis of Load Current using Modified ISCT

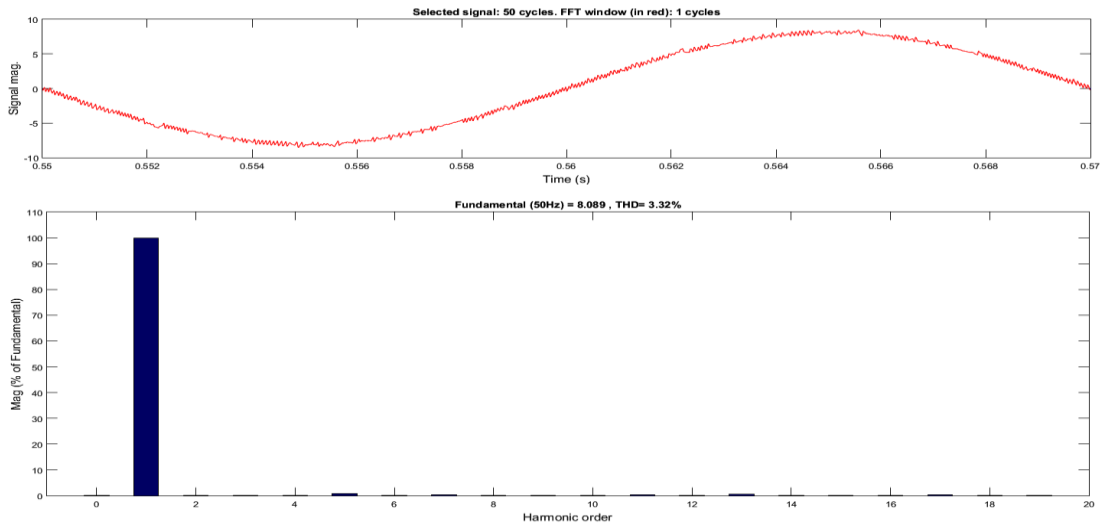

Fig. 3.35: FFT Analysis of Source Current using Modified ISCT

3.2.4 Notch Filter

There are many power quality problems such as poor power factor of loads, network pollution due to harmonics injection by the nonlinear. A notch filter extracts the fundamental frequency component of the load currents by allowing only a specific frequency to pass through it (which in this case is the fundamental frequency) [20]. These components of load currents are used to estimate reference supply currents. This fundamental frequency is called the notch frequency of the filter. Thus in the frequency spectrum of the filter's output, all frequencies except the notch frequency can exist [19].

$$e(t) = u(t) - \dot{x} \tag{3.33}$$

$$\ddot{x} + \theta^2 x = 2\xi\theta e(t) \tag{3.34}$$

Here,

u(t) is the input signal.

e(t) is the error signal or the harmonic signal.

$\dot{x}$ is the estimate signal for input signal u(t).

θ is the frequency in rad/sec.

ξ is a real positive number that determine the performance of notch filter in terms of accuracy.

The notch-filtering system uses two integrators to extract the fundamental component of input [18]. The gain 'ξ' can be tuned to adjust the bandwidth and settling time of the notch filter. The open loop response for the notch filter has been observed for various

values of 'ξ' and by inspection the 'ξ = 1' gives satisfactory transient and steady state response which is selected for simulation purpose.

If the notch frequency can follow the fundamental frequency of the input signal and change accordingly, the filter is then called an Adaptive Notch Filter (ANF) and its dynamic behaviour is characterized by the following set of differential equations i.e. Equations [19]
(3.33 to 3.35).

$$\dot{\theta} = -\gamma x \theta e(t) \quad \text{.....(3.35)}$$

Here γ is a real positive number that determines that determines performance of an ANF in terms of speed.

3.2.4.1 Control Algorithm for Notch Filter [20]

The load currents (i_{La}, i_{Lb}, i_{Lc}), Point of Common Coupling (PCC) Voltages (v_{sa}, v_{sb}, v_{sc}) and the DC bus voltage (V_{dc}) in the distribution system are sensed for generating the reference current signals. First we determine the amplitude of the instantaneous value of Load Currents in individual phase (i_{ma}, i_{mb}, i_{mc}) using a notch filter Equations 3.33 to 3.35. The amplitude of the input signal is given by:

$$i_{mi} = \sqrt{\theta^2 x^2 + \ddot{x}^2} \quad (3.36)$$

Unit templates (U_{ia}, U_{ib}, U_{ic}) are estimated by the fundamental components of PCC phase voltages ($\dot{x_a}, \dot{x_b}, \dot{x_c}$) and the amplitude of three phase PCC voltages 'V_t'.

$$\begin{bmatrix} U_{ia} \\ U_{ib} \\ U_{ic} \end{bmatrix} = \frac{1}{V_t} \begin{bmatrix} \dot{x_a} \\ \dot{x_b} \\ \dot{x_c} \end{bmatrix} \quad (3.37)$$

$$V_t = \sqrt{\frac{2}{3}(v_{sa}^2 + v_{sb}^2 + v_{sc}^2)} \quad (3.38)$$

Simulation diagram of estimating the amplitude of the instantaneous value of Load Current in single phase 'i_{ma}' and the fundamental component of PCC phase voltage in phase-a '$\dot{x_a}$' is shown in Fig. 3.36.

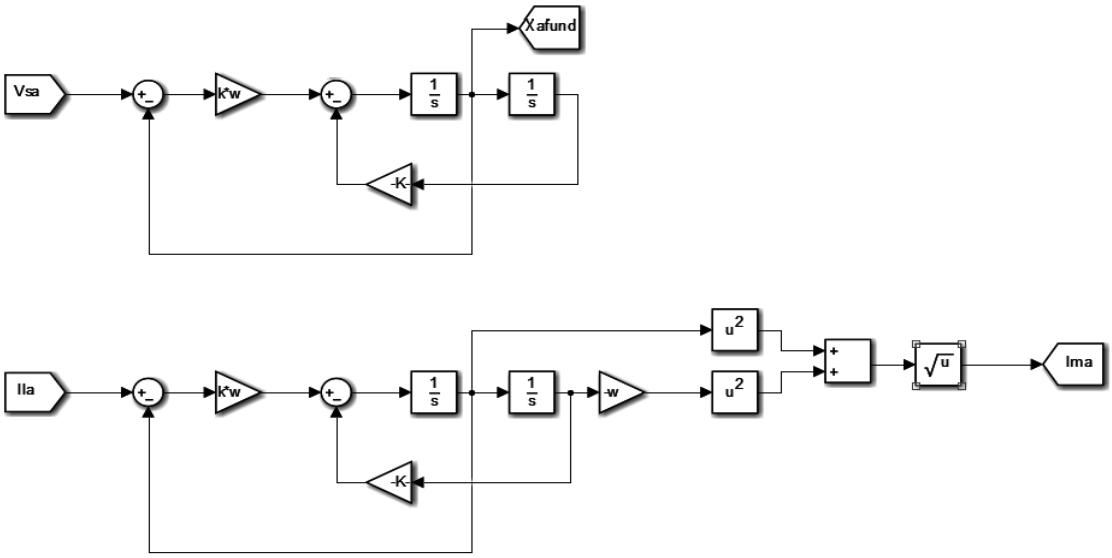

Fig. 3.36: Estimation of Amplitude of Load Current in Single-Phase 'i_{ma}' and the Fundamental Component of PCC Phase-Voltage '$\dot{x_a}$'

Simulation diagram of extracting Unit templates (U_{ia}, U_{ib}, U_{ic}) from the fundamental components of PCC phase voltages ($\dot{x_a}, \dot{x_b}, \dot{x_c}$) and the amplitude of three phase PCC voltages 'V_t' is shown in Fig 3.37.

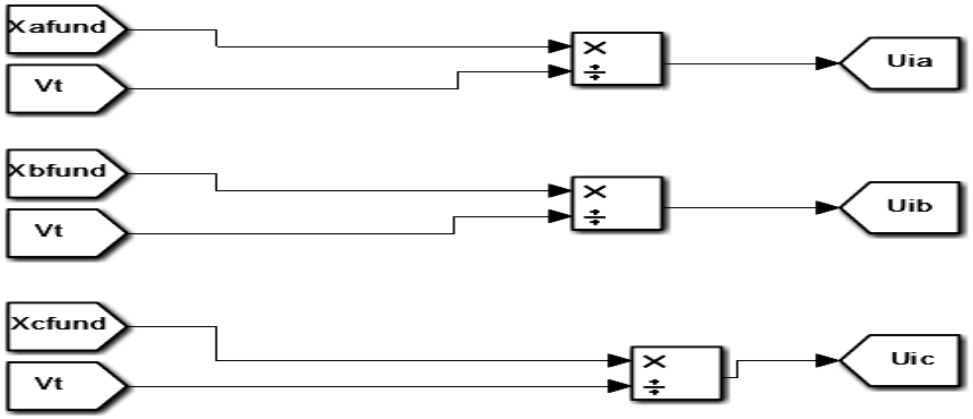

Fig. 3.37: Unit Templates

A PI controller is used to regulate the DC bus voltage 'V_{dc}'. The error in DC bus Voltage at nth sampling instant between the reference DC bus voltage 'V_{dc}^{*}' and the sensed DC bus voltage 'V_{dc}' is given as:

$$V_{DC}(n) = V_{dc}^{*}(n) - V_{dc}(n) \tag{3.39}$$

The output of the DC PI controller is known as the 'i_{Loss}'

$$i_{Loss}(n) = i_{Loss}(n-1) + K_{pd}\{V_{DC}(n) - V_{DC}(n-1)\} + K_{pi}V_{DC}(n) \tag{3.40}$$

Here, K_{pd} and K_{id} are the proportional and integral gain of the PI controller respectively.

The reference source currents ($i_{refa}, i_{refb}, i_{refc}$) are generated as shown:

$$\begin{bmatrix} i_{refa} \\ i_{refb} \\ i_{refc} \end{bmatrix} = \begin{bmatrix} U_{ia} \\ U_{ib} \\ U_{ic} \end{bmatrix} \left\{ \frac{1}{3}(i_{ma} + i_{mb} + i_{mc}) + i_{Loss} \right\} \tag{3.41}$$

Simulation diagram for extraction of reference source currents is shown in Fig. 3.38.

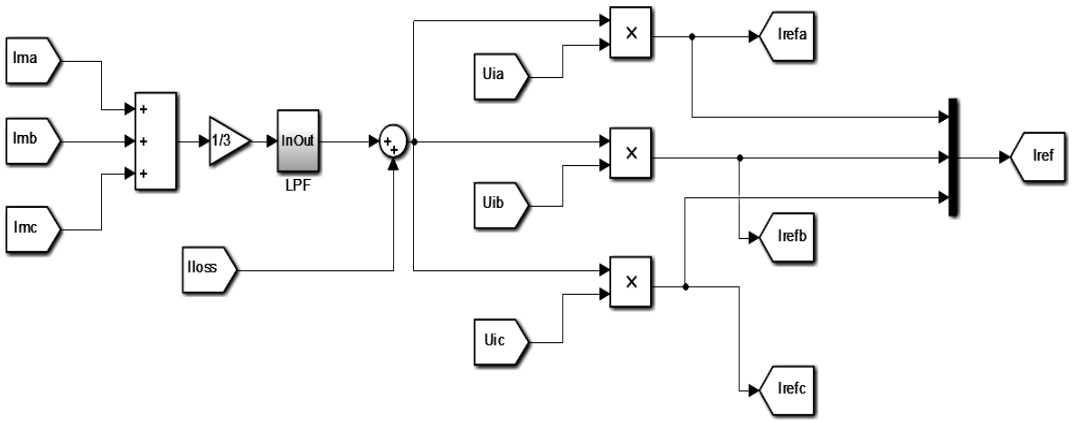

Fig. 3.38: Reference Source Currents

3.2.4.2 Results with Notch Filter.

The performance of VSC based DSTATCOM controlled by ISC theory in PFC mode is observed in Fig. 3.40 and the results of the intermediate in the control algorithm are also shown in Fig. 3.39 which shows a plot of $i_{mabc}, U_{abc}, i_{Loss} and\ i_{ref}$. Fig.3.40 as we can see the PCC voltage is sinusoidal, the phase 'a' of three phase non-linear load is disconnected at time t=0.4 sec. as we can see the dc link voltage V_{dc} rises momentarily and slowly starts to settle down at 200V. As we can also see that the source currents are sinusoidal and its magnitude reduces while phase-a of load is disconnected.

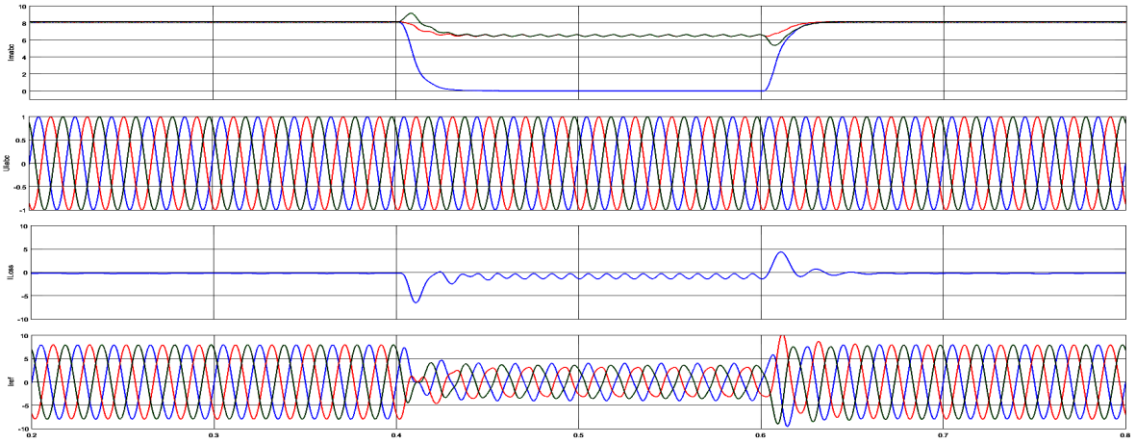

Fig. 3.39: Intermediate results using Notch Filter

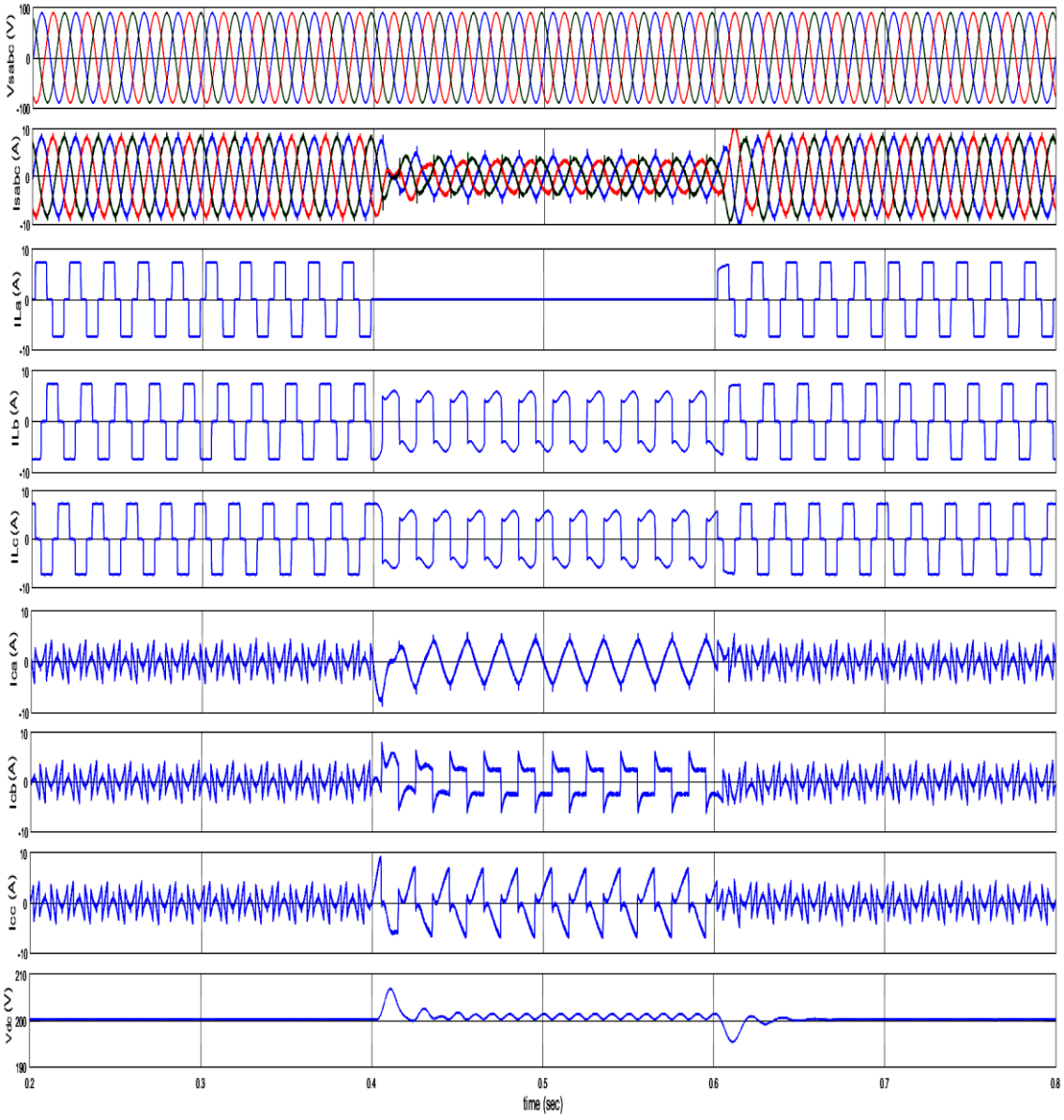

Fig. 3.40: Performance of DSTATCOM Controlled using Notch Filter in PFC mode

The FFT Analysis of PCC Voltage, Load Current and Source Current obtained by Notch Filter in distribution system is shown below. The Total Harmonic Disorder (THD) in %age of the load current, PCC Voltage and Source currents are observed to be 27.26%, PCC voltage 0.36% and the source current 4.25%.

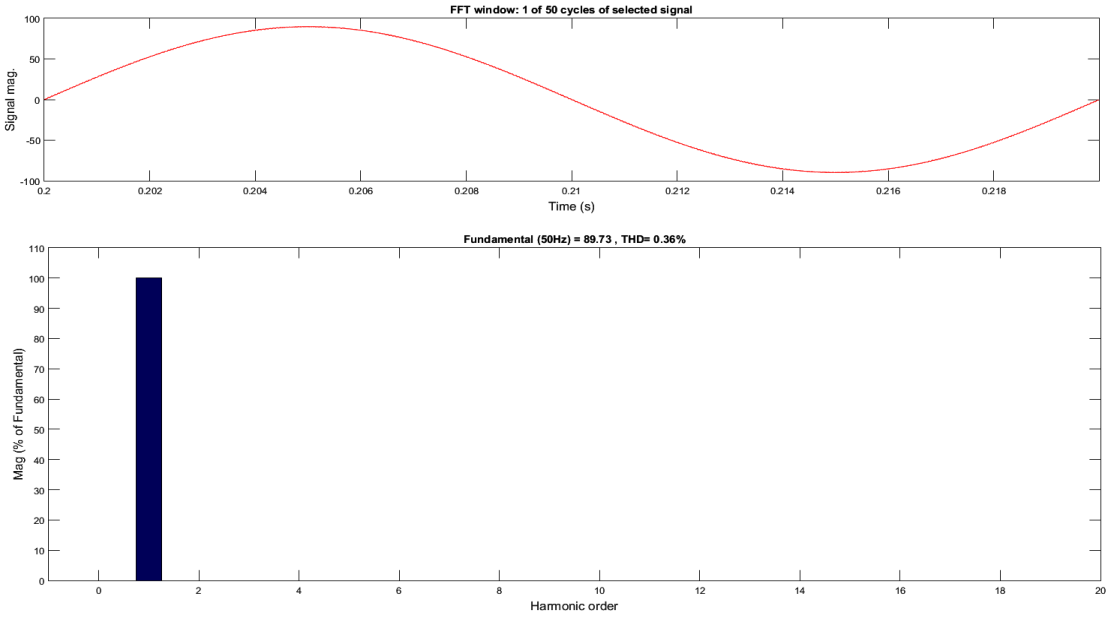

Fig. 3.41: FFT Analysis of PCC Voltage using Notch Filter

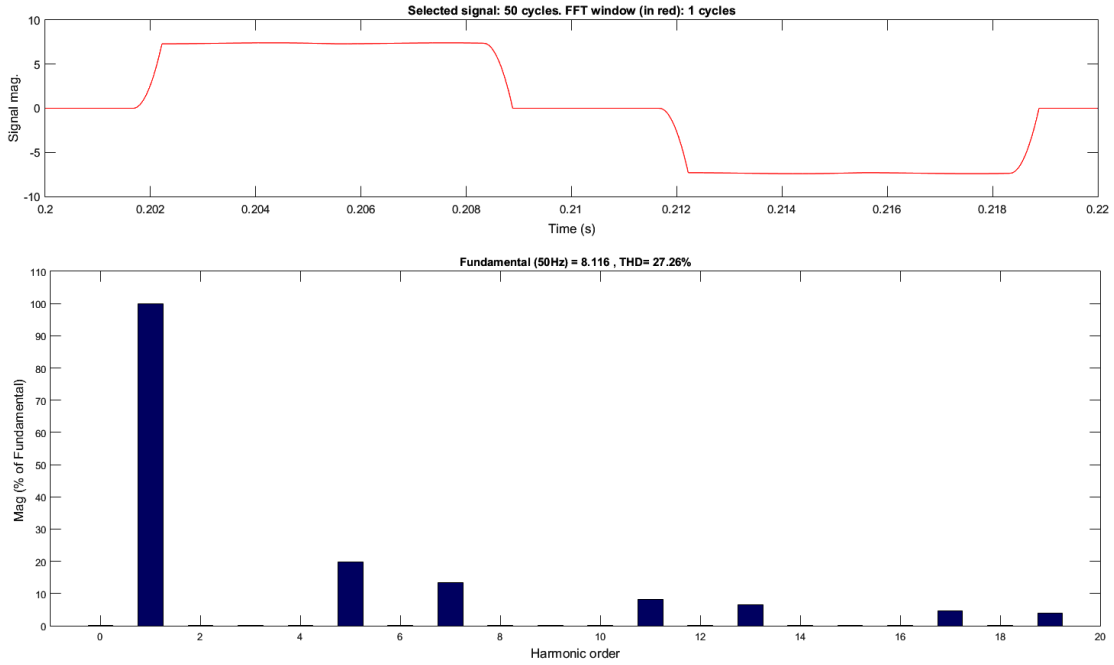

Fig. 3.42: FFT Analysis of Load Current using Notch Filter

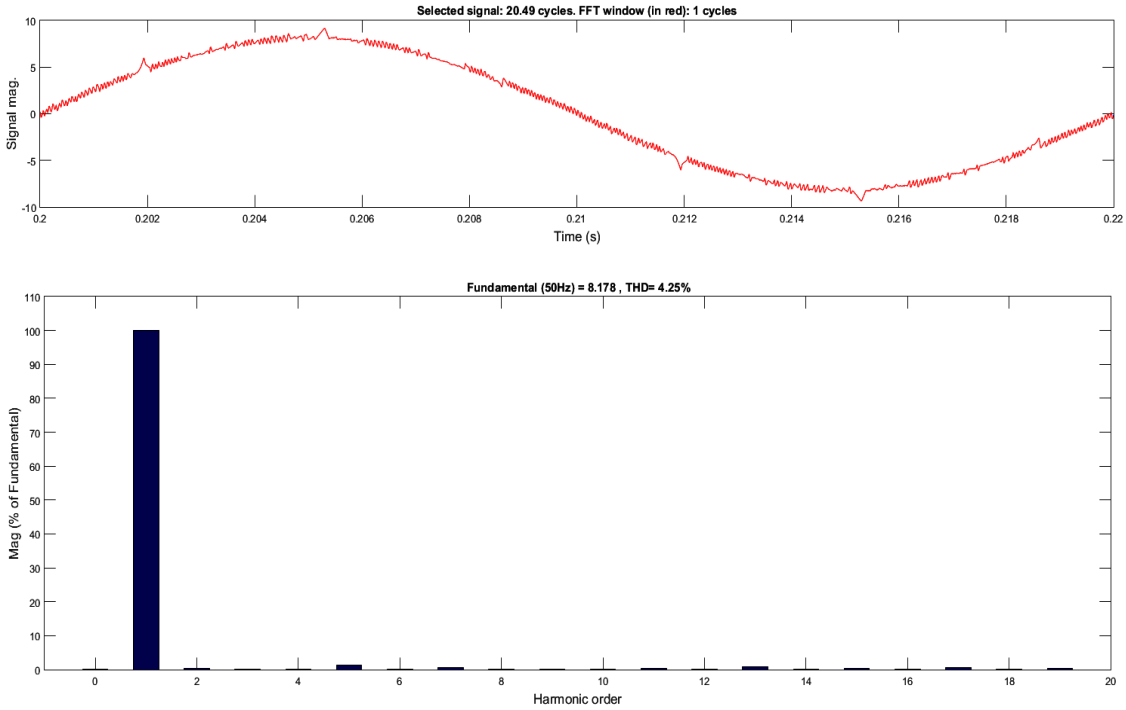

Fig. 3.43: FFT Analysis of Source Current using Notch Filter

3.3 COMPAISION OF ALGORITHMS

The comparison between all the algorithms for harmonics extraction studied in this chapter is shown in TABLE 3.2.

TABLE 3.2: THD IN PHASE-A OF SOURCE AND LOAD CURRENTS USING VARIOUS CONTROL ALGORITHMS.

SR.NO.	Control algorithm	% THD in load current	% THD in source current
1.	Synchronous Reference Frame (SRF) Theory	27.26% (PFC mode) 27.26%(ZVR mode)	2.20% (PFC mode) 2.04% (ZVR mode)
2.	Instantaneous Reactive Power (IRP) Theory	27.19% (PFC mode) 27.16%(ZVR mode)	3.87% (PFC mode) 3.70% (ZVR mode)
3.	Instantaneous Symmetrical Component (ISC) Theory	27.36% (PFC mode)	3.32% (PFC mode)
4.	Notch Filter	27.26% (PFC mode)	4.25% (PFC mode)

3.3 CONCLUSION

The performance of a VSC based DSTATCOM has been carried out for compensating the harmonics current using various control algorithms in power factor correction mode as well as zero voltage regulation mode. The algorithms discussed in this chapter include Synchronous Reference Frame (SRF) Theory, Instantaneous Reactive Power (IRP) Theory, Modified Instantaneous Symmetrical Component (ISC) Theory and Notch Filter. The proposed algorithms are found to be effective during balanced and unbalance non-linear loads. Table 3.2 shows the Total Harmonic Distortion (THD) in Phase-a of the source and load currents using the control algorithms explained before.

It is observed from the Table that for the same load current having a THD of 27.2%, SRFT gives a THD of 2.20%, IRPT gives THD of 3.87%, ISCT gives a THD of 3.32% and notch filter gives a THD of 4.25% in PFC mode.

Similarly in ZVR mode, SRFT gives a THD of 2.02% and IRPT gives THD of 3.70%, in supply current. All the algorithms are able to meet IEEE 519 standards, and %age of THD in supply currents is reduced to less than 5% level. Also, the performance of SRFT is observed to be best in PFC mode and in ZVR mode as it gives the least THD.

CHAPTER-4

CONTROL OF DSTATCOM UNDER DISTORTED GRID

INTRODUCTION

The function of a DSTATCOM is to compensate the current based power quality disturbances like reactive power, neutral currents, fluctuations, harmonics and unbalanced currents. As seen in previous chapter the performance of DSTATCOM controlled by various control algorithms was quite good [2]. This performance of DSTATCOM was observed when the source was supplying sinusoidal voltages, but in case the voltage is non-sinusoidal in the distribution system, a couple of problems are faced [10]. These problems include [21]:

- Perfect compensation of harmonic currents might not provide unity power factor.
- Perfect unity power factor operation might not provide perfect compensation of harmonics currents.

In this chapter a short review on the performance and structure of existing control algorithms is proposed in presence of non-sinusoidal voltages.

A block diagram of three-leg VSC-based three-phase-three-wire DSTATCOM in presence of non-sinusoidal voltages in the distribution system is shown in Fig. 4.1.

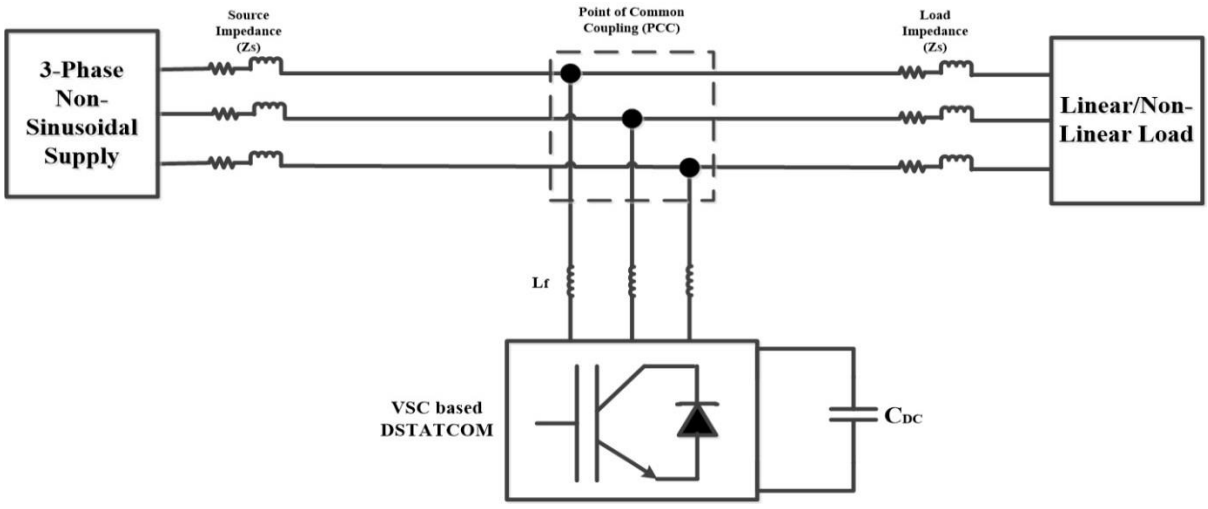

Fig. 4.1: Block Diagram of 3-Phase-3-Wire DSTATCOM in Presence of Non-Sinusoidal Voltages in Distribution System

The control algorithms used in this chapter are based on Instantaneous Reactive Power (IRP) Theory or p-q Theory. IRPT has been used in three different ways to generate the reference source currents for harmonics current compensation in presence of non-sinusoidal voltages in the distribution system. These control algorithms are as follows [21]:

- p-q Theory (PFC mode)
- p-q Theory (ZVR mode)
- Complete Harmonics Elimination (CHE) Theory

4.2 Control Algorithms

Along with the classical p-q theory in PFC and ZVR modes, CHE theory is also discussed.

4.2.1 p-q Theory (PFC mode)

The Instantaneous Reactive Power (IRP) Theory or the p-q Theory is based on a set of instantaneous powers defined in the time-domain. Three phase load currents $(i_{La}, i_{Lb}, i_{Lc})$and PCC Voltages (v_{sa}, v_{sb}, v_{sc}) and the DC bus voltage (V_{dc}) in the distribution system are sensed for generating the reference current signals. A block diagram showing the structure of p-q Theory is shown in Fig. 4.2.

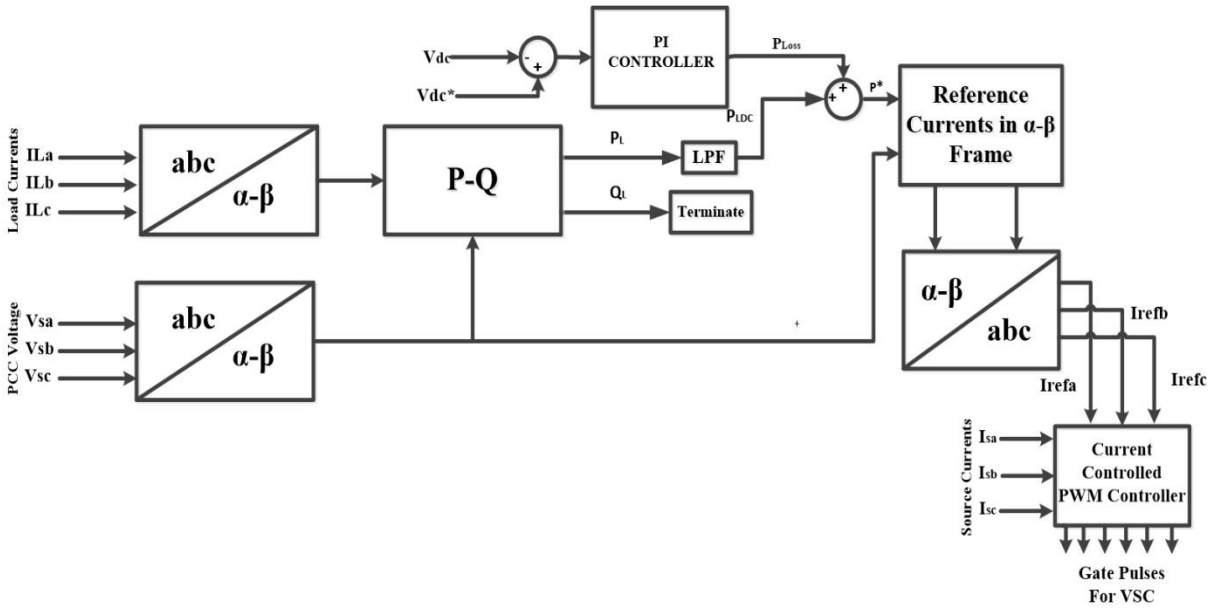

Fig. 4.2: Block Diagram of p-q Theory

4.2.1.1 Control Algorithm [13]

The p-q theory uses $\alpha\beta 0$ transformation, also known as the Clarke transformation to convert three phase voltages and currents in $\alpha\beta 0$ stationary reference frame.

$$\begin{bmatrix} v_\alpha \\ v_\beta \end{bmatrix} = \sqrt{\frac{2}{3}} \begin{bmatrix} 1 & -\frac{1}{2} & -\frac{1}{2} \\ 0 & \frac{\sqrt{3}}{2} & -\frac{\sqrt{3}}{2} \end{bmatrix} \begin{bmatrix} v_{sa} \\ v_{sb} \\ v_{sc} \end{bmatrix} \tag{4.1}$$

$$\begin{bmatrix} i_\alpha \\ i_\beta \end{bmatrix} = \sqrt{\frac{2}{3}} \begin{bmatrix} 1 & -\frac{1}{2} & -\frac{1}{2} \\ 0 & \frac{\sqrt{3}}{2} & -\frac{\sqrt{3}}{2} \end{bmatrix} \begin{bmatrix} i_{La} \\ i_{Lb} \\ i_{Lc} \end{bmatrix} \tag{4.2}$$

Simulation diagram of $\alpha\beta 0$ transformation or the Clarke transformation is shown in Fig. 4.3.

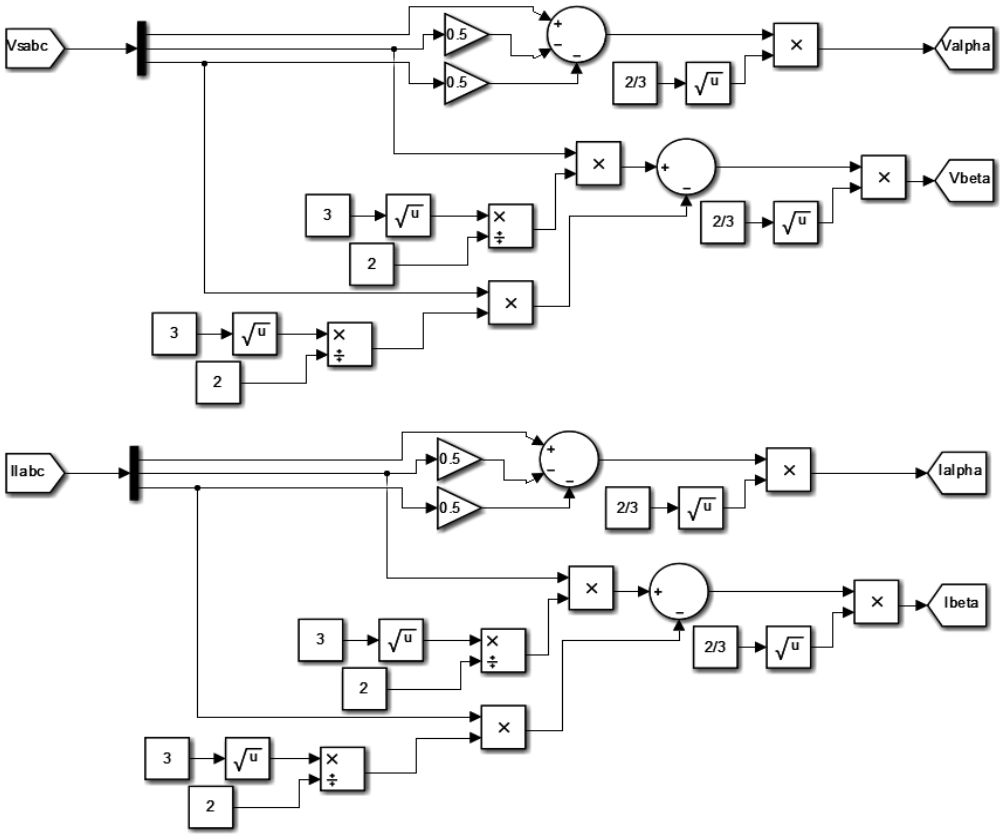

Fig. 4.3: Simulation Diagram of Clarke Transformation

The instantaneous active and reactive powers are calculated as:

$$\begin{bmatrix} P_L \\ Q_L \end{bmatrix} = \begin{bmatrix} v_\alpha & v_\beta \\ v_\beta & -v_\alpha \end{bmatrix} \begin{bmatrix} i_\alpha \\ i_\beta \end{bmatrix} \tag{4.3}$$

As these powers contain both the AC and DC components the AC component needs to be filtered out using a low pass filter.

$$\begin{bmatrix} P_L \\ Q_L \end{bmatrix} = \begin{bmatrix} \bar{P}_L + \tilde{P}_L \\ \bar{Q}_L + \tilde{Q}_L \end{bmatrix} \tag{4.4}$$

Here, $\bar{P}_L$ and $\bar{Q}_L$ are the DC components and $\tilde{P}_L$ and $\tilde{Q}_L$ are the AC components of the instantaneous active and reactive powers. A PI controllers is used to regulate the DC bus voltage 'V_{dc}'.

The error in DC bus Voltage at n^{th} sampling instant between the reference DC bus voltage 'V_{dc}^*' and the sensed DC bus voltage 'V_{dc}' is given as:

$$V_{DC}(n) = V_{dc}^*(n) - V_{dc}(n) \tag{4.5}$$

The output of the DC PI controller is known as the active power component loss 'P_{Loss}'

$$P_{Loss}(n) = P_{Loss}(n-1) + K_{pd}\{V_{DC}(n) - V_{DC}(n-1)\} + K_{pi}V_{DC}(n) \tag{4.6}$$

Here, K_{pd} and K_{id} are the proportional and integral gain of the PI controller respectively. P_{Loss} is added to the DC component of active power '$\bar{P}_L$' to acquire the fundamental component of active power given by 'P'.

$$P = \bar{P}_L + P_{Loss} \tag{4.7}$$

In Power Factor Correction (PFC) mode the instantaneous reactive power is not used for estimating the reference supply currents so,

$$Q = \bar{Q}_L + Q_{Loss} = 0$$

(4.8) Fig. 4.4 shows the simulation diagram of calculation of fundamental component of instantaneous active and reactive powers.

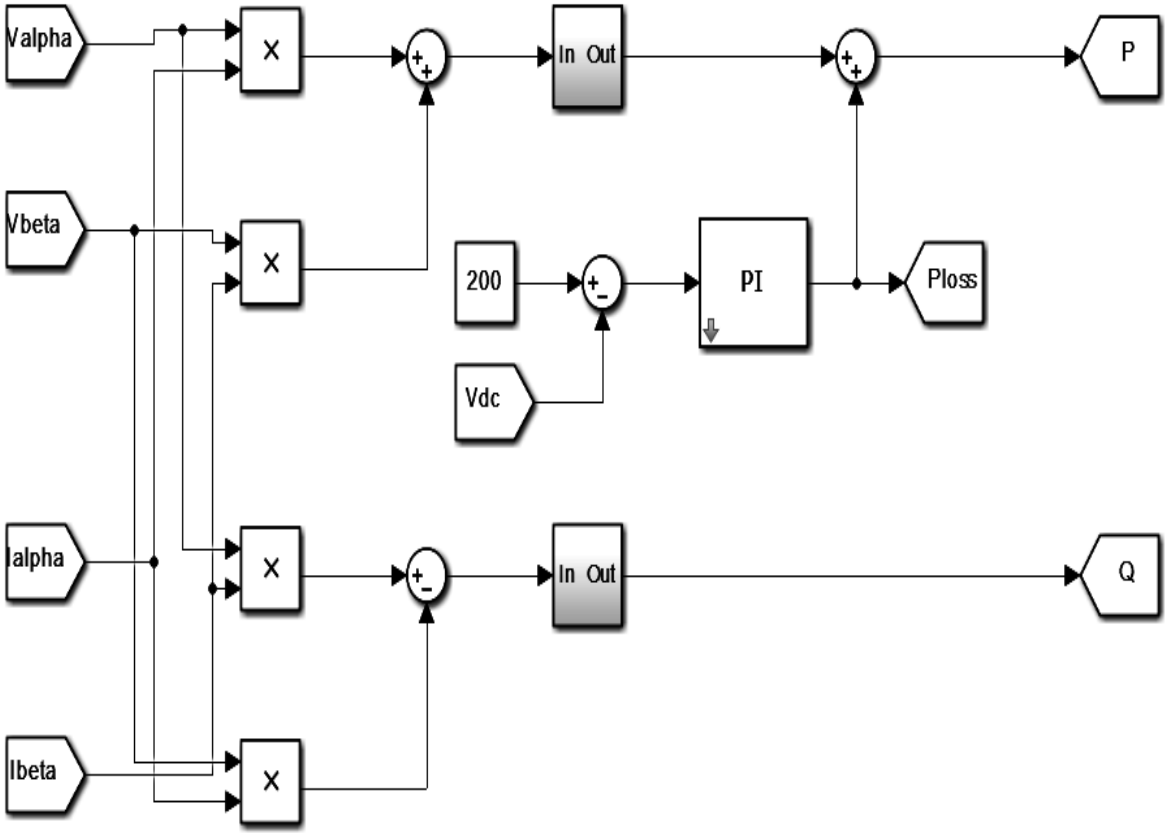

Fig.4.4: Simulation Diagram for Calculation of Fundamental Component of Instantaneous Active and Reactive Powers

The fundamental components of active power is used to obtain the reference currents in α-β frame known as 'i_α^*' and 'i_β^*'.

$$\begin{bmatrix} i_\alpha^* \\ i_\beta^* \end{bmatrix} = \frac{1}{V_\alpha^2 + V_\beta^2} \begin{bmatrix} v_\alpha & v_\beta \\ v_\beta & -v_\alpha \end{bmatrix} \begin{bmatrix} P \\ 0 \end{bmatrix} \quad (4.9)$$

Fig. 4.5 shows the simulation diagram of calculation of reference currents in α-β frame.

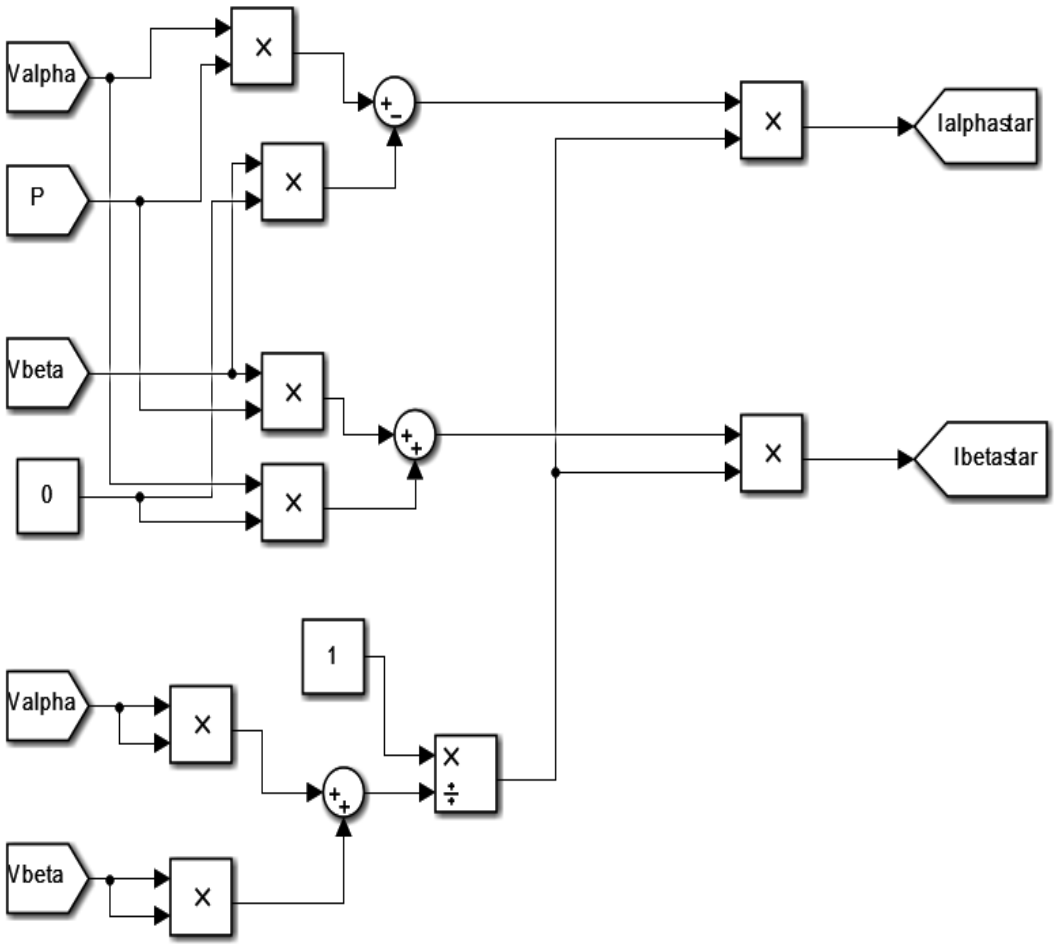

Fig. 4.5: Simulation Diagram of Calculation of Reference Currents in α-β Frame in PFC Mode.

The reference three-phase supply currents are estimated by inverse Clarke Transformation shown as:

$$\begin{bmatrix} i_{refa} \\ i_{refb} \\ i_{refc} \end{bmatrix} = \sqrt{\frac{2}{3}} \begin{bmatrix} 1 & 0 \\ -\frac{1}{2} & \frac{\sqrt{3}}{2} \\ -\frac{1}{2} & -\frac{\sqrt{3}}{2} \end{bmatrix} \begin{bmatrix} i_{\alpha}^{*} \\ i_{\beta}^{*} \end{bmatrix} \tag{4.10}$$

The Simulation diagram of estimation of reference three-phase supply currents by inverse Clarke transformation is shown in Fig. 4.6.

The generated reference currents are compared with the sensed source currents in order to generate the gating pulses required by the VSC based DSTATCOM.

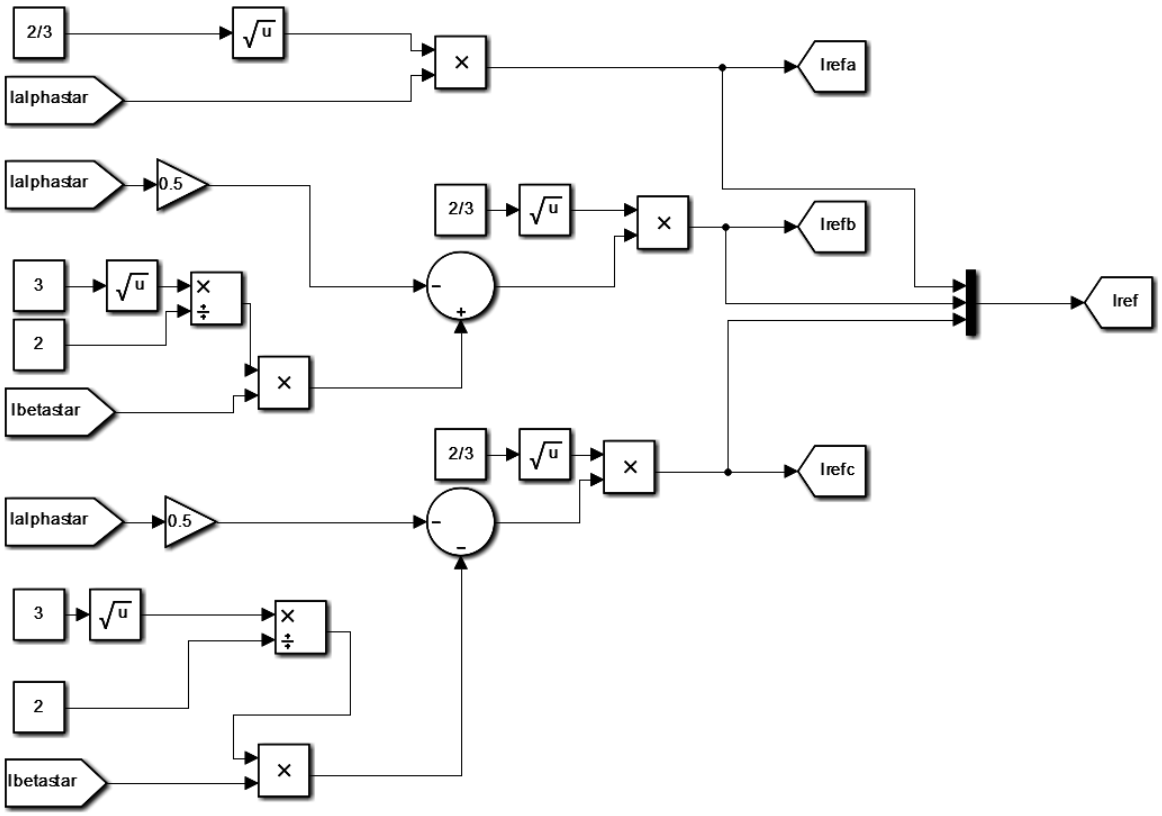

Fig. 4.6: Simulation Diagram of Estimation of Reference Three-Phase Supply Currents by Inverse Clarke Transformation.

4.2.1.2 Results with p-q Theory in PFC mode Under Distorted Grid

The performance of VSC based DSTATCOM controlled by p-q theory in PFC mode under distorted grid is observed in Fig. 4.8. The results of the intermediate in the control algorithm are also shown in Fig. 4.7.The intermediate signals shown in the figure includes a plot of $(v_\alpha, v_\beta), (i_\alpha, i_\beta), P, i_\alpha^*, i_\beta^*, P_{Loss} and\ i_{ref}$ in all three phases.

In Fig.4.8 , it is observed that the PCC voltage is non-sinusoidal, the phase 'a' of three phase non-linear load is disconnected at time t=3.2 sec. as we can see the dc link voltage V_{dc} rises momentarily and slowly starts to settle down at 200V. The generated reference currents are also non-sinusoidal in this case.

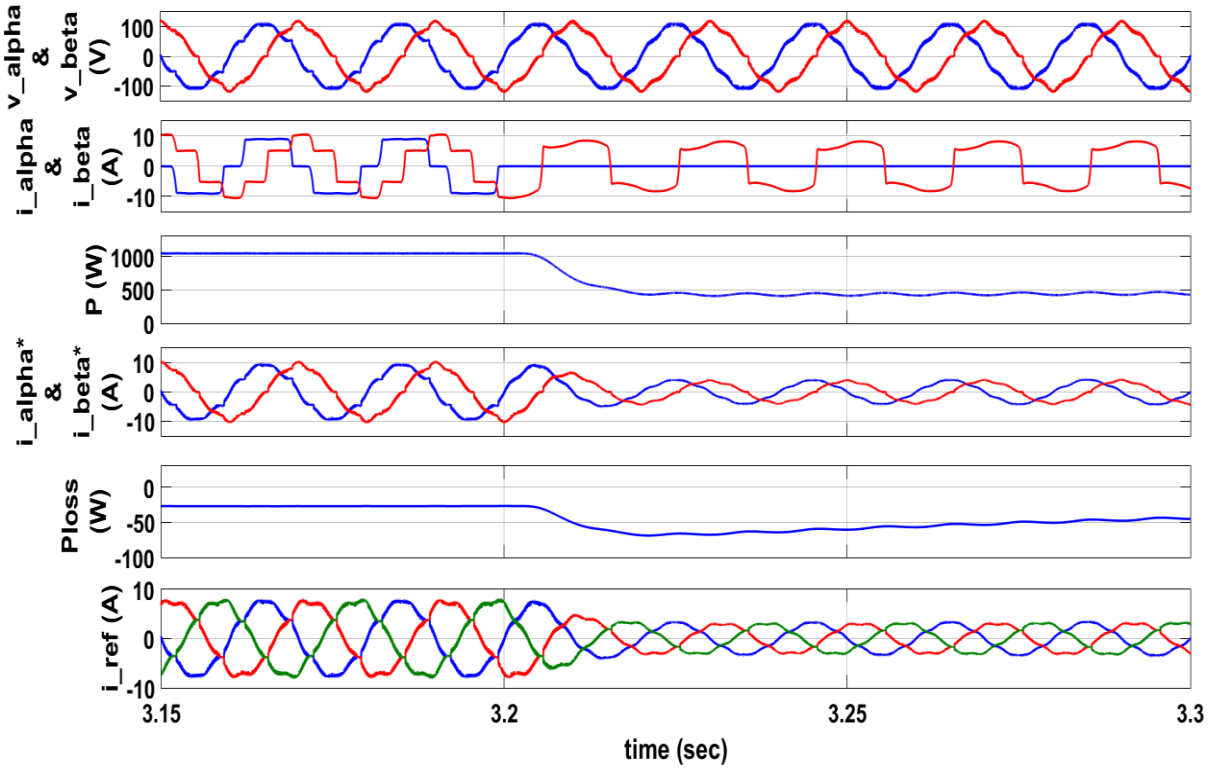

Fig. 4.7: Intermediate Results using p-q Theory in PFC mode Under Distorted Grid.

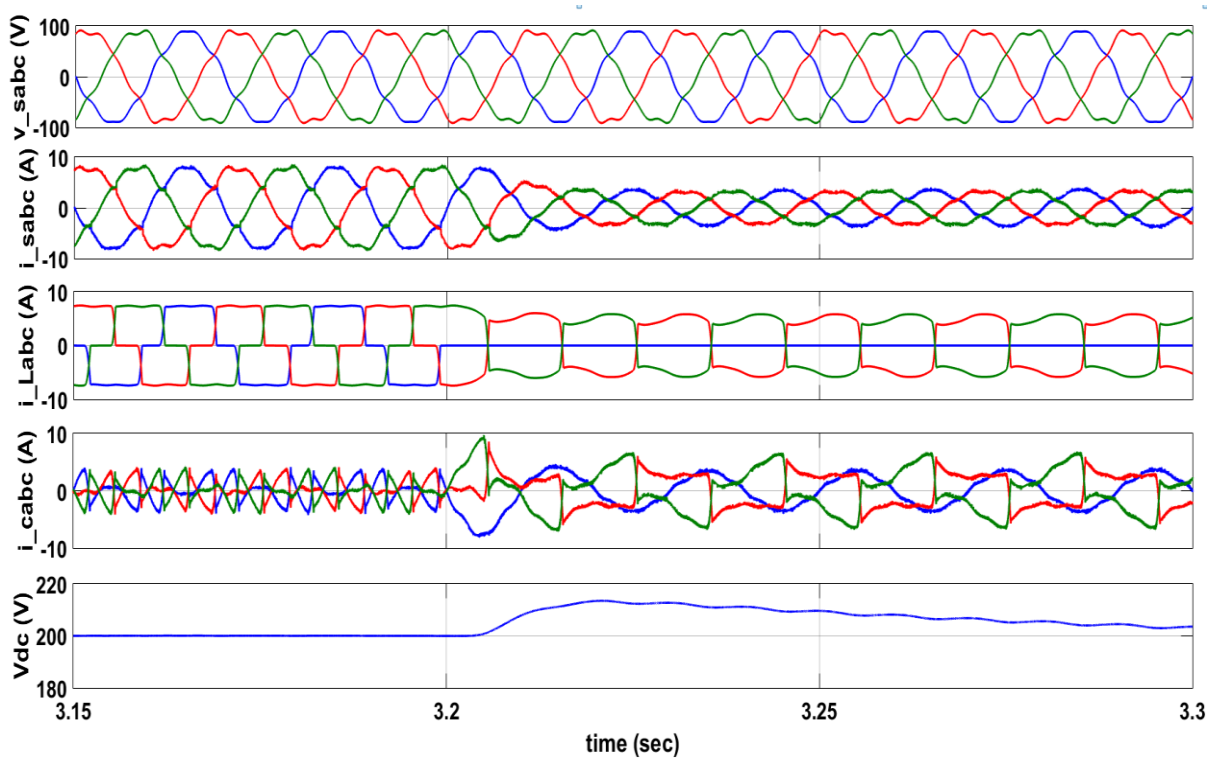

Fig. 4.8: Performance of DSTATCOM controlled by p-q theory (PFC mode) under distorted grid

The FFT Analysis of PCC Voltage, Load Current, Source Current, intermediate and the performance of DSTATCOM controlled by p-q theory in PFC mode under non-sinusoidal voltage in distribution system are shown below. The Total Harmonic Disorder (THD) in %age for the load current is observed to be 24.75%, PCC voltage 6.40% and the source current 8.52%.

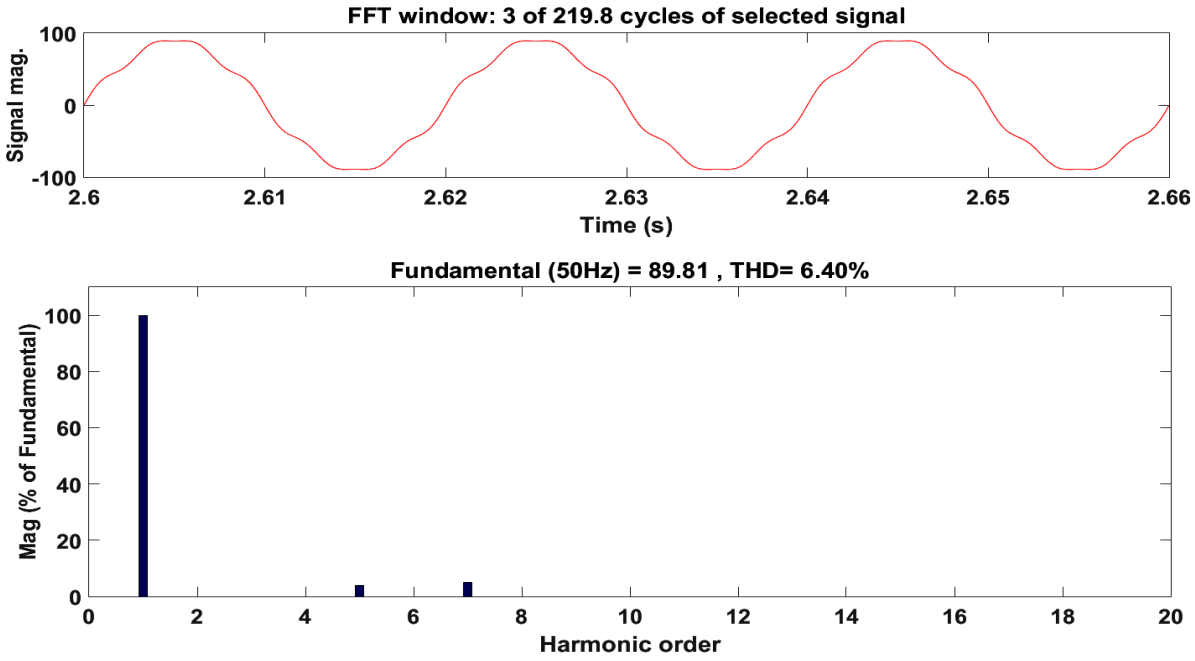

Fig. 4.9: FFT Analysis of PCC Voltage

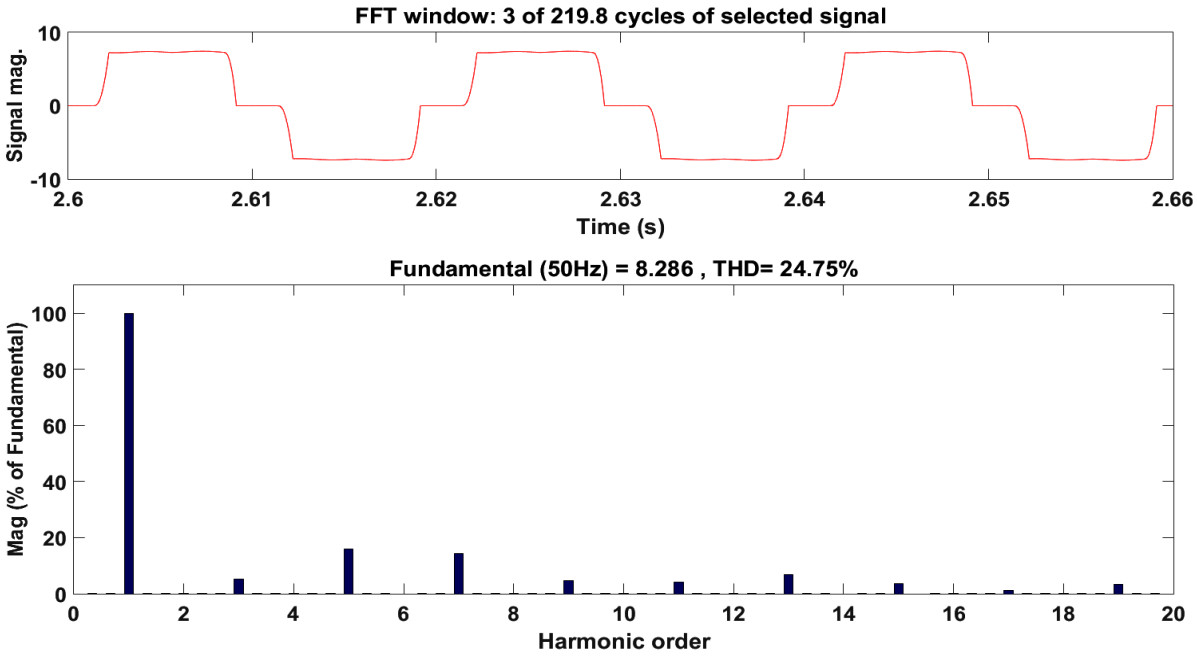

Fig. 4.10: FFT Analysis of Load Current

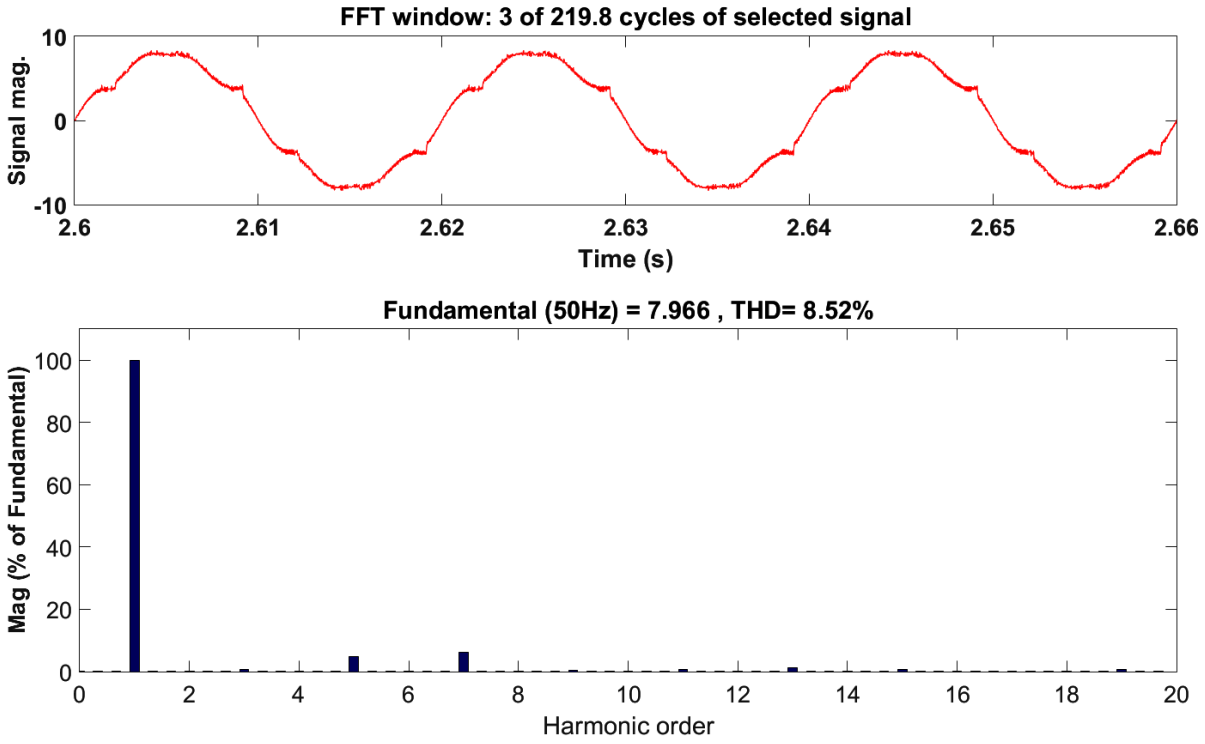

Fig. 4.11: FFT Analysis of Source Current

4.2.2 p-q Theory (ZVR mode) [2]

A block diagram of modified p-q theory is shown in Fig. 4.12.

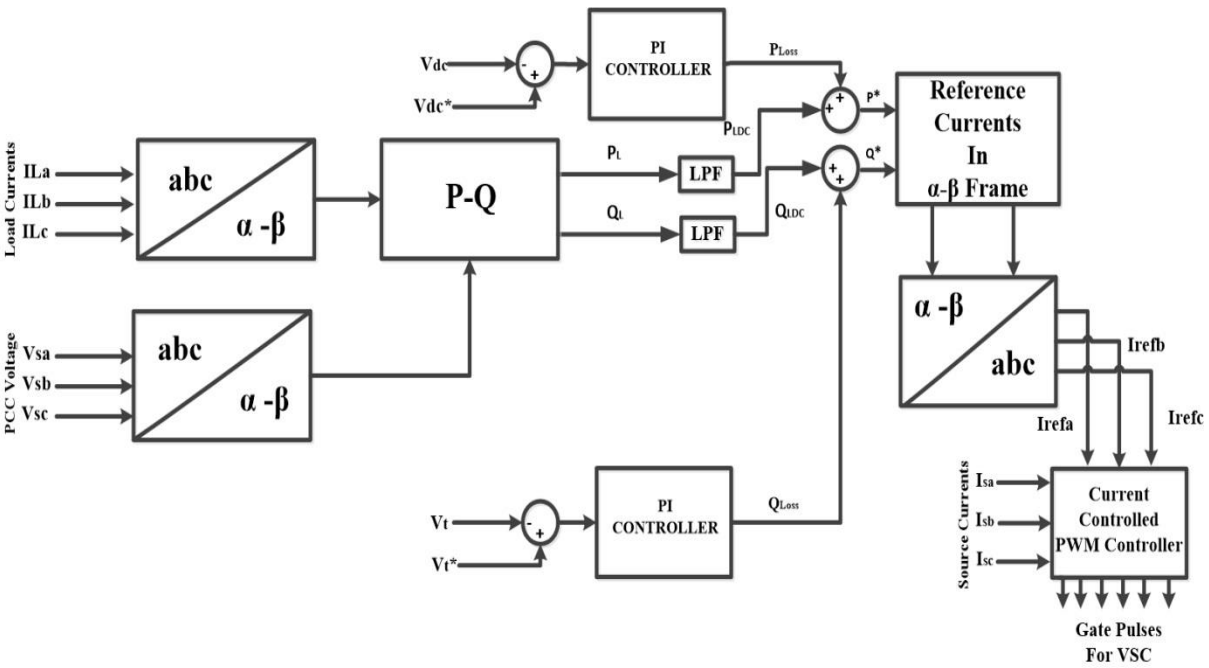

Fig. 4.12: Block Diagram of Modified p-q Theory.

4.2.2.1 Control Algorithm

Three phase load currents(i_{La}, i_{Lb}, i_{Lc}), PCC Voltages (v_{sa}, v_{sb}, v_{sc}) and the DC bus voltage (V_{dc}) in the distribution system are sensed for generating the reference current signals. The modified p-q theory also uses $\alpha\beta 0$ transformation, also known as the Clarke transformation to convert three phase voltages and currents in $\alpha\beta 0$ stationary reference frame.

$$\begin{bmatrix} v_\alpha \\ v_\beta \end{bmatrix} = \sqrt{\frac{2}{3}} \begin{bmatrix} 1 & -\frac{1}{2} & -\frac{1}{2} \\ 0 & \frac{\sqrt{3}}{2} & -\frac{\sqrt{3}}{2} \end{bmatrix} \begin{bmatrix} v_{sa} \\ v_{sb} \\ v_{sc} \end{bmatrix} \tag{4.11}$$

$$\begin{bmatrix} i_\alpha \\ i_\beta \end{bmatrix} = \sqrt{\frac{2}{3}} \begin{bmatrix} 1 & -\frac{1}{2} & -\frac{1}{2} \\ 0 & \frac{\sqrt{3}}{2} & -\frac{\sqrt{3}}{2} \end{bmatrix} \begin{bmatrix} i_{La} \\ i_{Lb} \\ i_{Lc} \end{bmatrix} \tag{4.12}$$

Simulation diagram of $\alpha\beta 0$ transformation or Clarke transformation is shown in Fig. 4.13.

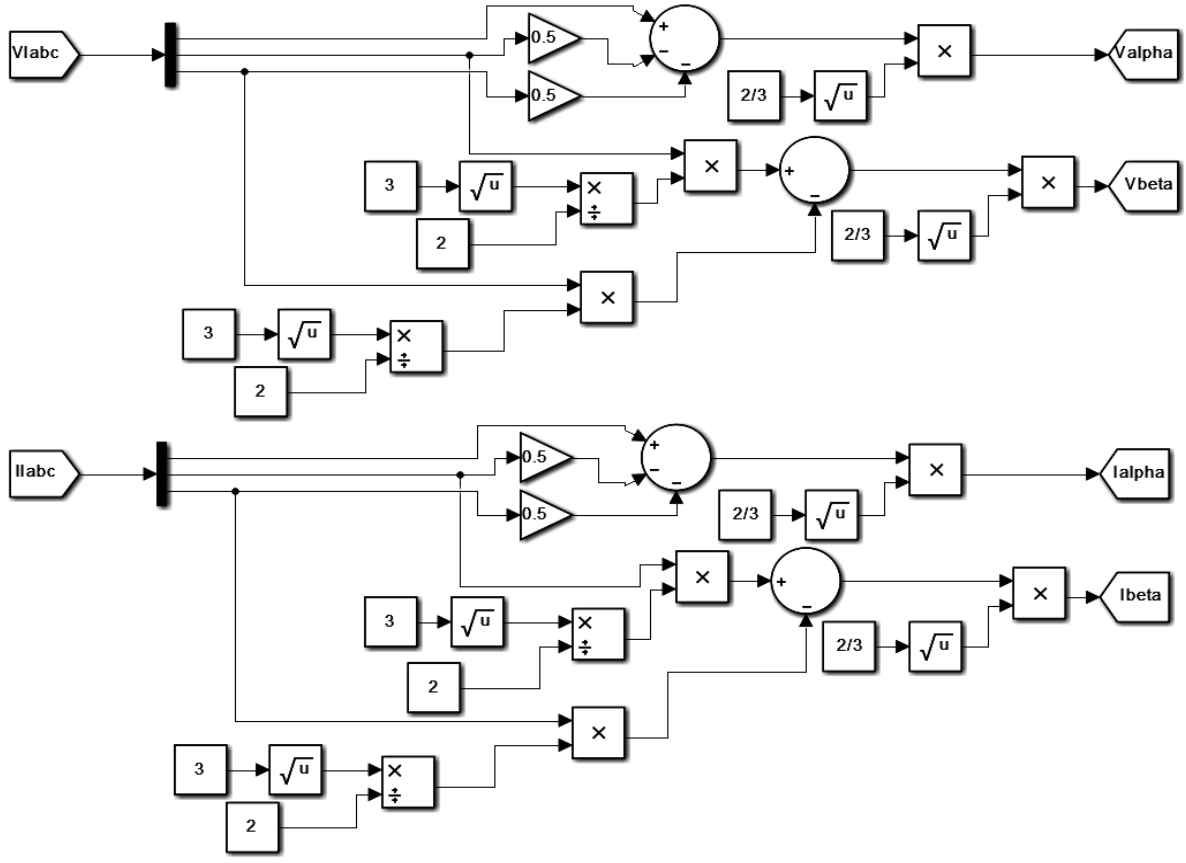

Fig. 4.13: Simulation Diagram of Clarke Transformation

The instantaneous active and reactive powers are calculated as:

$$\begin{bmatrix} P_L \\ Q_L \end{bmatrix} = \begin{bmatrix} V_\alpha & V_\beta \\ V_\beta & -V_\alpha \end{bmatrix} \begin{bmatrix} I_\alpha \\ I_\beta \end{bmatrix} \tag{4.13}$$

As these powers contain both the AC and DC components the AC component needs to be filtered out using a low pass filter.

$$\begin{bmatrix} P_L \\ Q_L \end{bmatrix} = \begin{bmatrix} \bar{P}_L + \tilde{P}_L \\ \bar{Q}_L + \tilde{Q}_L \end{bmatrix} \tag{4.14}$$

Here, $\bar{P}_L$ and $\bar{Q}_L$ are the DC components and $\tilde{P}_L$ and $\tilde{Q}_L$ are the AC components of the instantaneous active and reactive powers. A PI controllers is used to regulate the DC bus voltage 'V_{dc}'.

The error in DC bus Voltage at nth sampling instant between the reference DC bus voltage 'V_{dc}^*' and the sensed DC bus voltage 'V_{dc}' is given as:

$$V_{DC}(n) = V_{dc}^*(n) - V_{dc}(n) \tag{4.15}$$

The output of the DC PI controller is known as the active power component loss 'P_{Loss}'

$$P_{Loss}(n) = P_{Loss}(n-1) + K_{pd}\{V_{DC}(n) - V_{DC}(n-1)\} + K_{pi}V_{DC}(n) \tag{4.16}$$

Here, K_{pd} and K_{id} are the proportional and integral gain of the PI controller respectively. P_{Loss} is added to the DC component of active power '$\bar{P}_L$' to acquire the fundamental component of active power given by 'P'. Q_{Loss} is added to the DC component of reactive power $\bar{Q}_L$ to acquire the fundamental component of reactive power given by 'Q'.

$$P = \bar{P}_L + P_{Loss} \tag{4.17}$$

The error in PCC voltage at nth sampling instant between the amplitude of the reference PCC voltage 'V_t^*' and the amplitude of sensed PCC voltage 'V_t' is given as:

$$V_{te}(n) = V_t^*(n) - V_t(n) \tag{4.18}$$

$$V_t = \sqrt{\frac{2}{3}(V_{sa}^2 + V_{sb}^2 + V_{sc}^2)} \tag{4.19}$$

The output of the second PI controller is used to maintain constant PCC voltage at nth sampling instant and is given by 'Q_{Loss}'.

$$Q_{Loss}(n) = Q_{Loss}(n-1) + K_{pd}\{V_{te}(n) - V_{te}(n-1)\} + K_{pi}V_{te}(n) \tag{4.20}$$

Here, K_{pd} and K_{id} are the proportional and integral gain of the PI controller respectively. Q_{Loss} is added to the DC component of active power '$\bar{Q}_L$' to acquire the fundamental component of active power given by 'Q'.

$$Q = \bar{Q}_L + Q_{Loss} \tag{4.21}$$

Fig. 4.14 shows the simulation diagram of calculation of fundamental component of instantaneous active and reactive powers.

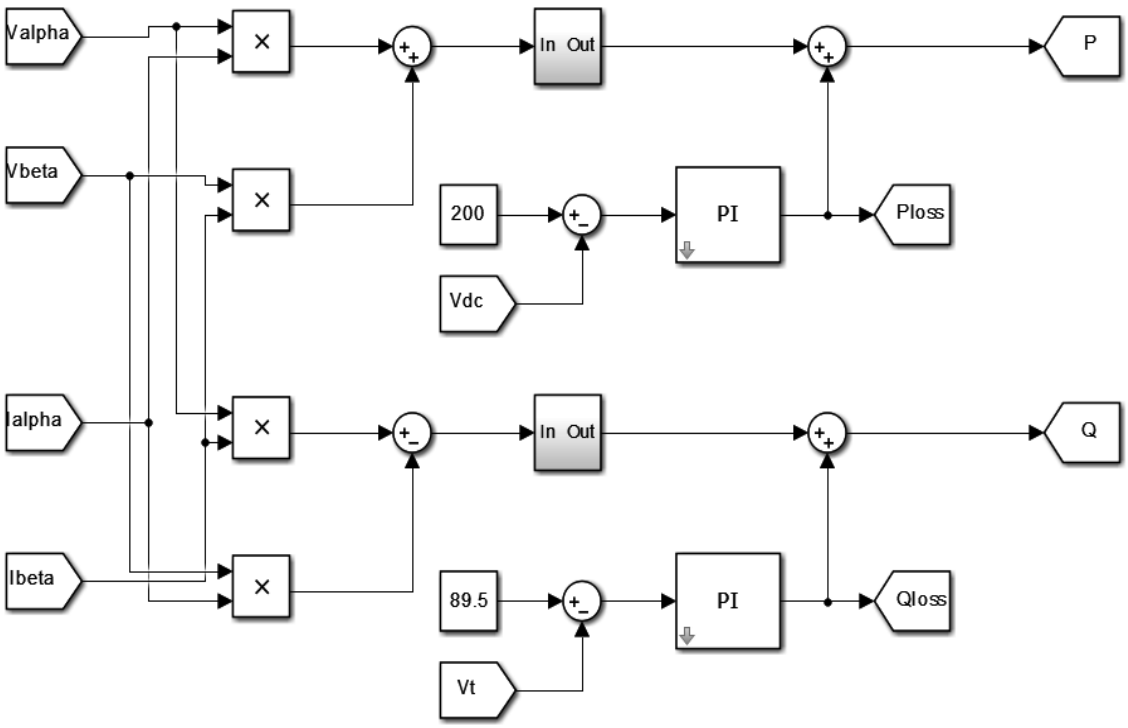

Fig. 4.14: Fundamental Component of Instantaneous Active and Reactive Powers

The fundamental components of active power is used to obtain the reference currents in α-β frame known as 'i_α^*' and 'i_β^*'.

$$\begin{bmatrix} i_\alpha^* \\ i_\beta^* \end{bmatrix} = \frac{1}{V_\alpha^2 + V_\beta^2} \begin{bmatrix} v_\alpha & v_\beta \\ v_\beta & -v_\alpha \end{bmatrix} \begin{bmatrix} P \\ Q \end{bmatrix} \tag{4.22}$$

Fig. 4.15 shows the simulation diagram of calculation of reference currents in α-β frame.

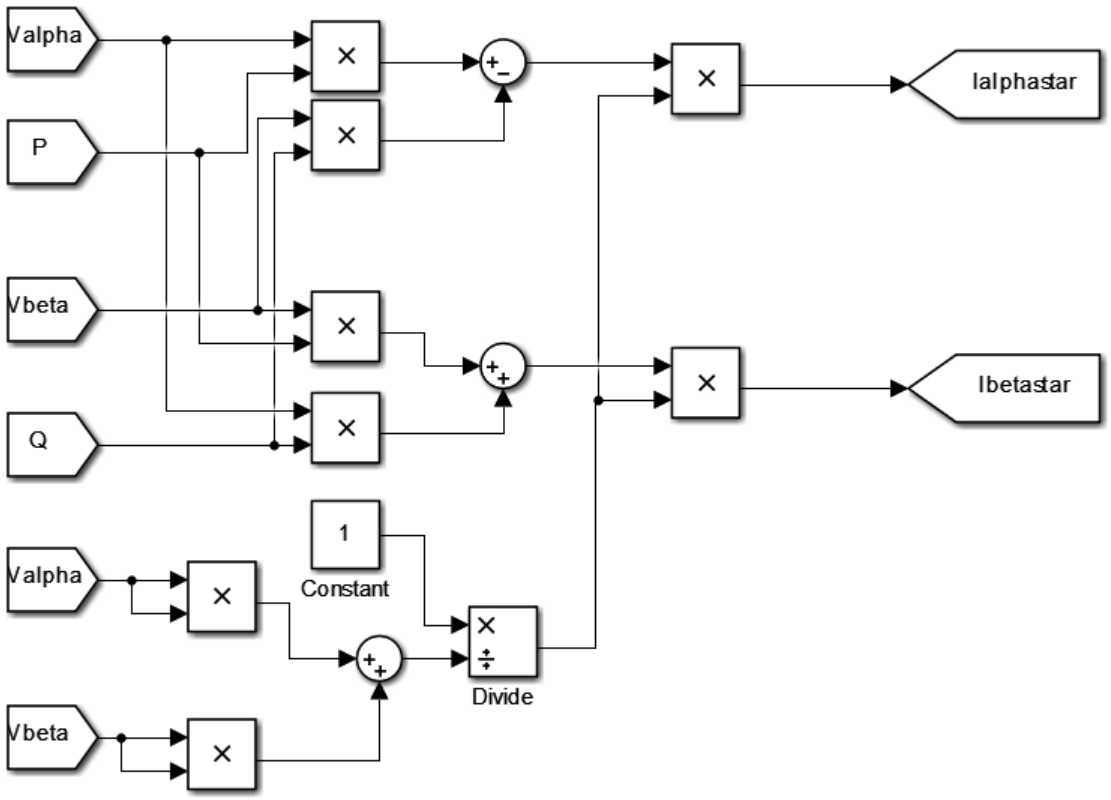

Fig. 4.15: Simulation Diagram of Calculation of Reference Currents in α-β Frame in ZVR Mode

The reference three-phase supply currents are estimated by inverse Clarke Transformation shown as:

$$\begin{bmatrix} i_{refa} \\ i_{refb} \\ i_{refc} \end{bmatrix} = \sqrt{\frac{2}{3}} \begin{bmatrix} 1 & 0 \\ -\frac{1}{2} & \frac{\sqrt{3}}{2} \\ -\frac{1}{2} & -\frac{\sqrt{3}}{2} \end{bmatrix} \begin{bmatrix} i_\alpha^* \\ i_\beta^* \end{bmatrix} \tag{4.23}$$

The Simulation diagram of estimation of reference three-phase supply currents by inverse Clarke transformation is shown in Fig. 4.16.

The generated reference currents are compared with the sensed source currents in order to generate the gating pulses required by the VSC based DSTATCOM.

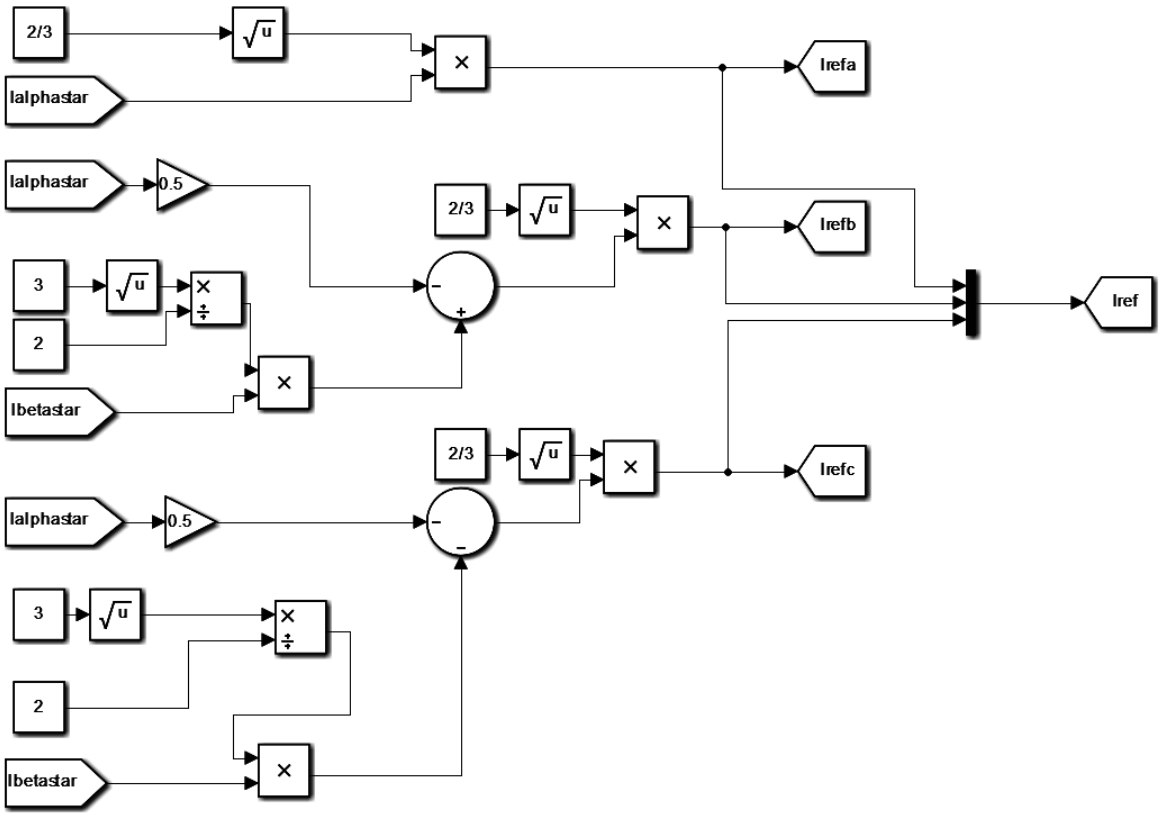

Fig.4.16: Simulation Diagram of Estimation of Reference Three-Phase Supply Currents by Inverse Clarke Transformation

4.2.2.1 Results with p-q Theory in ZVR mode Under Distorted Grid

The performance of VSC based DSTATCOM controlled by p-q theory in ZVR mode under distorted grid is observed in Fig. 4.18, the results of the intermediate in the control algorithm are also shown in Fig. 4.17.

These include waveforms for $v_\alpha, v_\beta, i_\alpha, i_\beta, P, Q, i_\alpha^*, i_\beta^*, P_{Loss}, Q_{Loss} and\ i_{ref}$.

In Fig.4.18 as we can see the PCC voltage is non-sinusoidal, the phase 'a' of three phase non-linear load is disconnected at time t=1.05 sec. as we can see the dc link voltage V_{dc} rises momentarily and slowly starts to settle down at 200V. The magnitude of PCC voltage is also regulated in ZVR mode, as the input voltages are distorted there is a lot

of oscillations in the magnitude of PCC voltage but at time t=1.05 sec the magnitude of PCC voltage rises momentarily and slowly begins to settle down near 89.8V.

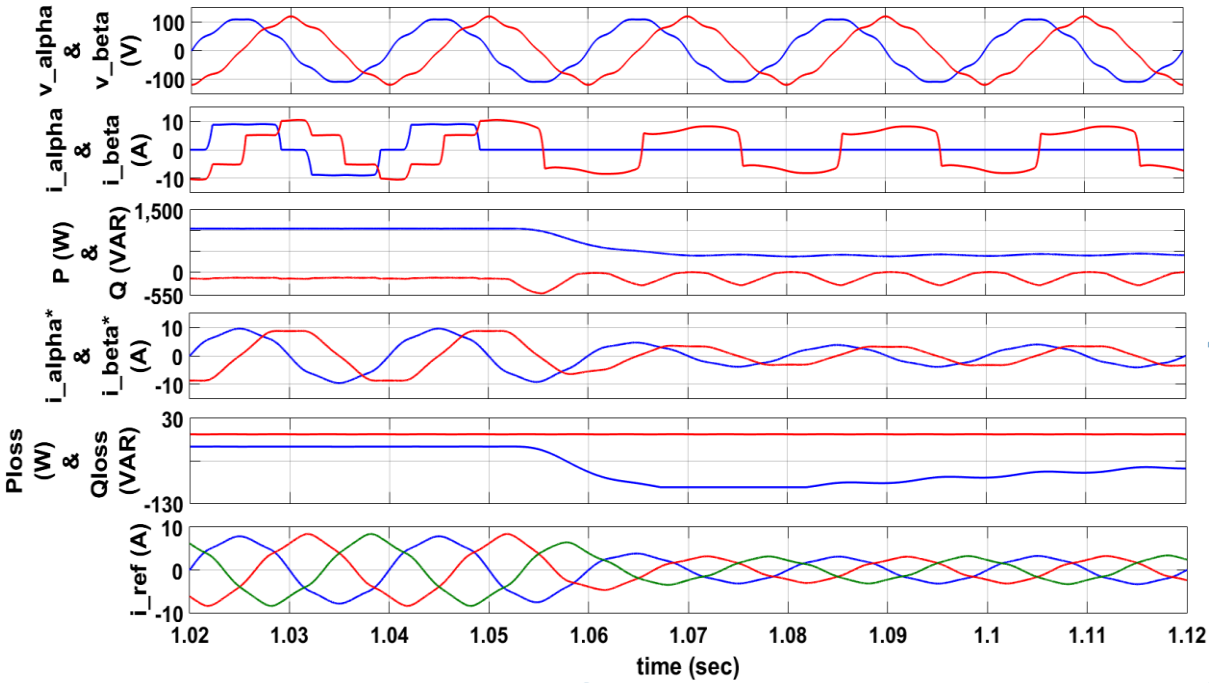

Fig. 4.17: Intermediate Results for p-q Theory in ZVR mode Under Distorted Grid

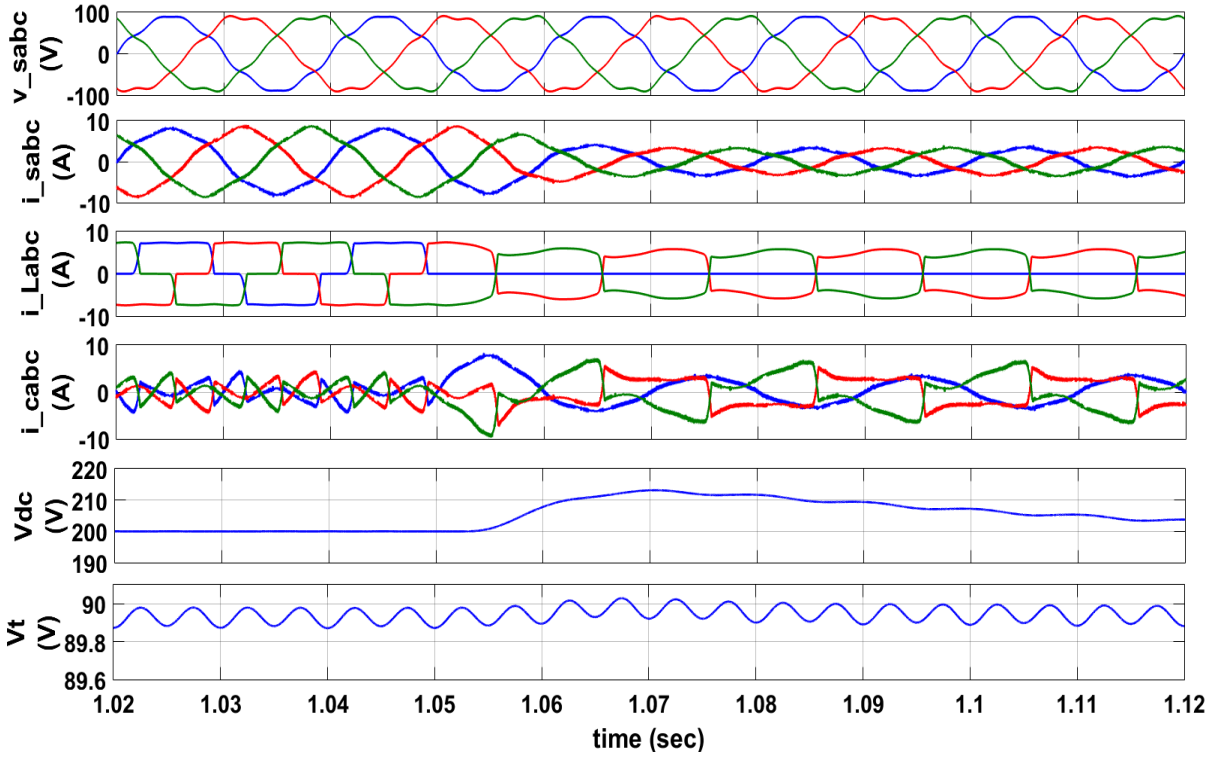

Fig. 4.18: Performance of DSTATCOM controlled by p-q theory (ZVR mode) under distorted grid

The FFT Analysis of PCC Voltage, Load Current, Source Current, intermediate and the performance of DSTATCOM controlled by p-q theory in ZVR modes under non-sinusoidal voltage in distribution system are shown. The Total Harmonic Disorder (THD) in %age of the load current is observed to be 24.74%, PCC voltage 6.40% and the source current 7.60%. The source currents are observed to have high distortion index.

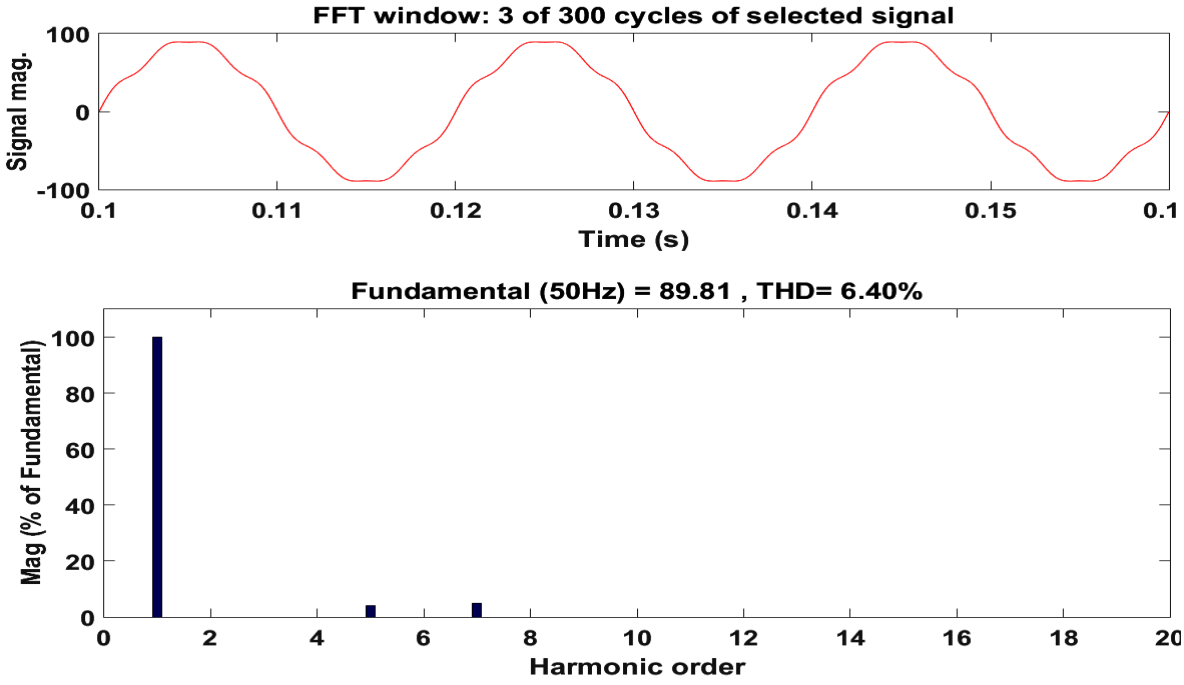

Fig. 4.19: FFT Analysis of PCC Voltage

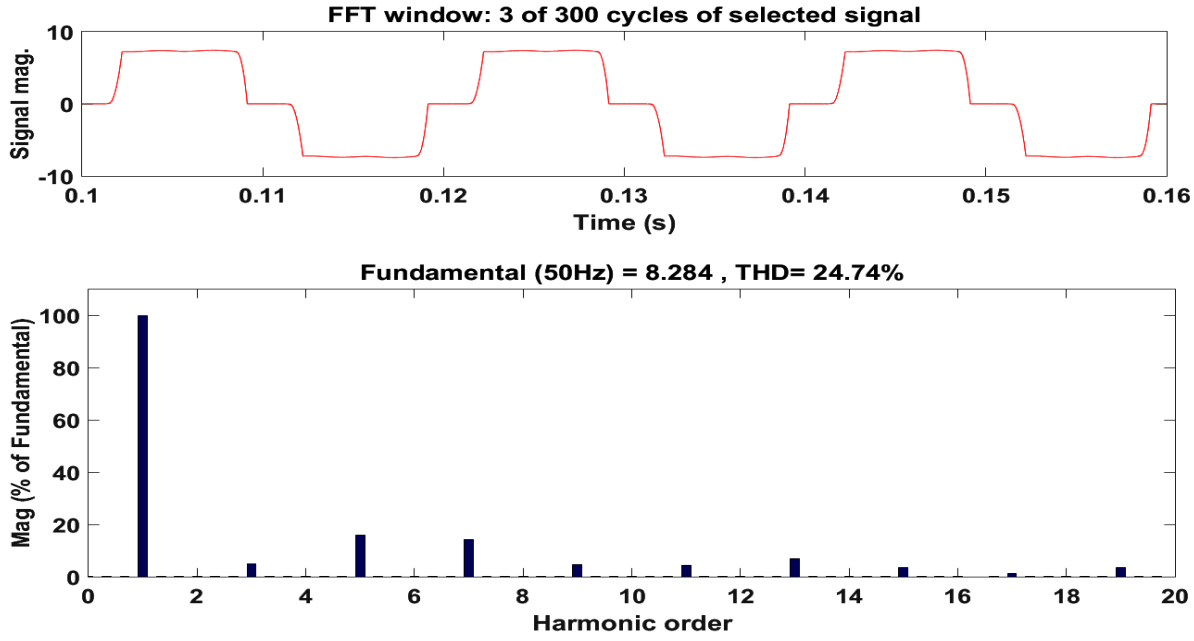

Fig. 4.20: FFT Analysis of Load Current

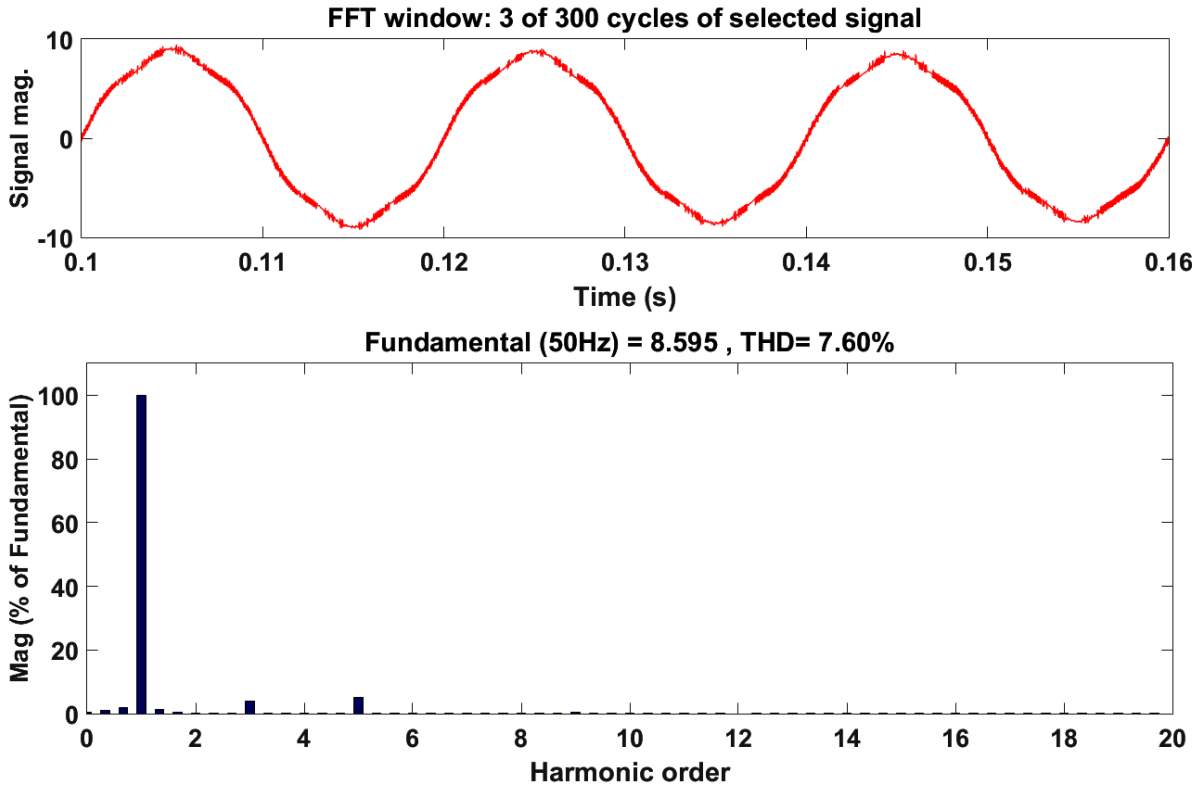

Fig. 4.21: FFT Analysis of Source Current

4.2.3 Complete Harmonic Elimination mode [20]

Both PFC and ZVR mode are observed to be incapable of completely eliminating the harmonics currents, so a modification of the PFC mode for harmonic elimination in the distribution system is considered. So in Complete Harmonic Elimination strategy, the three phase voltages and load currents are transformed into αβ0 stationary reference frame by Clarke Transformation as shown in Eq 4.1 and Eq. 4.2. The instantaneous value of load active power is calculated as shown in Fig 4.3 to Fig 4.8.

The DC component of load active power is filtered out using a low pass filter. The fundamental value of 'v_α' and 'v_β' are $\dot{v}_\alpha$, $\dot{v}_\beta$ obtained by using two band-pass filters tuned to extract the fundamental components of these voltages.

The band pass filters used to extract the fundamental components of v_α' and 'v_β' comprises of a second order butter-worth filter with a lower pass-band frequency of $2\pi 40$ rad/sec and an upper pass-band frequency of $2\pi 60$ rad/sec.

The reference currents generated using these components in α-β frame known as 'I_{α}^{*}' and 'I_{β}^{*}'.

$$\begin{bmatrix} i_{\alpha}^{*} \\ i_{\beta}^{*} \end{bmatrix} = \frac{\bar{P}_L}{v_{\alpha}^2 + v_{\beta}^2} \begin{bmatrix} v_{\alpha} \\ v_{\beta} \end{bmatrix} \quad (4.24)$$

Fig 4.22 shows the simulation diagram of generation of reference source currents in α-β frame.

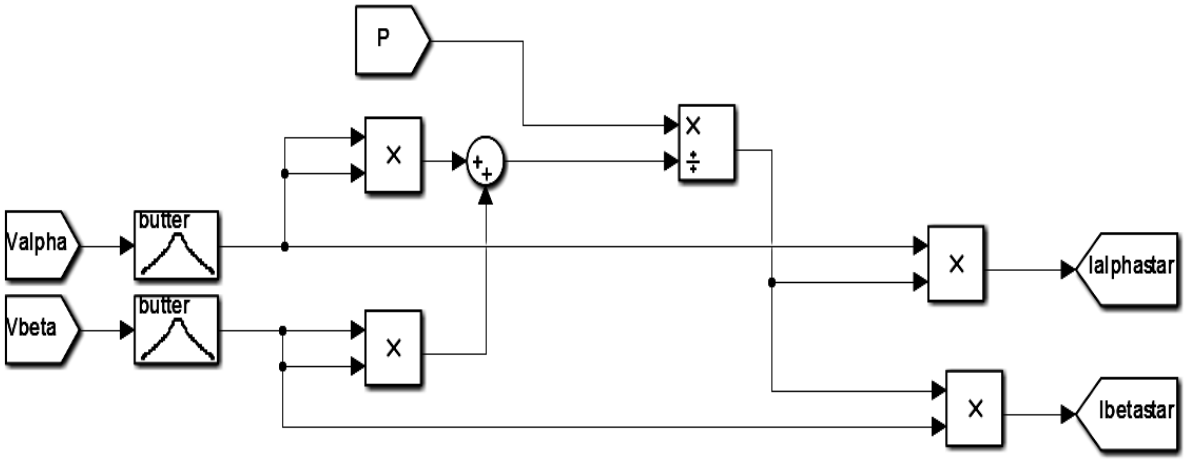

Fig. 4.22: Simulation of Extracting Reference Source Currents in α-β Frame using CHE.

The reference source currents in a-b-c frame can be calculated using Eq.4.10. The essence of CHE strategy focuses on filtering the distorted voltages first and using filtered $\bar{P}_L$. Once the reference source currents are generated, these are compared with the sensed source currents (i_{sa}, i_{sb}, i_{sc}) to generate gating pulses of VSC based DSTATCOM.

4.2.3.2 Results with Complete Harmonic Elimination.

The performance of VSC based DSTATCOM controlled by p-q theory in ZVR mode under distorted grid is observed in Fig. 4.24 and the results of the intermediate in the control algorithm are also shown in Fig. 4.23.

In Fig.4.24 as we can see the PCC voltage is non-sinusoidal, the phase 'a' of three phase non-linear load is disconnected at time t=4.2 sec. as we can see the dc link voltage V_{dc} rises momentarily and slowly starts to settle down at 200V.

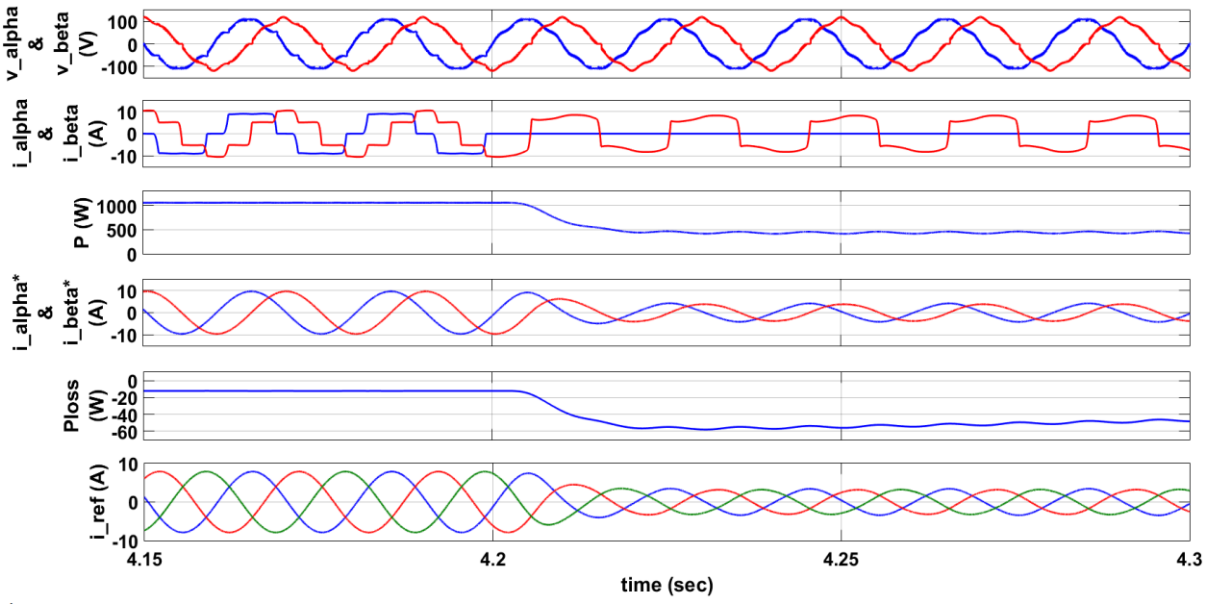

Fig. 4.23: Intermediate Results with CHE

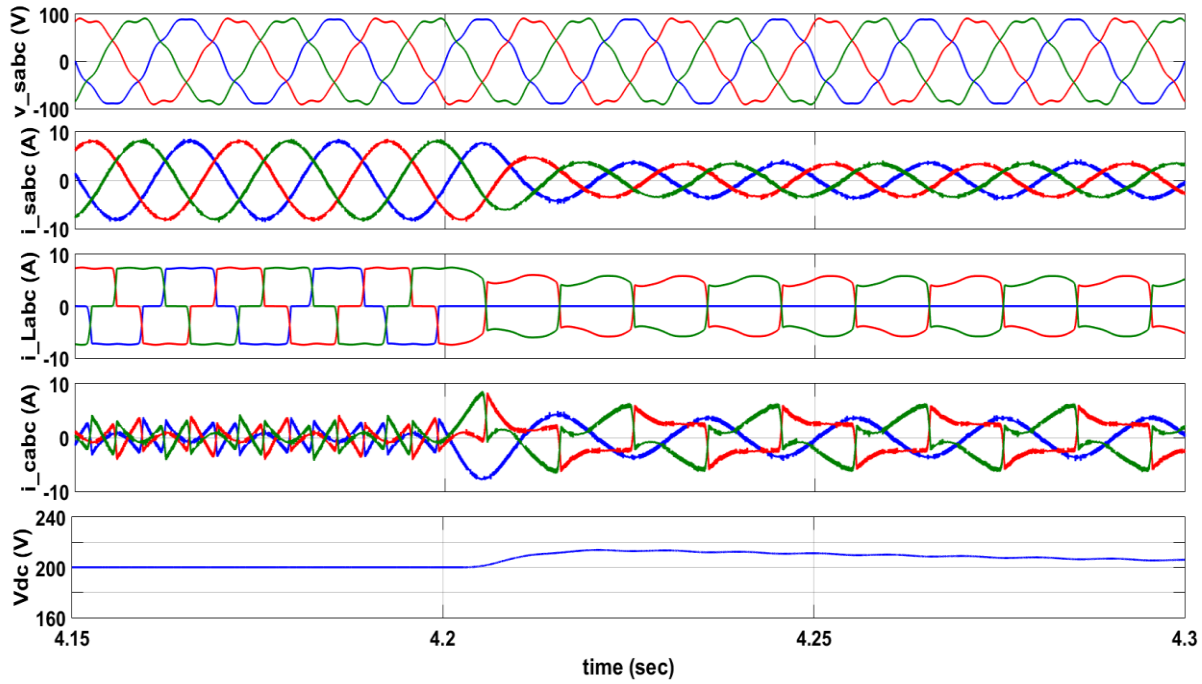

Fig. 4.24: Performance of DSTATCOM controlled by CHE under distorted grid

The FFT Analysis of PCC Voltage, Load Current, Source Current, intermediate and the performance of DSTATCOM controlled by CHE under non-sinusoidal voltage in distribution system are shown below. The Total Harmonic Disorder (THD) in %age of

the load current is observed to be 24.75%, PCC voltage 6.40% and the source current 3.64%.

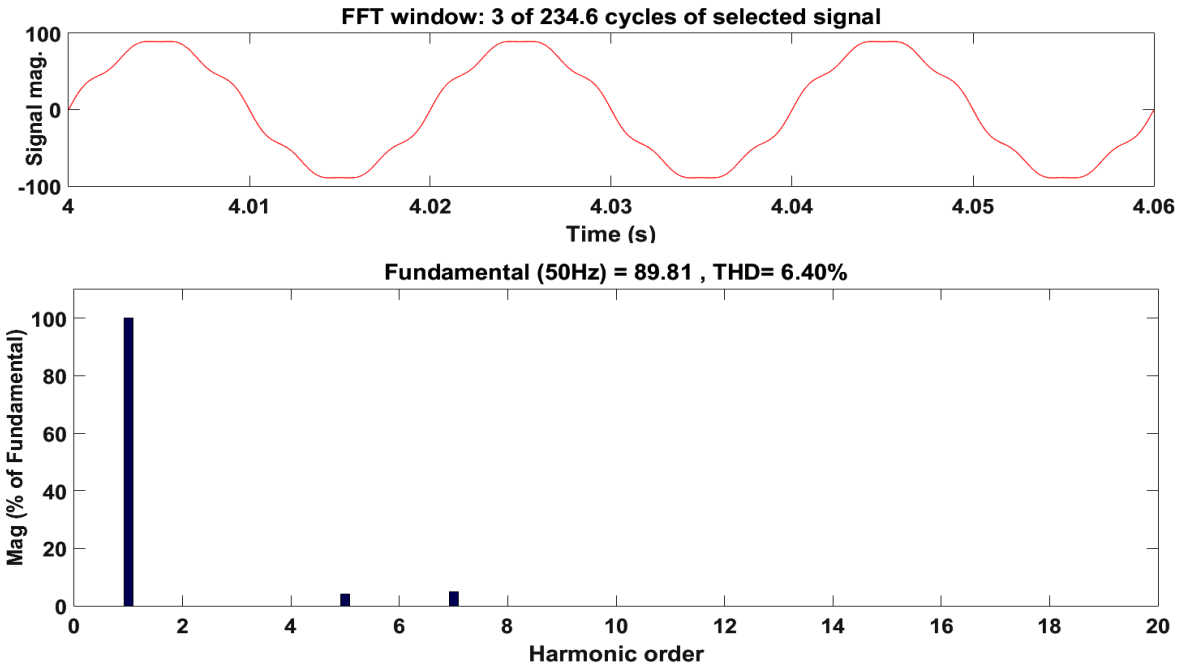

Fig. 4.25: FFT Analysis of PCC Voltage

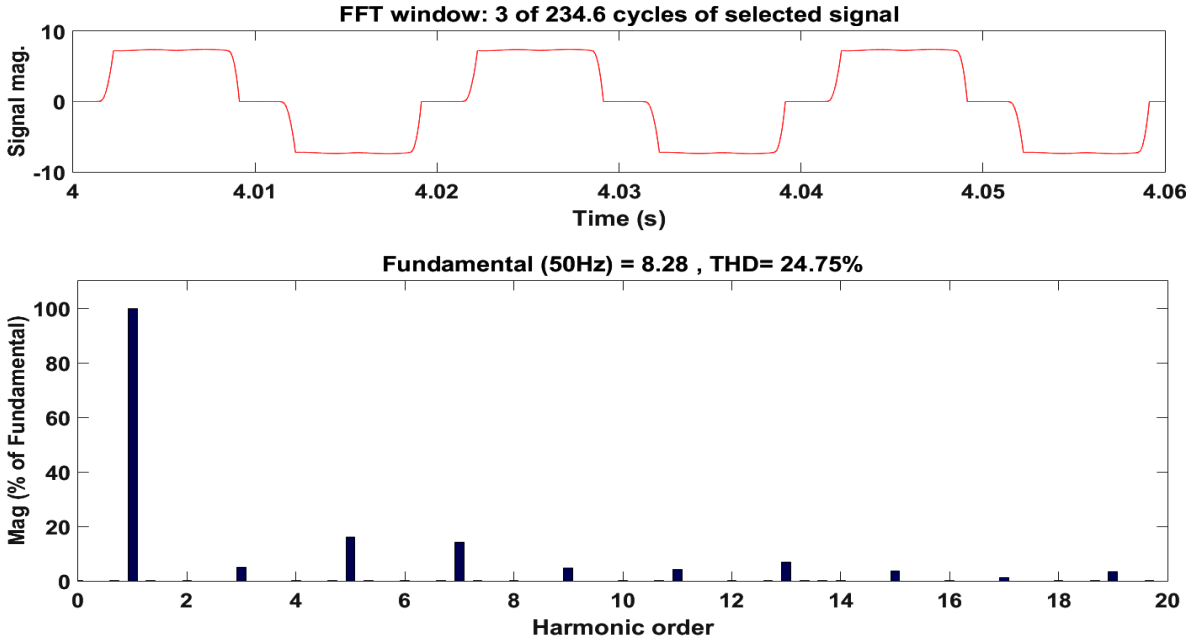

Fig. 4.26: FFT Analysis of Load Current

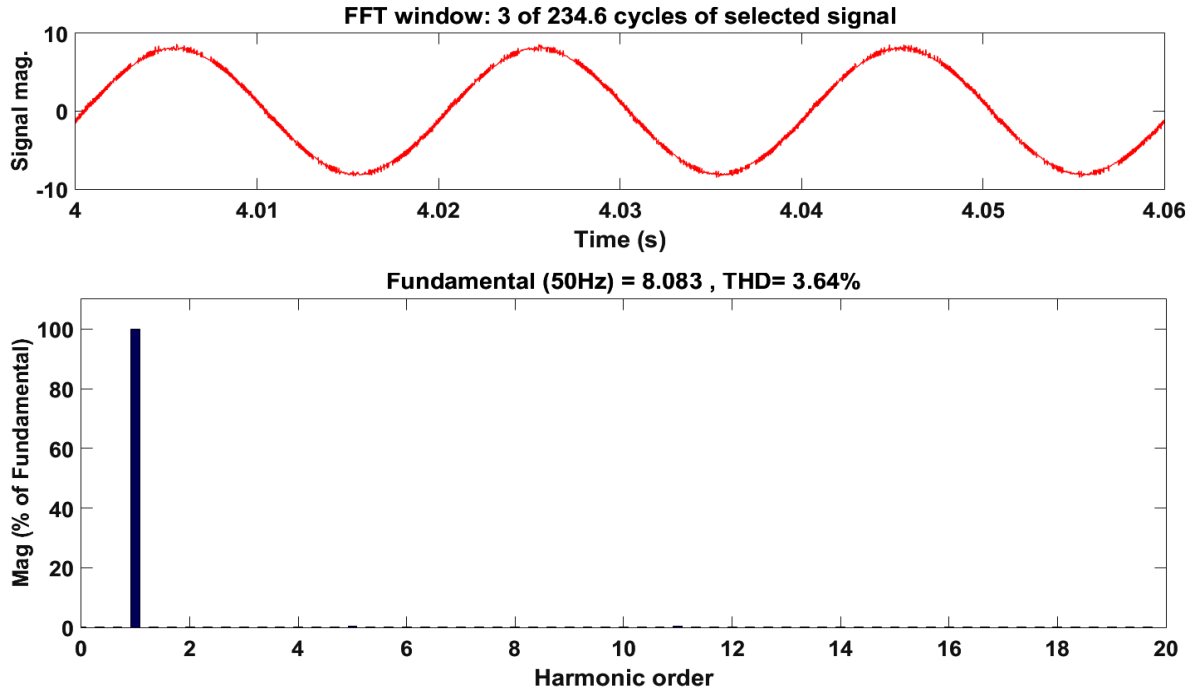

Fig. 4.27: FFT Analysis of Source Current

4.4 COMPAISON OF ALGORITHMS.

The comparison between all the algorithms for harmonics extraction studied in this chapter is shown in TABLE 4.1.

TABLE 4.1: THD IN PHASE-A OF PCC VOLTAGE, SOURCE AND LOAD CURRENTS USING VARIOUS CONTROL ALGORITHMS.

CONTROL ALGORITHM	THD IN PCC VOLTAGE	THD IN LOAD CURRENT	THD IN SOURCE CURRENT
p-q Theory (PFC) mode	6.40%	24.75%	8.52%
p-q Theory (ZVR) mode	6.40%	24.74%	7.60%
CHE	6.40%	24.75%	3.64%

4.3 CONCLUSION

The performance of a VSC based DSTATCOM has been carried out for compensating the harmonics current using p-q theory in PFC/ZVR mode and using CHE strategy under distorted grid. The proposed algorithms are found to be effective during balanced and unbalance non-linear loads. Table 4.1 shows the Total Harmonic Distortion (THD) in Phase-A of PCC Voltage, Source and Load currents using the control algorithms explained before.

It is observed from the Table 4.1 that for the same load current, p-q theory gives a THD of 8.52% in PHC mode, THD of 7.60% in ZVR mode and CHE gives a THD of 3.64%.

So, under non sinusoidal voltage CHE strategy gives the lowest THD of 3.64% in source current after compensation. Conventional IRPT strategy in PFC/ ZVR mode will not be able to reduce THD in source current to less than 5% level as per IEEE 519 standards as simulation results clearly indicate.

CHAPTER-5

MODELING AND CONTROL OF SELF EXCITED INDUCTION GENERATOR

INTRODUCTION

Today the main sources for generation of electricity are fossil fuels like coal, oil and natural gas and these sources are non-renewable in nature. These fossil fuels have limited reserves in nature and will be exhausted in the near future. Apart from these limitations, the fossil fuels produce pollutant gases when they burn which is of great concern for the ecosystem. So, more attention is being given to renewable energy such as wind, micro-hydro, tidal, solar, bio-fuel etc. Out of these, wind energy seems to be most promising source because it is clean and abundant resource without producing any emissions.

Induction generators are commonly used for wind powered energy generation [24]. SEIG system consists of a squirrel cage induction machine, prime mover, excitation capacitor and three phase load. The primary requirement for the induction machine to work as an induction generator is excitation current to produce rotating magnetic field. For grid connected machine it takes reactive current from grid whereas for a standalone machine reactive power is supplied locally by the help of shunt and series passive elements [23-25].

An induction generator has low cost, has rugged construction and gives a good dynamic response over the conventional synchronous generator.

A three phase induction machine can act as self-excited induction generator (SEIG) when a capacitor bank is used to supply the reactive power required by the generator to start operating. In grid connected induction generator driven by wind turbine, the magnetic field is produced by excitation current drawn from the grid. Fig. 5.1 shows the operation of self-excited induction generator driven by wind turbine [38].

The main drawback of SEIG is that the terminal voltage and frequency are sensitive to load and speed variation and a voltage controller is required for controlling and maintaining the ac mains voltage to its rated value.

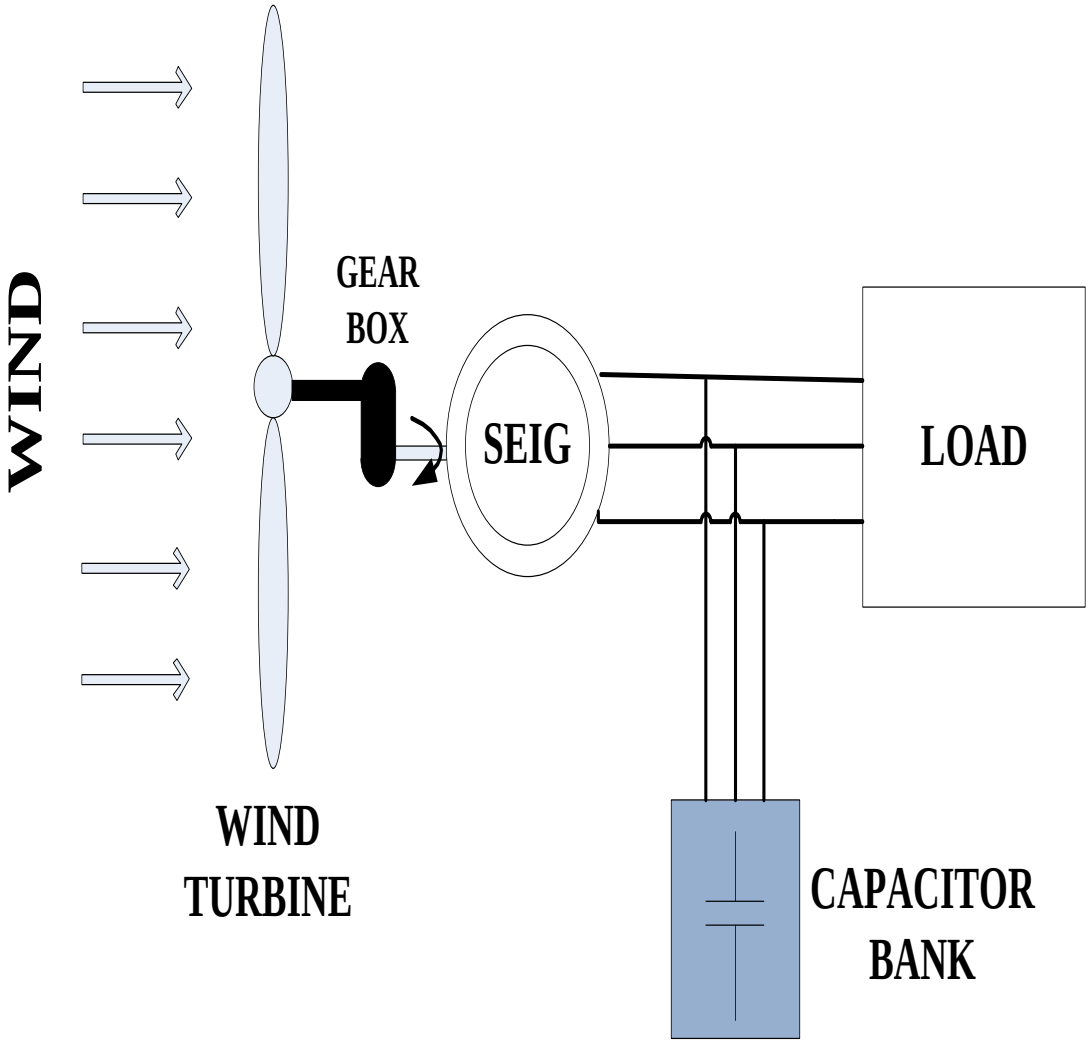

Fig. 5.1: Schematic Diagram of Wind Driven SEIG [38].

5.2 MODELING OF SEIG [40]

In electrical machine analysis a three-axes to two-axes transformation is done to produce simpler expressions that make complex systems simple to analyse. So an induction machine is generally modelled in d-q frame using Park's Transformation. In order to model the dynamic behaviour of SEIG in stand-alone mode, it is best to express the machine equivalent circuit using stationary frame of reference as shown in Fig. 5.2.

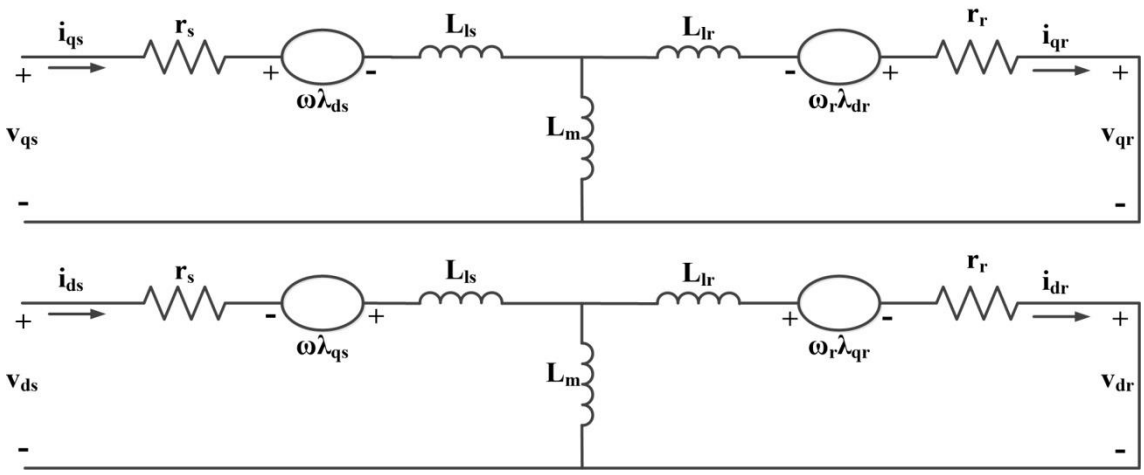

Fig. 5.2: Circuit Model of SEIG in d-q Stationary Reference Frame [40]

The stator and rotor flux linkage of induction machine 'λ_s' and 'λ_r' respectively in SI units can be represented in term of column-vector as:

$$\frac{d\lambda_s}{dt} = v_s - (r_s I)i_s \tag{4.1}$$

$$\frac{d\lambda_r}{dt} = v_r + (\omega_r J)\lambda_r - (v_r I)i_r \tag{4.2}$$

Here;

$$v_s = \begin{bmatrix} v_{ds} \\ v_{qs} \end{bmatrix};\ v_r = \begin{bmatrix} v_{dr} \\ v_{qr} \end{bmatrix};\ i_s = \begin{bmatrix} i_{ds} \\ i_{qs} \end{bmatrix};\ i_r = \begin{bmatrix} i_{dr} \\ i_{qr} \end{bmatrix};$$

$$\lambda_s = \begin{bmatrix} \lambda_{ds} \\ \lambda_{qs} \end{bmatrix};\ \lambda_r = \begin{bmatrix} \lambda_{dr} \\ \lambda_{qr} \end{bmatrix};\ I = \begin{bmatrix} 1 & 0 \\ 0 & 1 \end{bmatrix};\ J = \begin{bmatrix} 0 & -1 \\ 1 & 0 \end{bmatrix}$$

Here; v_s is the stator terminal voltage and v_r is the rotor terminal voltage

i_s is the stator currents and i_r is the rotor currents of machine

J is the moment of inertia in kg.m^2.

Here subscripts 'd' and 'q' represents the d-axis and q-axis values of these quantities.

In Equations 4.1 and 4.2, v_{dr}= v_{qr}=0 as the rotor is short circuited in case of an induction machine. The subscripts 's' and 'r' represent stator and rotor quantities respectively. The stator and rotor current in Equation 4.1 and 4.2 can be shown as:

$$i_s = L_R\lambda_s - L_M\lambda_r \tag{4.3}$$

$$i_r = L_S\lambda_r - L_M\lambda_s \tag{4.4}$$

where;

$$L_S = \left(\frac{L_{ls}+L_m}{L_m(L_{lr}+L_{ls})+L_{ls}L_{lr}}\right) I \tag{4.5}$$

$$L_R = \left(\frac{L_{lr}+L_m}{L_m(L_{lr}+L_{ls})+L_{ls}L_{lr}}\right) I \tag{4.6}$$

$$L_M = \left(\frac{L_m}{L_m(L_{lr}+L_{ls})+L_{ls}L_{lr}}\right) I \tag{4.7}$$

L_{ls} and L_{lr} are the stator and rotor leakage inductances, and L_M is the mutual inductance respectively. For operating the induction machine as a generator its saturation effects are to be considered. The non-linear characteristics between L_m and magnetizing current i_m must be determined. This non-linear characteristic can be expressed as a quadratic function where $a_0, a_1, a_2, a_3, \dots, a_n$ are constants.

$$L_m = a_0 + a_1 i_m + a_2 i_m^2 + a_3 i_m^3 + \cdots + a_n i_m^n \tag{4.8}$$

$$i_m = \sqrt{(i_{ds} + i_{dr})^2 + \left(i_{qs} + i_{qr}\right)^2} \tag{4.9}$$

The expression for electromagnetic torque (T_e) is given by:

$$T_e = \left(\frac{3}{2}\right)\left(\frac{P}{2}\right) i_m\left[i_{qs}i_{dr} - i_{ds}i_{qr}\right] \tag{4.10}$$

Torque balance equation is represented as:

$$T_{shaft} = T_e + J\left(\frac{2}{P}\right)\frac{d\omega_r}{dt} \tag{4.11}$$

Here,

P= no. of poles

ω_r= electrical rotor speed

The instantaneous phase voltages can be obtained by inverse Park's Transformation.

$$\begin{bmatrix} v_a \\ v_b \\ v_c \end{bmatrix} = \frac{2}{3}\begin{bmatrix} \cos(0) & \cos(-\frac{2\pi}{3}) & \cos(\frac{2\pi}{3}) \\ -\sin(0) & -\sin(-\frac{2\pi}{3}) & -\sin(\frac{2\pi}{3}) \end{bmatrix}\begin{bmatrix} v_{ds} \\ v_{qs} \end{bmatrix} \quad (4.12)$$

where,

$$\begin{bmatrix} v_a \\ v_b \\ v_c \end{bmatrix} = \begin{bmatrix} \sqrt{2}v_s cos(\omega_s t) \\ \sqrt{2}v_s cos(\omega_s t - 2\pi/3) \\ \sqrt{2}v_s cos(\omega_s t + 2\pi/3) \end{bmatrix} \quad (4.13)$$

5.2.2 Modeling of Excitation Capacitor

The excitation capacitor bank is connected to SEIG stator terminals in shunt and it consists of three capacitors for each phase connected in delta.

As we know,

Apparent power S=$\sqrt{3}$vi (4.14)

Active Power, P=Scosθ ;where cosθ is power factor (4.15)

Reactive power, Q=$\sqrt{S^2 - P^2}$ (4.16)

Capacitive Currents, i_c=Q/3v (4.17)

Capacitive Reactance per phase, X_c=v/i_c (4.18)

Minimum Capacitance per phase, C=(1/2πfX_c)μF (4.19)

The value of capacitance required per phase is calculated to be 13.68μF.

5.3 EQUIVALENT CIRCUIT PAPRAMETERS OF IM [36].

The equivalent circuit parameters of three phase induction machine can be determined from open circuit, short circuit and stator winding dc resistance test.

5.3.1 No Load Test

To conduct the no load test on IM, rated voltage is supplied to the stator while running the induction machine at its synchronous speed using an external prime mover at no load. The no load test is conducted on a Squirrel cage induction motor to measure the rotational losses of the motor and to determine some of its equivalent circuit parameters. Input power, voltage, and phase currents are measured in the no-load condition. The schematic of no-load test is shown in Fig. 5.3.

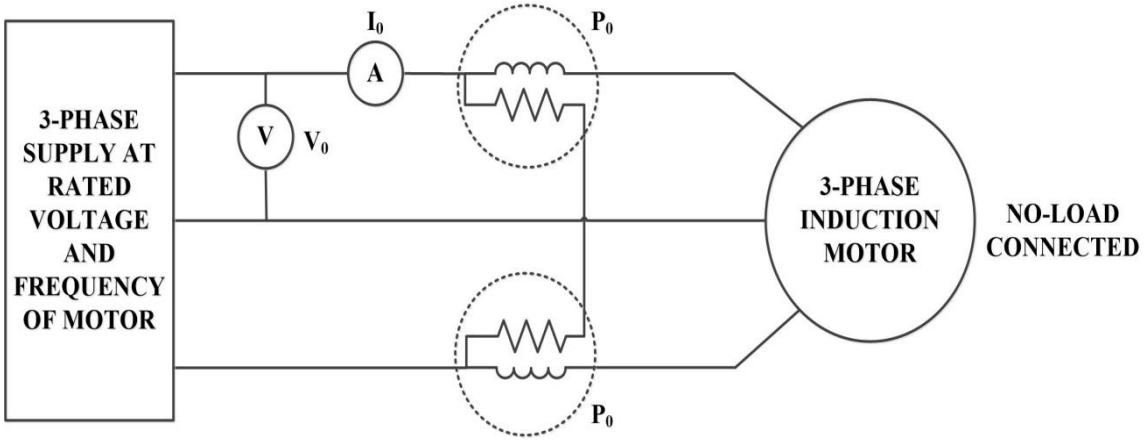

Fig. 5.3: Schematic of no-Load Test

The parameters that can be calculated from the no-load test are as follows at slip (s=0):

$$R_0 = \frac{P_0}{3I_0^2} \tag{4.20}$$

$$Z_0 = \frac{V_0}{I_0} \tag{4.21}$$

$$X_0 = \sqrt{Z_0^2 - R_0^2} \tag{4.22}$$

Here;

V_0= measured no load phase-voltage

I_0= measured no load phase current

P_0= measured no load three-phase power

R_0= total input resistance under no load condition

Z_0= total input impedance under no load condition

X_0= total input reactance under no load condition

5.3.2 Blocked Rotor Test

The short-circuit test (or block rotor or standstill test) is conducted by blocking the motor using a locking mechanism to hold the induction motor at zero speed. At standstill, rated current is supplied to the stator. When the speed of the rotor is zero, the slip will be unity. The blocked-rotor test on an induction motor is performed to determine some of its equivalent circuit parameters. In this test, input power, voltage, and current are measured.

The schematic of blocked rotor test is shown in Fig. 5.4.

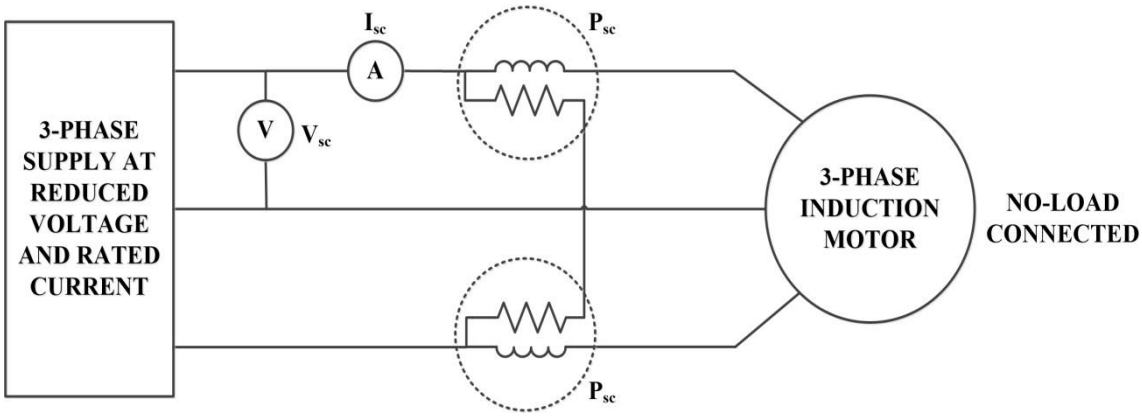

Fig. 5.4: Schematic of Blocked Rotor Test

The parameters that can be calculated from the blocked rotor test are as follows:

$$R_{sc} = \frac{P_{sc}}{3I_{sc}^2} \tag{4.23}$$

$$Z_{sc} = \frac{V_{sc}}{I_{sc}} \tag{4.24}$$

$$X_{sc} = \sqrt{Z_{sc}^2 - R_{sc}^2} \quad (4.25)$$

Here;

V_{sc}= measured blocked rotor phase-voltage

I_{sc}= measured blocked rotor phase current

P_{sc}= measured blocked rotor three-phase power

R_{sc}= total input resistance under blocked rotor condition

Z_{sc}= total input impedance under blocked rotor condition

X_{sc}= total input reactance under blocked rotor condition

5.3.3 Synchronous Speed Test:

Following steps are followed to perform the synchronous speed test:

1. The stator is connected to supply through auto- transformer. Rotor is coupled to external prime mover. This experiment is conducted at synchronous speed of rotor. It is similar to no load test because slip is zero.

2. A separately excited DC motor acts as prime mover.

3. Then the terminal voltage, per phase current drawn by machine and power taken from supply were obtained by varying the stator voltage of the induction machine in steps, while varying adjust dc machine supply to retain the rotor speed equal to synchronous speed.

4. From the series of data taken, relationship between air gap voltage and magnetizing current can be determined from curve fitting method.

The relationship between gap voltage 'v_g' and magnetizing current 'i_m' follow a non-linear characteristic:

$$v_g = Fi_m(K_1 e^{K_2 i_m^2} + K_3) \quad (4.26)$$

Here K_1, K_2, K_3 are constants, and F is the ratio of rotor frequency and reference frequency.

$$F = \frac{f}{f_{base}} \tag{4.27}$$

Here f is the rotor frequency and f_{base} is the reference frequency used in the test to obtain the excitation curve.

5.4 SELF-EXCITED INDUCTION GENERATOR

A self-excited induction generator is basically an asynchronous generator driven by prime mover whose stator terminals are connected to a capacitor bank that provides the excitation currents required by the asynchronous generator in order to start operating. An induction generator has poor voltage and frequency regulation. Fig.5.5 shows a block diagram of self-excited induction generator.

The parameters of Induction Generator used in modelling and simulation are: 2.7KW, 415V, 50Hz Y-connected 4 pole asynchronous machine.

R_s=3.715Ω; R_r =6.2533Ω

L_{ls}=L_{lr}=0.01888 H

J=Moment of Inertia=0.6175kg.m^2

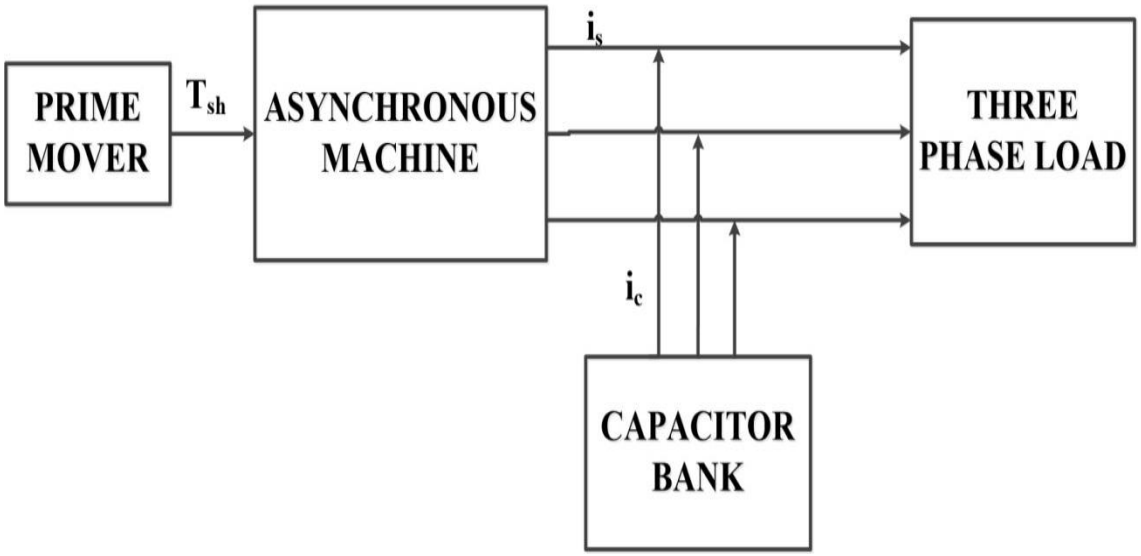

Fig. 5.5: Block Diagram of SEIG.

Fig. 5.6 shows the Block Diagram of a Self Excited Induction Generator

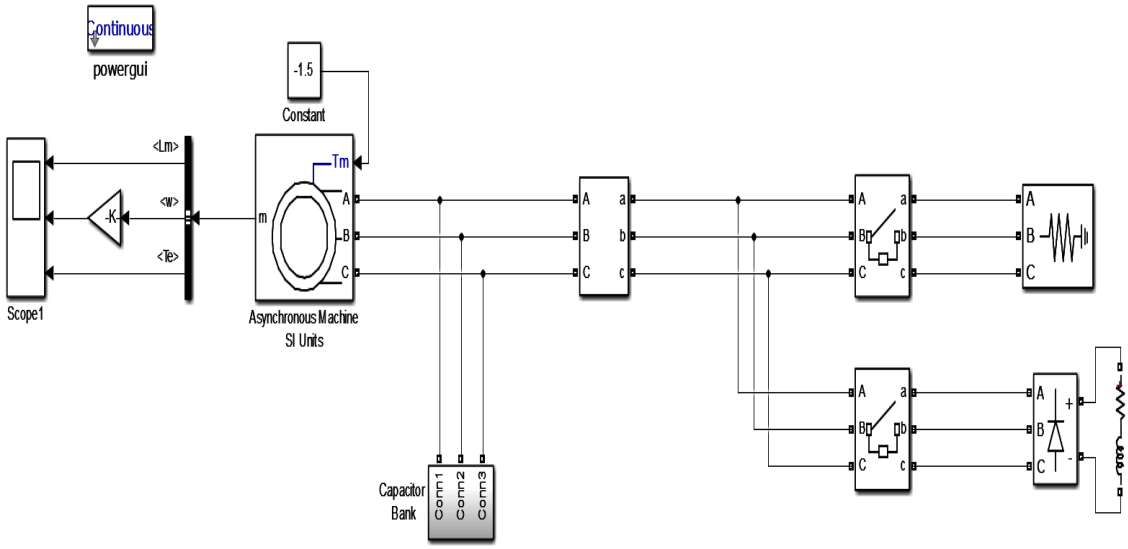

Fig.5.6: Simulation Diagram of Self Excited Induction Generator

After the modeling and simulation, performance of SEIG is tested under no load condition, under resistive load condition and under non-linear load condition. The voltage and currents shown in these results are obtained from three phase VI measurement with line to line voltage.

5.4.1 SEIG operation under No Load

As shown in Fig. 5.7 and Fig. 5.8, the stator terminal voltage rises and settles down to a peak voltage of 586.5V in t=0.5 sec. with the excitation capacitor bank of 13.68µF (in each phase connected in delta), the rotor speed rises to 314 rad/sec. It is also found that the value of L_m drops from 0.45 mH to 0.23 mH with a variation in magnetizing current i_m.

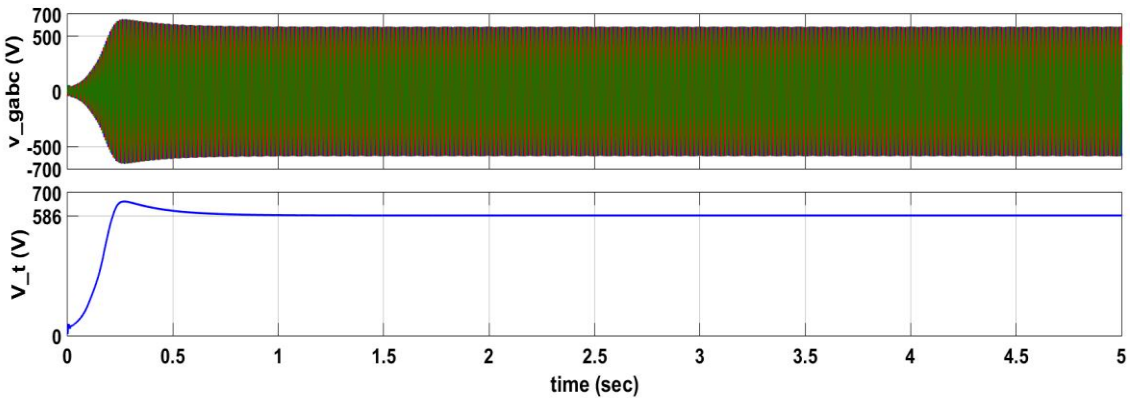

Fig. 5.7: Stator Terminal Voltage at No-Load

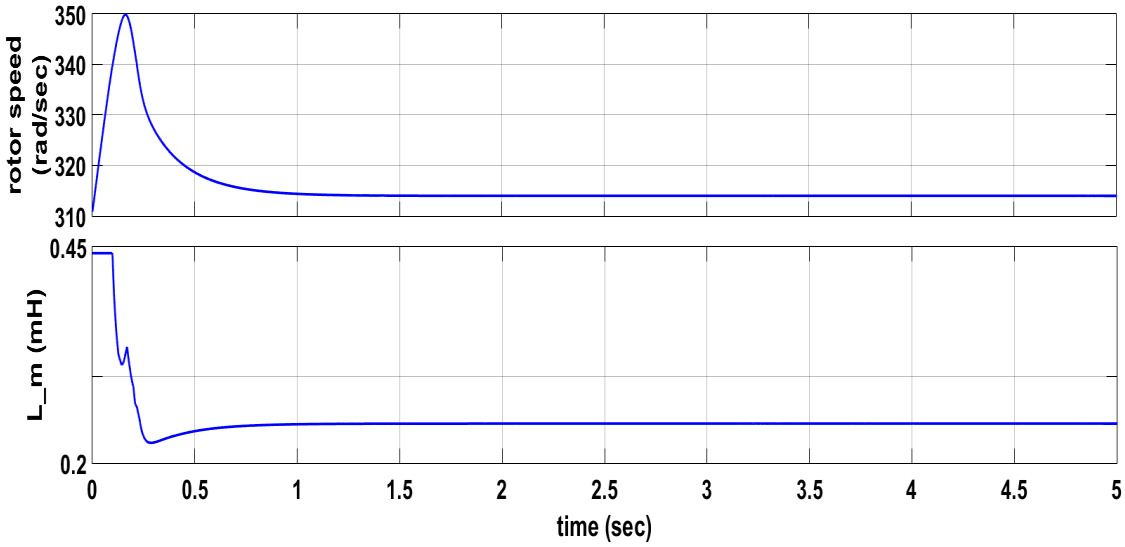

Fig. 5.8: Rotor Speed and Magnetizing Inductance at No-Load

5.4.2 SEIG operation under Resistive Load

A load of 0.08KW, upf is applied to machine at time t=3 sec. It is observed in Fig. 5.9 that the voltage drops immediately from 586V and settle down to 366.84 V in 0.5 sec. Also the rotor speed changes from 314 rad/sec and settles down to 285 rad/sec. In Fig. 5.10, the value of L_m rises from 0.23 mH to 0.315 mH in 0.5 sec with a variation in magnetizing current i_m.

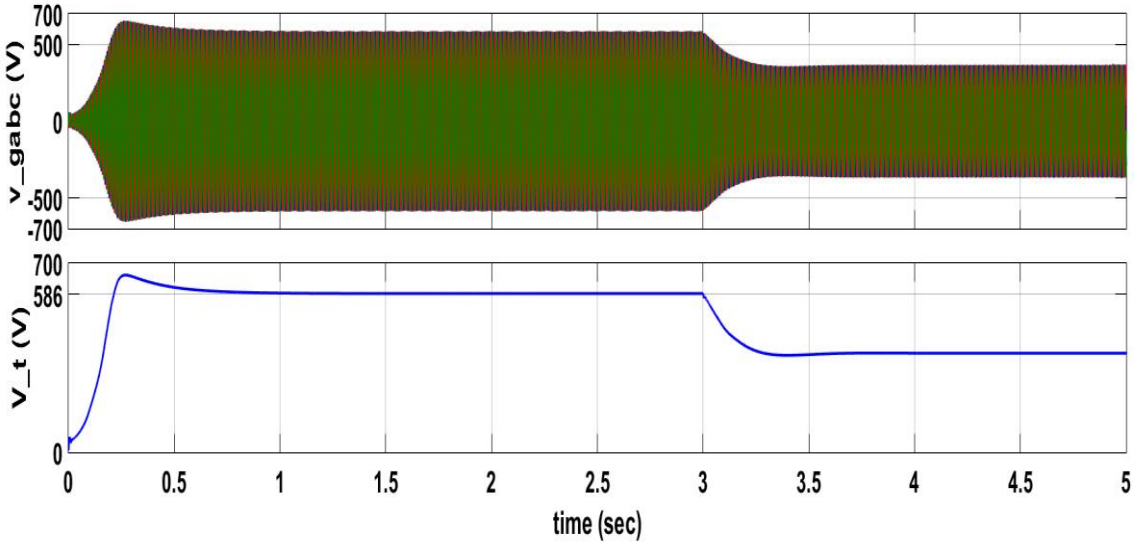

Fig. 5.9: Stator Terminal Voltage at upf load

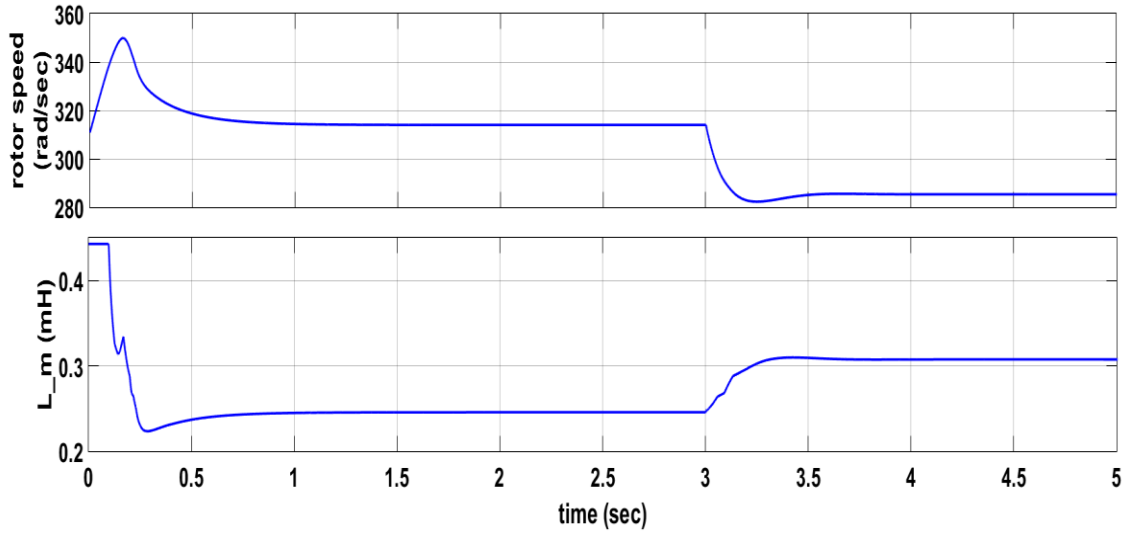

Fig. 5.10: Rotor Speed and Magnetizing Inductance at upf load

5.4.3 SEIG operation under Non-Linear Load

A non-linear load represented by an uncontrolled rectifier with R-L branch (R=500Ω and L=100 mH) is applied to machine at time t=3 sec. It is observed in Fig. 5.11 that the voltage drops immediately from 586V and settle down to 209.7 V in 1.5 sec. Also the rotor speed changes from 314 rad/sec and settles down to 299 rad/sec. In Fig. 5.12, the value of L_m rises from 0.23 mH to 0.33 mH in 1 sec with a variation in magnetizing current i_m.

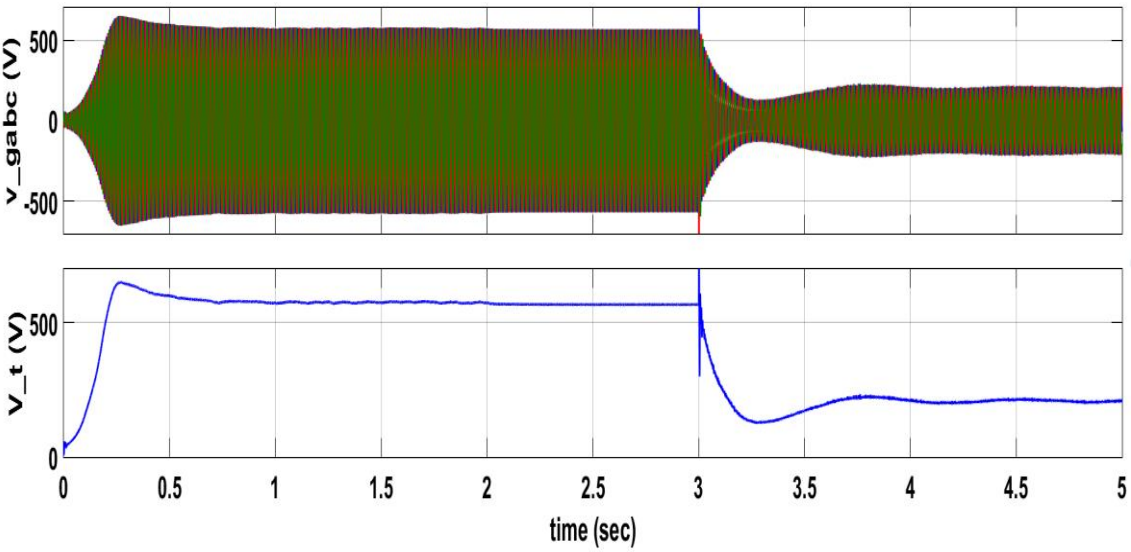

Fig. 5.11: Stator Terminal Voltage and Load Current under Non-Linear Load

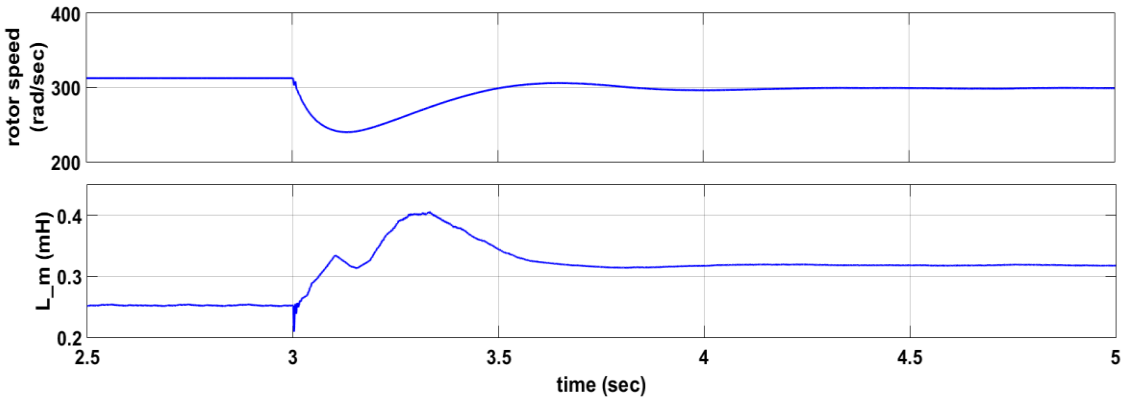

Fig. 5.12: Rotor Speed and Magnetizing Inductance under Non-Linear Load

5.5 VOLTAGE CONTROLLER FOR GRID CONNECTED IG

In a grid connected induction generator, the reactive power requirement of induction generator is fulfilled by the grid itself, hence there is no need of adding a capacitor bank. The main drawback of using induction generators is their inherently poor voltage regulation and uncontrollable frequency of operation.

The output voltage of a SEIG can be controlled by introducing an appropriate voltage regulation scheme. A number of schemes for voltage control have been recommended by many authors [24-30]. The voltage control method using switched capacitor [37] does not allow smooth control, it either increases or decreases voltage in steps. Voltage regulation with the help of saturating reactor is not economically considerable because it involves a potentially large size and weight. The series capacitor in long shunt configuration has better performance than shunt capacitance but there is a possibility of occurrence of series resonance when load is particularly inductive[]. An isolated induction generator connected to current controlled VSI with a single capacitor on the DC link side draws lagging or leading current to regulate the terminal voltage.

5.5.2 Control Algorithm for Voltage Control in Grid Connected IG

Synchronous Reference Frame (SRF) Theory as explained in Chapter 3 is used for voltage control of grid connected induction generator. The DC link is kept constant

throughout the process and only the voltage regulation of the induction generator is modelled and simulated. The reference currents are generated using SRFT in ZVR mode. Here, the load currents are first converted into d-q frame using Park's transformation and the d-axis and q-axis component of load current are passed through a low pass filter that allows only the DC components of the values to pass through it. Then the q axis component of load current is subtracted from the component i_{qr} (the q aais component obtained as the output of a PI regulator for regulating the PCC Voltage, explained in CHAPTER-3) and these new d-axis and q axis components are converted back into a-b-c- frame using inverse Park's Transformation.

Fig. 5.13 shows the simulation diagram of grid connected Induction Generator.

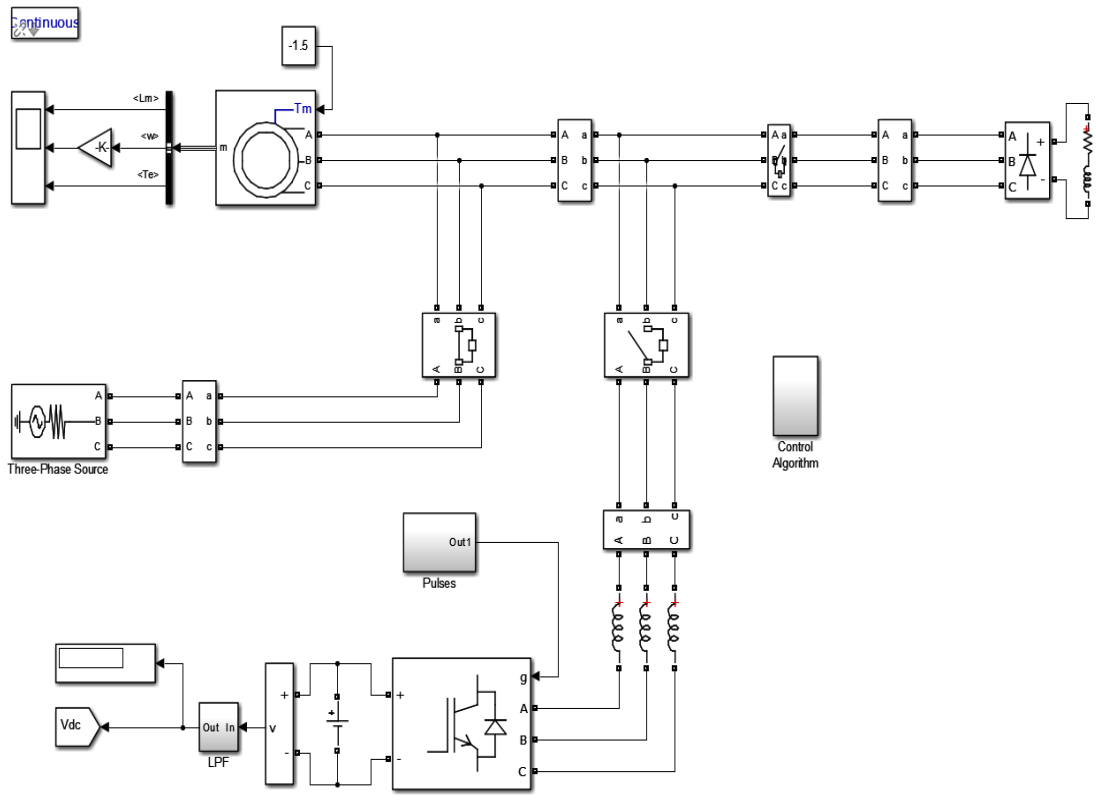

Fig. 5.13: Simulation Diagram of grid connected IG

5.5.2.1 Results of Grid Connected IG with Non-Linear Load

Fig 5.15 shows that results for grid connected IG feeding non-linear loads. For the time period t=0-2.5 sec, the grid connected IG runs on no load. and hence the voltage and current wave form are shown in first two plots of Fig. 5.14 the voltage of IG stator

terminal is constant at 338.5 V due to the grid and the source currents shown during no load period is basically the amount of excitation current that IG receives from the grid in order to start operationg. At time t=2.5 sec, the DSTATCOM is turned on, and load is turned on at time t=3 sec, after oscillations for about 1.8 sec, the voltage and currents settles down.

Fig. 5.15 shows the load current and source current waveform after the DSTATCOM and load are turned on. It is observed that the load currents have a peak magnitude of 6A and are distorted, while the supply currents are sinusoidal due to DSTATCOM action.

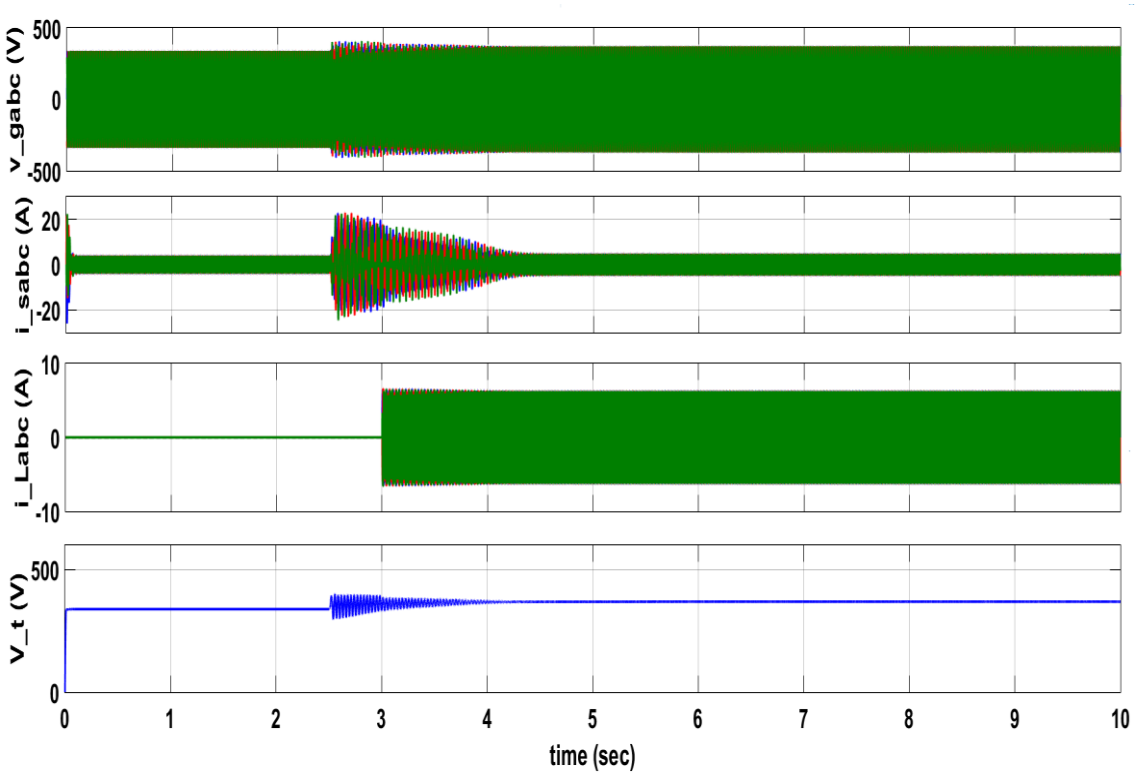

Fig.5.14: Voltage Control in Grid Connected IG using DSTATCOM controlled by SRFT

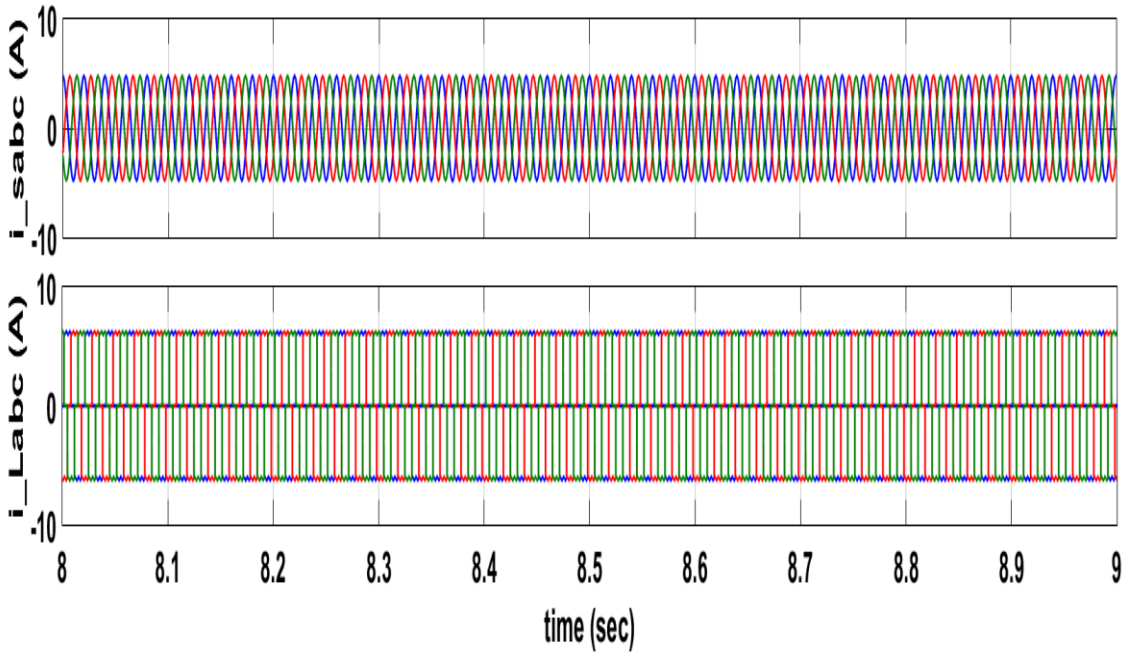

Fig. 5.15: source and load currents

5.6 CONCLUSION

Modeling and simulation of 2.5KW, 415V, 50Hz Y-connected IG has been performed. Its performance shows poor voltage regulation in standalone condition. Also the grid connected SEIG is simulated. For improving the voltage regulation, PI controller over the terminal voltage is used in the control scheme for DSTATCOM. It helps to improve various pq features and harmonic reduction is one of them. The grid supply is observed to be close to sinusoidal. Thus DSTATCOM can be used in grid connected SEIG for improving power quality problems.

CHAPTER-6

FUTURE SCOPE OF WORK

1. Other harmonic extraction and mitigation technique can be studied and some of these include conventional and new algorithms viz.
    i. Power Balance Theory
    ii. Neural Network theory
    iii. Adaptive Detecting Control algorithm
    iv. Hilbert Huang Transformation
    v. Wavelet Transformation
    vi. Kalman Filter based algorithm
    vii. Stockwell Transformation Theory
    viii. Enhanced Phase Locked Loop (EPLL) based Control Algorithm
    ix. Empirical Decomposition Transformation Theory
    x. Recursive Discrete Fourier Transformation theory
2. Implementation of different the mitigation techniques on three-phase-four wire system.
3. Implementation of all the mitigation techniques with grid connected Induction Generator and Self-Excited Induction Generator in the laboratory on a prototype hardware.

APPENDIX

Different system parameters and control gains are shown below:

1. CHAPTER-2

   A three phase 110V, 50Hz supply with source resistance, R_s=0.1Ω and source inductance L_s=0.1mH. A three Phase non-linear load; basically a three-phase uncontrolled bridge rectifier with R-L load where R=20Ω and L=100mH.

2. CHAPTER-3

   AC Supply: 110V, 3-phase, 50Hz; Rs=0.1Ω, Ls=0.1mH; dc link voltage V_{dc}=200V; dc link capacitor C_{dc}=1500μF; Interfacing inductor L_f=2.25mH; Nonlinear load: three phase uncontrolled diode rectifier with *R*=20Ω, *L*=100mH.
   PI CONTROLLER GAINS

SRFT:	(V_{dc})	k_{pd}=0.4, k_{id}=0.02
	(V_t)	k_{pd}=0.4, k_{id}=0.02
IRPT:	(V_{dc})	k_{pd}=5, k_{id}=15
	(V_t)	k_{pd}=0.4, k_{id}=0
ISCT:		k_{pd}=5, k_{id}=50
NOTCH FILTER:		k_{pd}=0.95, k_{id}=0

3. CHAPTER-4

   AC Supply: 110V, 3-phase, 50Hz; Source Impedance: Rs=0.01Ω, Ls=0.1mH; dc link voltage V_{dc}=200V; dc link capacitor C_{dc}=1500μF; Interfacing inductor L_f=2.25mH; Gains of dc link PI controller: k_{pd}=5, k_{id}=20; Nonlinear load: three phase uncontrolled diode rectifier with R=20Ω, L=100mH.

4. CHAPTER-5

   AC Supply: 415V, 3-phase, 50Hz; : Rs=0.01Ω, Ls=0.1mH; dc link voltage V_{dc}=700V; dc link capacitor C_{dc}=4000μF; Interfacing inductor L_f=4.25mH; Gains of dc link PI controller: k_{pd}=0.9, k_{id}=1; 0.08 KW upf Load, Nonlinear load: three phase uncontrolled diode rectifier with R=500Ω, L=100mH.

REFERENCES

[1] Xiao-Ping Zhang, Christian Rehtanz and Bikash Pal, "Flexible AC Transmission Systems: Modeling and Control", Springer-Verlag Berlin Heidelberg 2006.

[2] Bhim Singh, Ambrish Chandra, Kamal Al-Haddad' "Power Quality: Problems and Mitigation Techniques", John Wiley and Sons Ltd 2015.

[3] Hirofumi Akagi, Edson Hirokazu Watanabe, Mauricio Aredes, "Instantaneous Power Theory and Applications to Power Conditioning", IEEE Press, John Wiley and Sons Ltd. 2007.

[4] Boli Chen, Gilberto Pin, Wai Man Ng, Thomas Parisini and S.Y. Ron Hui, "A Fast Convergent Modulation Integral Observer for Online Detection of the Fundamental and Harmonics in Grid-Connected Power Electronics System", IEEE Transaction on Power Electronics, 2016.

[5] Lewei Qian, David Cartes, and Hui Li, "Experimental Verification and Comparision of MAFC Method and D_Q Method for Selective Harmonic Detection", IECON 2006 -32nd Annual Conference on IEEE Industrial Electronics.

[6] B. Singh and J. Solanki, "A Comparison of Control Algorithms for DSTATCOM," IEEE Trans. Ind. Electron., vol. 56, no. 7, pp. 2738–2745, 2009.

[7] B. Singh and S. R. Arya, "Design and control of a DSTATCOM for power quality improvement using cross correlation function approach," International Journal of Engineering, Science and Technology, vol. 4, no. 1, pp. 74–86, 2012.

[8] B. Chen, G. Pin, W. Ng, T. Parisini, and S. Hui, "A Fast-Convergent Modulation Integral Observer for Online Detection of the Fundamental and Harmonics in Grid-Connected Power Electronics Systems," IEEE Trans. Power Electron., vol. 8993, no. c, pp. 1–1, 2016.

[9] L. Qian, D. Cartes and L. Hui, 'Experimental Verification and Comparision of MAFC method and D_Q method for Selective Harmonic Detection", IECON Proc. (Industrial Electron Conf.), pp. 25-30, 2006.

[10] S. Kumar, B. Singh, and S. Member, "Control of 4-Leg VSC Based DSTATCOM using Modified Instantaneous Symmetrical Component Theory," Third International Conference on Power System, Kharagpur, INDIA December, 2009.

[11] J. Bangarraju and V. Rajagopal, “Implementation of Three -Leg VSC based DVR using IRPT Control Algorithm,” IEEE 6th India International Conference on Power Electronics (IICPE), 2014.

[12] L. S. Czarnecki, “Effect of Supply Voltage Harmonics on IRP-based Switching Compensator Control,” IEEE Trans. Power Electron., vol. 24, no. 2, pp. 483–488, 2009.

[13] Y. S. Prabhu, A.A. Dharme and D.B. Talaange, “A Three Phase Shunt Active Power Filter Based on Instantaneous Reactive Power Theory,” Annual IEEE India Conference (INDICON), 2014.

[14] B. Singh, A. Adya, A.P. Mittal and J.R.P. Gupta, “Modeling and Control of DSTATCOM for Three Phase, Four Wire Distribution System,” 40th IAS Annual Meeting Conference Record of the 2005 Industry Applications Conference, 2005.

[15] L. Zhu, L. Chang, J. Yan, F. Li, Y. Yang, Xiaoying Su, Z. Wu and Di Cui, “Research on Shunt Active Power Filter based on the Improved Instantaneous Reactive Power Theory”, 6th International Conference on Intelligent Control and Information Processing, Wuhan, China; November 26-28, 2015.

[16] G. W. Chang, “A new method for determining reference compensating currents of three-phase shunt active power filters,” IEEE Power Eng. Rev., vol. 22, no. 4, pp. 68–70, 2002.

[17] P. K. Dash, B. R. Mishra, R. K. Jena, and a. C. Liew, “Estimation of power system frequency using adaptive notch filters,” Proc. EMPD ’98. 1998 Int. Conf. Energy Manag. Power Deliv. (Cat. No.98EX137), vol. 1, no. 6, pp. 2470–2477, 1998.

[18] M. Karimi-Ghartemani, A.R. Bakhshai, and M. Mojiri, “Estimation of Power System Frequency Using Adaptive Notch Filter,” 2005 IEEE Instrumentationand Meas. Technol. Conf. Proc., vol. 2, no. May, pp. 1494–1497, 2005.

[19] M. Malekpour and M. Farshadnia, “Monitoring and Measurement of Power Quality Indices Using an Adaptive Notch Filter,” 5th International Power Engineering and Optimization Conference (PEOCO2011), Shah Alam, Selangor, Malaysia; 6-7 June 2011.

[20] B. Singh, K. Kant and S.R. Arya, “Notch Filter Based Fundamental Frequency Component Extraction to Control DSTATCOM for Mitigating Current Related Power Quality Problems”, IET Power Electronics, IET Journals & Magazines, Vol. 8, Issue: 9, 2015.

[21] P. Salmerón and R. S. Herrera, “Distorted and Unbalanced Systems Compensation within Instantaneous Reactive Power Framework,” IEEE Trans. Power Deliv., vol. 21, no. 3, pp. 1655–1662, 2006.

[22] S. Mohammad-Reza Rafiei, H. A. Toliyat, R. Ghazi, and T. Gopalarathnam, “An Optimal and Flexible Control Strategy for Active Filtering and Power Factor Correction Under Non-Sinusoidal Line Voltages,” IEEE Trans. Power Deliv., vol. 16, no. 2, pp. 297–305, 2001.

[23] M. Aggarwal, S. K. Gupta, and M. Singh, “Analysis and Control of Grid Connected Wind Energy System with DSTATCOM,” 2012 IEEE Fifth Power India Conf., no. 2, pp. 1–6, 2012.

[24] M. Aggarwal, S. K. Gupta, M. Singh, and G. Kasal, “D-STATCOM Control in Low Voltage Distribution System with Distributed Generation,” 2010 3rd Int. Conf. Emerg. Trends Eng. Technol., pp. 426–429, 2010.

[25] M. Aggarwal, S. . Gupta, and M. Singh, “Integration of Wind Generation System in Low Voltage Distribution System,” 2012 IEEE 5th India Int. Conf. Power Electron., pp. 1–6, 2012.

[26] P. Aree and S. Lhaksup, “Dynamic Simulation of Self-Excited Induction Generator Feeding Motor Load using Matlab/Simulink,” 2014 11th Int. Conf. Electr. Eng. Comput. Telecommun. Inf. Technol. ECTI-CON 2014, 2014.

[27] P. Arora, R. S. Reddy, B. Singh, and S. S. Murthy, “Implementation of Modified Current Synchronous Detection Method for Voltage Control of Self-Excited Induction Generator,” IET Power Electron., vol. 8, no. 7, pp. 1146–1155, 2015.

[28] Y. K. Chauhan, S. K. Jain, and B. Singh, “A Prospective on Voltage Regulation of Self-Excited Induction Generators for Industry Applications,” IEEE Trans. Ind. Appl., vol. 46, no. 2, pp. 720–730, 2010.

[29] Y. K. Chauhan, S. K. Jain, and B. Singh, “Performance of a three-phase Self-Excited Induction Generator with Static Synchronous Series Compensator,” 2010 Jt. Int. Conf. Power Electron. Drives Energy Syst. PEDES 2010 2010 Power India, no. Cc, pp. 1–6, 2010.

[30] R. R. Chilipi, B. Singh, and S. S. Murthy, “Performance of a Self-Excited Induction Generator with DSTATCOM-DTC Drive-based Voltage and Frequency Controller,” IEEE Trans. Energy Convers., vol. 29, no. 3, pp. 545–557, 2014.

[31] A. Eid, “Utility Integration of PV-Wind-Fuel Cell Hybrid Distributed Generation Systems under Variable Load Demands,” Int. J. Electr. Power Energy Syst., vol. 62, pp. 689–699, 2014.

[32] T. S. I. Generator, a K. Tandon, and S. Member, “Transient Performance of Series-Compensated Feeding Dynamic Loads,” IEEE Trans. Ind. Appl., vol. 46, no. 4, pp. 1271–1280, 2010.

[33] U. K. Kalla, B. Singh, and S. S. Murthy, “Normalised Adaptive Linear Element-based Control of Single-Phase Self-Excited Induction Generator Feeding Fluctuating Loads,” IET Power Electron., vol. 7, no. 8, pp. 2151–2160, 2014.

[34] G. K. Kasal and B. Singh, “Decoupled Voltage and Frequency Controller for Isolated Asynchronous Generators Feeding Three-Phase Four-Wire Loads,” IEEE Trans. Power Deliv., vol. 23, no. 2, pp. 966–973, 2008.

[35] C. Kathirvel, K. Porkumaran, and S. Jaganathan, “Design and Implementation of Improved Electronic Load Controller for Self-Excited Induction Generator for Rural Electrification,” vol. 2015, 2015.

[36] S. Khandelwa, A. Agarwal, and V. Agarwal, “Matlab Based Analysis of 3-Phase Self-Excited Induction Generator with Nonlinear Load,” vol. 6, no. 4, pp. 21–29, 2013.

[37] A. Kumari, A. G. Thosar, and S. S. Mopari, “A Review on Various Approaches for Determination of Excitation Capacitance of a Three Phase Self Excited Induction Generator,” Www.Ijmer.Com, vol. 5, no. 13, pp. 4069–4074, 2015.

[38] E. Muljadi, J. Sallan, M. Sanz, and C. P. Butterfield, “Investigation of Self-Excited Induction Generators for Wind Turbine Applications,” Conf. Rec. 1999 IEEE Ind. Appl. Conf. Thirty-Forth IAS Annu. Meet. (Cat. No.99CH36370), vol. 1, no. February, pp. 509–515, 1999.

[39] S. S. Murthy and A. J. P. Pinto, “A Generalized Dynamic and Steady State Analysis of Self Excited Induction Generator (SEIG) Based,” Int. Conf. Electr. Mach. Syst. ICEMS 2005. Proc. Eighth, vol. 3, pp. 1933–1938, 2005.

[40] N. Rahaman and H. V Govindraju, “Modeling & Simulation of a Three-Phase Electric Traction Induction Motor Using Matlab Simulink,” no. 5, pp. 18–25, 2014.

[41] B. Singh, S. S. Murthy, and S. Gupta, “Transient Analysis of Self-Excited Induction Generator with Electronic Load Controller (ELC) Supplying Static and

Dynamic Loads," Proc. Int. Conf. Power Electron. Drive Syst., vol. 1, no. 5, pp. 771–776, 2003.

[42] B. Singh, S. S. Murthy, and S. Gupta, "Analysis and Design of Electronic Load Controller for Self-Excited Induction Generators," IEEE Trans. Energy Convers., vol. 21, no. 1, pp. 285–293, 2006.

[43] B. Singh, S. S. Murthy, and S. Gupta, "An Electronic Voltage and Frequency Controller for Single-Phase Self-Excited Induction Generators for Pico Hydro Applications," 2005 Int. Conf. Power Electron. Drives Syst., vol. 1, pp. 0–5, 2005.

[44] B. Singh, "SRF Theory for Voltage and Frequency Control of IAG Based Wind Power Generation," pp. 25–30, 2009.

[45] B. Singh, "SRF Theory for Voltage and Frequency Control of IAG Based Wind Power Generation," pp. 25–30, 2009.

[46] B. Singh and G. K. Kasal, "Solid State Voltage Regulator for Isolated Asynchronous Generators Supplying 3-Phase 4-Wire Loads," Proc. India Int. Conf. Power Electron. IICPE 2006, pp. 144–149, 2006.

[47] B. Singh and G. K. Kasal, "Voltage and Frequency Controller for Isolated Asynchronous Generators Feeding 3-Phase 4-Wire Loads," Proc. IEEE Int. Conf. Ind. Technol., pp. 2773–2778, 2006.

[48] B. Singh, S. Member, S. S. Murthy, and S. Gupta, "Analysis and Design of STATCOM-Based Voltage Regulator for Self-Excited Induction Generators," Trans. Energy Convers., vol. 19, no. 4, pp. 783–790, 2004.

[49] B. Singh, S. S. Murthy, and S. Gupta, "Modeling of STATCOM Based Voltage Regulator for Self-Excited Induction Generator," Annu. Conf. IEEE Ind. Electron. Soc., vol. 00, 2003.

[50] B. Singh, S. S. Murthy, and S. Gupta, "STATCOM-based Voltage Regulator for Self-Excited Induction Generator Feeding Non-Linear Loads," IEEE Trans. Ind. Electron., vol. 53, no. 5, pp. 1437–1452, 2006.

[51] B. Singh and R. Niwas, "Power Quality Improvements in Diesel Engine Driven Induction Generator System using SRF Theory," 2012 IEEE 5th Power India Conf. PICONF 2012, pp. 3–7, 2012.

[52] B. Singh and L. B. Shilpakar, "Analysis of a Novel Solid State Voltage Regulator for a Self-Excited Induction Generator," IEE Proc. Gener. Transm. Distrib., vol. 145, no. 6, p. 647, 1998.

[53] V. Verma, P. Pant, and B. Singh, “VSC Supported Active Load Control for SEIG under Load Perturbations,” India Int. Conf. Power Electron. IICPE 2010, 2011.

[54] K. H. Youssef, M. A. Wahba, H. A. Yousef, and O. A. Sebakhy, “A New Method for Voltage and Frequency Control of Stand-Alone Self-Excited Induction Generator using PWM Converter with Variable DC Link Voltage,” Proc. Am. Control Conf., pp. 2486–2491, 2008.

LIST OF PUBLICATION

1. Performance of DSTATCOM control with Instantaneous Reactive Power Theory under Ideal and Polluted grid, submitted for second international conference on Innovative Applications of Computational Intelligence on Power Energy and Control with their Impact on Humanity (Technical sponsored by IEEE UP Section).